Special Issue

IMI Pathologic Myopia

Kyoko Ohno-Matsui,[1] Pei-Chang Wu,[2] Kenji Yamashiro,[3,4] Kritchai Vutipongsatorn,[5] Yuxin Fang,[1] Chui Ming Gemmy Cheung,[6] Timothy Y. Y. Lai,[7] Yasushi Ikuno,[8–10] Salomon Yves Cohen,[11,12] Alain Gaudric,[11,13] and Jost B. Jonas[14]

[1]Department of Ophthalmology and Visual Science, Tokyo Medical and Dental University, Tokyo, Japan
[2]Department of Ophthalmology, Kaohsiung Chang Gung Memorial Hospital and Chang Gung University College of Medicine, Kaohsiung, Taiwan
[3]Department of Ophthalmology and Visual Sciences, University Graduate School of Medicine, Kyoto, Japan
[4]Department of Ophthalmology, Otsu Red-Cross Hospital, Otsu, Japan
[5]School of Medicine, Imperial College London, London, United Kingdom
[6]Singapore Eye Research Institute, Singapore National Eye Center, Singapore
[7]Department of Ophthalmology & Visual Sciences, The Chinese University of Hong Kong, Hong Kong Eye Hospital, Hong Kong
[8]Ikuno Eye Center, 2-9-10-3F Juso-Higashi, Yodogawa-Ku, Osaka 532-0023, Japan
[9]Department of Ophthalmology, Osaka University Graduate School of Medicine, Osaka, Japan
[10]Department of Ophthalmology, Kanazawa University Graduate School of Medicine, Kanazawa, Japan
[11]Centre Ophtalmologique d'Imagerie et de Laser, Paris, France
[12]Department of Ophthalmology and University Paris Est, Creteil, France
[13]Department of Ophthalmology, APHP, Hôpital Lariboisière and Université de Paris, Paris, France
[14]Department of Ophthalmology, Medical Faculty Mannheim, Heidelberg University, Mannheim, Germany

Correspondence: Kyoko Ohno-Matsui, Department of Ophthalmology and Visual Science, Tokyo Medical and Dental University, Tokyo, Japan; k.ohno.oph@tmd.ac.jp.

Received: January 6, 2021
Accepted: January 8, 2021
Published: April 28, 2021

Citation: Ohno-Matsui K, Wu P-C, Yamashiro K, et al. IMI Pathologic myopia. *Invest Ophthalmol Vis Sci.* 2021;62(5):5. https://doi.org/10.1167/iovs.62.5.5

Pathologic myopia is a major cause of visual impairment worldwide. Pathologic myopia is distinctly different from high myopia. High myopia is a high degree of myopic refractive error, whereas pathologic myopia is defined by a presence of typical complications in the fundus (posterior staphyloma or myopic maculopathy equal to or more serious than diffuse choroidal atrophy). Pathologic myopia often occurs in eyes with high myopia, however its complications especially posterior staphyloma can also occur in eyes without high myopia.

Owing to a recent advance in ocular imaging, an objective and accurate diagnosis of pathologic myopia has become possible. Especially, optical coherence tomography has revealed novel lesions like dome-shaped macula and myopic traction maculopathy. Wide-field optical coherence tomography has succeeded in visualizing the entire extent of large staphylomas. The effectiveness of new therapies for complications have been shown, such as anti-VEGF therapies for myopic macular neovascularization and vitreoretinal surgery for myopic traction maculopathy.

Myopia, especially childhood myopia, has been increasing rapidly in the world. In parallel with an increase in myopia, the prevalence of high myopia has also been increasing. However, it remains unclear whether or not pathologic myopia will increase in parallel with an increase of myopia itself. In addition, it has remained unclear whether genes responsible for pathologic myopia are the same as those for myopia in general, or whether pathologic myopia is genetically different from other myopia.

Keywords: pathologic myopia, myopic maculopathy, optical coherence tomography, gene analyses, myopic macular neovascularization, myopic foveoschisis, myopic traction maculopathy, dome-shaped macula

Definition of Pathologic Myopia

According to the IMI,[1] pathologic myopia is an excessive axial elongation associated with myopia that leads to structural changes in the posterior segment of the eye (including posterior staphyloma, myopic maculopathy, and high myopia-associated optic neuropathy) and that can lead to loss of best-corrected visual acuity. The term "pathologic myopia" is often confused with "high myopia." These two entities are distinctly different; high myopia is defined as a high degree of myopic refractive error, whereas "pathologic myopia" is characterized by the presence of typical myopic lesions in the posterior fundus. Duke-Elder[2] defined pathologic myopia as "that type of myopia which is accompanied by degenerative changes occurring especially in the posterior pole of the globe."

Characteristic myopic lesions in the posterior fundus include myopic maculopathy equal to or more serious than

Investigative Ophthalmology & Visual Science

diffuse chorioretinal atrophy (equal to category 2 in the META-analysis for Pathologic Myopia [META-PM] classification[3]) and/or the presence of a posterior staphyloma.[4] The cut-off values of the myopic refractive error and axial length were not set for the definition of pathologic myopia because a posterior staphyloma has been reported to occur in eyes with normal axial length[5] or in eyes with an axial length of less than 26.5 mm,[6] although long axial length is one of the risk factors for fundus complications.

Because progressive choroidal thinning and formation of Bruch's membrane defects in the macular region are key phenomena associated with myopic maculopathy, the lesions of myopic maculopathy are better classified by their appearance in the optical coherence tomography (OCT) images than by the morphology as detected on fundus photographs.[7]

Basic Aspects of Pathologic Myopia

Epidemiology of Pathologic Myopia

Prevalence and Its Impact on Vision. It has been reported that pathologic myopia affects up to 3% of the world's population, with racial differences regarding the prevalence of the disease.[8] Approximately 1% to 3% of Asians and 1% of Caucasians have pathologic myopia. However, the definition of pathologic myopia used in earlier studies was not consistent and pathologic myopia was confused with high myopia. Thus, an accurate prevalence needs to be determined based on the new standard definition of pathologic myopia.

Pathologic myopia causes vision impairment or blindness in 0.2% to 1.5% of Asians and 0.1% to 0.5% of Caucasians.[8] Particularly, it is one of the major causes of low vision in working-aged populations, as well as in the elderly population. In Asia, pathologic myopia is the leading cause of irreversible blindness in Taiwan, Japan, and China. In Taiwan, pathologic myopia is the second leading cause of vision impairment in individuals aged 65 years or older.[9] In Japan, pathologic myopia is the third leading cause of bilateral low vision and the leading cause of monocular blindness in individuals aged 40 years or older.[10] In China, pathologic myopia is the leading cause of blindness and low vision in individuals aged 40 to 49 years.[11] In Western countries, pathologic myopia is the third cause of blindness according to the Rotterdam Study, the Copenhagen City Eye Study, and the Los Angeles Latino Eye Study.[12–14]

High Myopia and Myopia. Recently, owing to changes in environmental and lifestyle factors, the prevalence of myopia and high myopia has increased rapidly. Therefore, the associated prevalence of pathologic myopia may also increase dramatically in the near future.

High myopia can be defined as a refractive error of at least –5.00 diopters (D).[15] High myopia is linked to pathologic myopia. Most pathologic myopia occurs in eyes with high myopia, although low myopia and some individuals with emmetropia will also develop pathologic myopia. Approximately 28.7%, 44.4%, 45.9%, 47.6%, 58.31%, 72.7%, and 65% of high myopia cases in adult or elderly populations have pathologic myopia in Singapore, Australia, Japan, rural China, South China, Taiwan, and Beijing, respectively.[9,16–21] This means that approximately one-half of subjects with high myopia in the adult population would develop pathologic myopia.

The prevalence of high myopia is linked to the overall prevalence of myopia. In Taiwan, the prevalence of myopia is as high as 84% in 18-year-old individuals and the prevalence of high myopia is about 21%.[22] Approximately 22.9% of the world population were diagnosed with myopia in 2000, and 11.6% had high myopia among the myopia population. It is estimated that by 2050, approximately one-half of the world's population will have myopia and up to one-fifth of the myopia population will be highly myopic.[23] Thus, areas with high prevalence rates of myopia would have increased rates of high myopia and pathologic myopia. Pathologic myopia will be associated with a high number of individuals suffering from vision impairment and will have a significant negative impact on society.

The degree of myopia is associated with the risk of pathologic myopia. The prevalence of pathologic myopia is only 1% to 19% in the low-to-moderate myopia (–3 D) population, but its prevalence is as high as 50% to 70% in the high myopia population.[17,18,24] A 1-D increase in myopia is associated with a 67% increase in the prevalence of pathologic myopia.[25] A linear trend is observed for increasing myopia diopters until −7.00 D, followed by an exponential trend in the prevalence rates of pathologic myopia.[26]

Age. In addition to the degree of myopia, age is an important factor in the development of pathologic myopia. The prevalence of myopic maculopathy increased and exponentially with increasing spherical equivalent and age in Singapore.[19] The prevalence of pathologic myopia is low in children and adolescents, but increases with advancing age. In individuals with high myopia aged 40 years or older, a progressive increase was noted in the prevalence and severity of maculopathy. Pathologic myopia changes with chorioretinal atrophy were found in 52.9% and 19.3% of the Chinese and Singaporean adult groups with high myopia, respectively.[27,28] In the Taiwanese elderly population, myopic maculopathy increased from 2.2% in individuals aged 65 years to 14.8% in relatively older adults. Myopic maculopathy is rare in children with high myopia.[29] However, a long-term follow-up study showed that 83% of adults with pathologic myopia and myopic maculopathy had already had diffuse choroidal atrophy around the optic disc in their childhood.[30] This finding suggested the possibility that children who eventually develop pathologic myopia may be different, even at an early age.

Genetic or Acquired. There are two types of myopia—congenital myopia or infantile myopia and acquired myopia or school myopia. Congenital myopia has family aggregation and is strongly influenced by genetic factors. However, the prevalence of congenital myopia is low, less than 1% among Caucasian population.[31] The initial degree of infantile myopia is often high and progression of myopia is also observed.[32] A longer life span with high myopia may be linked to the high prevalence of pathologic myopia.

Acquired or school myopia occurs in children who develop myopia in the primary school or early secondary school years, with the exclusion of congenital myopia of strong familial inheritance.[33] It should be noted that, from age 6, the annual progression rate for children with myopia is approximately 1 D until the end of adolescence, with the development of high myopia between the ages of 11 and 13 years.[34] Considering the myopia boom in children worldwide, the severity of pathologic myopia associated with vision impairment is predictable.

Investigative Ophthalmology & Visual Science

Environmental Factors. In the case of acquired myopia, there might be a genetic susceptibility owing to a variation in the prevalence observed in different areas. Although more than 200 gene variants have been found to be associated with myopia, none predominately contribute to acquired myopia.[35] Therefore, environmental factors play a more important role in the development of myopia and high myopia. Risk factors include educational stress, near-work time and intensity, and lack of outdoor time.[36,37] In addition, increased digital screen time because of the smartphone era and the popularity of online education owing to the coronavirus disease 2019 pandemic may aggravate the prevalence of myopia in the near future.[38]

Genetics

Genome-wide association studies (GWASs) have identified more than hundreds susceptibility genes for myopia.[39–44] However, the genetic background for pathologic myopia has not been elucidated fully. For example, little is known about whether all subjects with high myopia have the same risk of developing pathologic myopia or if the risk of developing pathologic myopia depends on the patient's genetic background.

Candidate Gene Analysis for Pathologic Myopia. Several studies have examined the association between myopic macular neovascularization (MNV) and susceptibility genes for myopia, high myopia, and AMD. Among the susceptibility genes for AMD and their related genes, ARMS2, CFH, C2/CFB, C3, CFI, ABCA1, APOE, LIPC, CETP, TIMP3, COL8A1, COL10A1, VEGFA, and PEDF were evaluated for their association with MNV.[45–50] CFI, COL8A1, and PEDF were suggested as susceptibility genes for MNV,[48–50] and it has been reported that VEGFA is associated with the size of MNV and the visual prognosis after treatment for MNV.[47,51] However, these associations were not confirmed in later studies. Among the susceptibility genes for myopia and high myopia, GJD2, RASGRF1, TOX, RDH5, and SHISA6 were evaluated for association with MNV, but no association was found.[52,53]

In 2015, a photographic classification and grading system for myopic maculopathy was proposed.[3] Since then, the Myopic Maculopathy Classification System (META-PM classification) has been used to study pathologic myopia. In 2019, the genotype distribution of 50 susceptibility genes for myopia were compared between 348 highly myopic cases with myopic maculopathy and 898 highly myopic controls without myopic maculopathy, but none of the genes showed a significant association with myopic maculopathy in the highly myopic eyes.[54]

GWAS for Pathologic Myopia. In 2018, a GWAS on myopic maculopathy in a Japanese population identified *CCDC102B* as a susceptibility gene for myopic maculopathy.[55] The genotype distribution of *CCDC102B* was significantly different between the 1381 highly myopic cases with myopic maculopathy and the 936 highly myopic controls without myopic maculopathy. In contrast, *CCDC102B* was not significantly associated with axial length, and previous GWASs on myopia have not reported any association between *CCDC102B* and myopia. *CCDC102B* is a susceptibility gene for myopic maculopathy, but not for myopia. Given that the genetic background for developing myopia and the genetic background for developing myopic maculopathy are different, we would be able to develop preventive methods for myopic maculopathy, even for patients who have already developed myopia or high myopia. The role of *CCDC102B* in the development of myopic maculopathy should be elucidated.

The discovery of *CCDC102B* suggests that we might be able to prevent the development of myopic maculopathy, even after the development of high myopia. To control the development of pathologic myopia in highly myopic patients, further studies need to discover more susceptibility genes for myopic maculopathy that are not associated with high myopia. Because posterior staphyloma is associated with myopic maculopathy in highly myopic eyes, the identification of susceptibility genes for posterior staphyloma and/or posterior eye shape would also contribute to future control of the development of pathologic myopia. The posterior fundus shape can be quantitatively evaluated using OCT.[56] GWASs on fundus shape might be able to discover genes associated with fundus shape and/or staphyloma and contribute to future control of the development of pathologic myopia.

Animal Models of Pathologic Myopia

Since Wiesel and Raviola[57] discovered in 1977 that lid-sutured monkeys developed axial elongation, animal models have been a vital tool to understand and develop treatments for myopia. This section summarizes animals that spontaneously, or via monocular deprivation, developed features of pathologic myopia.

A search on Embase database using the following keywords: "animal model" with "posterior staphyloma," "lacquer cracks," "myopic maculopathy," "choroidal neovascularization," and "Fuchs spot" one feature at a time revealed 1502 results. There were 1466 entries from "choroidal neovascularization," which were almost entirely induced artificially through laser photocoagulation and, hence, were excluded. A summary of screened studies is found in Table 1, which included retinopathy, globe enlarged (*rge*) chicks, normal chicks, and LRP2 knockout mice.

The murine model is widely used because its genetics and physiology are well-understood.[58] Similar to in humans, murine sclera and fibroblasts contain five types of muscarinic receptors.[59,60] However, they are nocturnal animals that lack a fovea and ability to accommodate.[61] Additionally, their lenses are more spherical compared with human lenses and occupy most of the vitreal cavity.[62]

Chick eyes are relatively larger and make up 50% of the cranial volume compared with 5% in adult human.[63] Additionally, they contain pecten, a comb-like structure of blood vessels that provides nutrition and oxygenation to the retina. Crucially, chick sclera has a cartilaginous layer and ossicles, unlike any mammals.[64,65] Nonetheless, there is a rod-free region called the area centralis in the chick retina that contains a greater concentration of cone photoreceptors, resembling the macula in human.[66] Similar to mice, chicks have no fovea.

Animal Models of Lacquer Cracks. Lacquer cracks are the yellowish linear lesions in the macular region and seem to lack choriocapillaris under OCT angiography (OCTA). They are seen in 4.3% to 15.7% of patients with pathologic myopia.[67–70] These lesions are believed to represent mechanical breaks in the Bruch's membrane–RPE–choriocapillaris complex. In pathologic myopia, lacquer cracks are commonly found temporal to the fovea in a horizontal direction.[71] One may discuss that because a horizontal tension within Bruch's membrane may be relieved

Table 1. Summary of Animal Models That Demonstrated Features of Pathologic Myopia Spontaneously or Induced Through Monocular Deprivation

Authors	Animal	*n*	Relevant Phenotypes	Method	Time of First Intervention	Degree of Induced Myopia	Other Features
Cases et al.,[95] 2015	Mouse	20	Peripapillary staphyloma after 21 days, chorioretinal atrophy after 60 days	Spontaneous in LRP2 knockout model. Mutation associated with Stickler syndrome and Donnai-Barrow or facio-acoustico-renal syndrome (DBS/FOAR), which present with ocular defect	Day 0	Day 90: About 40% increase in axial length	Increase in vitreous chamber, retina thinning (owing to increased cell death), scleral thinning at the posterior pole, and collagen fibrils formed fewer lamellae
Wen et al.,[295] 2006	Chick	45	Lacquer cracks after 12 weeks	Form-deprivation via lid suturing	Day 2	Week 4: −10.23 ± 2.15 D, Week 8: −15.57 ± 2.52 D, Week 12: −17.01 ± 3.29 D. Axial length increases by 13.5%, 11.4% and 11.1% respectively	—
Hirata and Negi,[72] 1998	Chick	40	Lacquer cracks after 8 weeks, chorioretinal atrophy (choriocapillaris significantly less dense) after 4 weeks	Form deprivation via lid suturing	Day 1	Week 8: 28.3% increase in axial length	—
Montiani-Ferreira et al.,[76] 2004	Chick	9 *rge/rge*, 12 *rge/+*, 5 +/+	Lacquer cracks after 6.4 weeks, patchy chorioretinal atrophy and scleral displacement after 134 weeks	Spontaneous in congenital stationary night blindness model (mutation in GNB3 gene), animals known as retinopathy globe enlarged (*rge*) chicks	Day 0	Hyperopia. At Day 92, *rge/rge* shows 9.8 ± 7.4 D, *rge/+* shows 4.3 ± 0.57 D. Axial length increases by 14.8%	Areas of ruptured Bruch's membrane with focal absence of RPE Fibroblasts covered the interface of the abnormal Bruch's membrane and choriocapillaris
Mao et al.,[296] 2006	Chick	32	Chorioretinal atrophy after 12 weeks	Form deprivation via lid suturing	Day 1	Week 12: −18.0 ± 2.25 D, 23.1% increase in axial length	TUNEL-positive cells in ONL and INL of myopic chick eyes

INL, inner nuclear layer; ONL, outer nuclear layer.

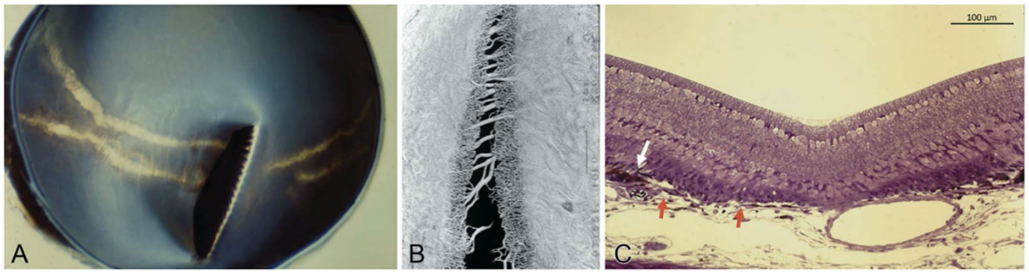

Figure 1. Images taken from 8-week-old lid-sutured chick. (**A**) Macroscopic appearance of the eyecup of a lid-sutured eye. Horizontal lacquer cracks could be seen running perpendicularly to the pecten. (**B**) Vascular cast at site of the LC and showing a central gap surrounded by areas of decreased choriocapillaris density and some large choroidal bridging vessels between the gap. (**C**) Histology image at the site of the LC. The white arrow depicts the proliferation and accumulation of RPE while the red arrows indicates both ends of Bruch's membrane.

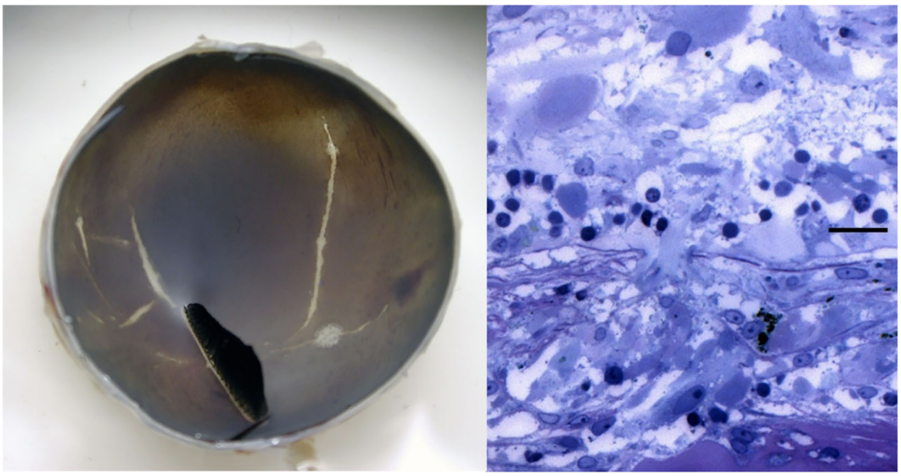

Figure 2. Images taken from *rge* chick. (**A, Left**) Macroscopic appearance of an eyecup taken from a 7-week-old *rge* chick showing lacquer cracks as white linear lesions. Reprinted with permission from Montiani-Ferreira F, Kiupel M, Petersen-Jones SM. Spontaneous lacquer crack lesions in the retinopathy, globe enlarged (*rge*) chick. *J Comp Pathol*. 2004;131(2-3):105-11. Copyright © 2004 Elsevier Ltd. (**B, Right**) Histology image taken from 48-week-old *rge* chick showing Bruch's membrane rupture and absence of RPE (Toluidine blue. Bar, 20 mm).

by a temporally located parapapillary gamma zone, lacquer cracks may be orientated in a horizontal direction to relieve the remaining excess tension in the vertical direction.

Lid-sutured Chick. Chicks that undergo monocular deprivation through lid suturing on the first day after hatching develop lesions that resemble lacquer cracks after 8 weeks[72] (Fig. 1A). Similar to human, these lesions are frequently orientated horizontally, which may be due to the vertically orientated pectin in its retina. Vascular casts show that lacquer cracks are not sharply demarcated. There is a central gap that is void of Bruch's membrane and choriocapillaris. This gap is surrounded by an area with reduced choriocapillaris density, possibly owing to atrophy from increased tension on the vessel bed (Fig. 1B). Large choroidal vessels bridging the gap could also be seen. Proliferation and accumulation of RPE, seen as a white arrow in Figure 1C, suggest that this lacquer crack has developed over a period of time and the RPE had sufficient time to respond.

Retinopathy, Globe Enlarged (rge) Chick. Rge chicks have a progressive, early onset visual loss and a deletion in *GNB3*, a gene that encodes guanine nucleotide binding protein b3 (Gbeta3),[73] resulting in a nonfunctional protein. Physiologically, Gbeta3 forms a part of phototransduction cascade and is an integral part of the G-protein signaling within ON-bipolar cells.[74] In humans, GNB3 mutation is seen in patients with congenital stationary night blindness with normal retinal thickness.[75]

Lacquer cracks in *rge* chicks are seen as early as 45 days after hatching[76] (Fig. 2A). Histologic images show a rupture of Bruch's membrane and a lack of RPE compared with the surrounding area where these structures are intact (Fig. 2B).

Long-term Follow-up Observation of Lacquer Cracks in Humans and Chicks. Studies show that lacquer cracks in patients with pathologic myopia tend to deteriorate by elongating, increasing in number, or progressing to patchy atrophy.[71,77,78] Interestingly, the chick models also develop similar progression patterns. In Figure 3, a 50-week-old lid-sutured chick eye developed a greater number of lacquer cracks and a marked elongation as compared with an 8-week-old eye shown in Figure 2. Although there was no obvious formation of a patchy atrophy during the long-term observation of lid-sutured chicks, 134-week-old *rge* chicks developed circular lesions that resembled a patchy atrophy (Fig. 3). OCT images at the lesions showed areas of tissue thinning and posterior bowing of sclera, which were consistent with a patchy chorioretinal atrophy in patients with pathologic myopia. This finding suggests that both features

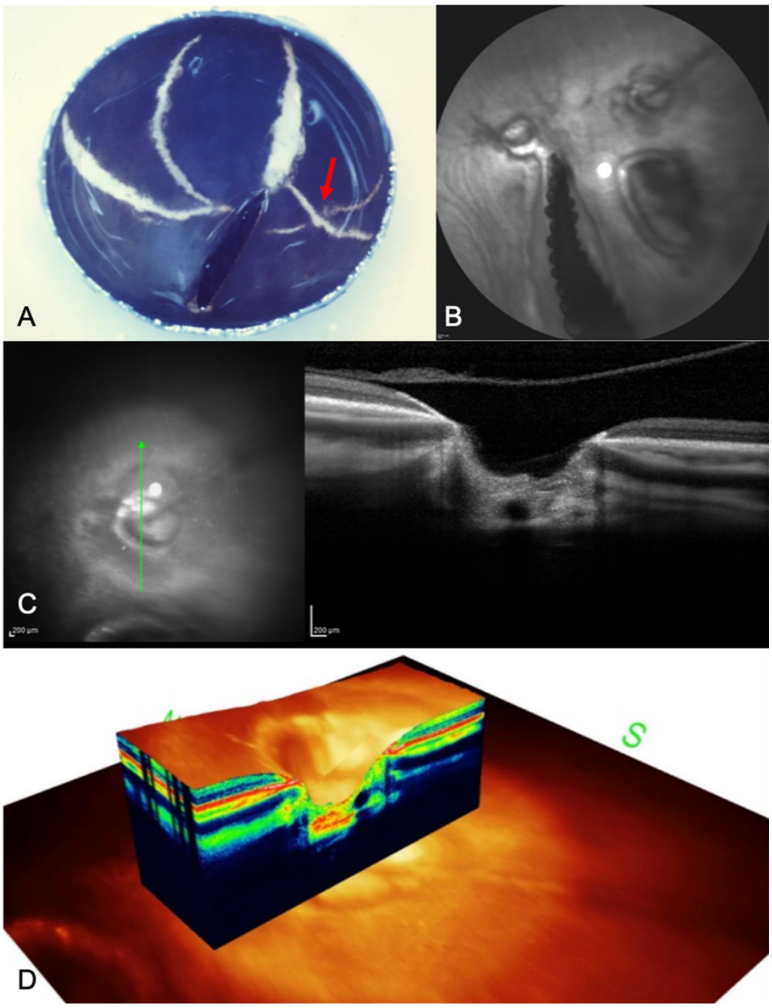

Figure 3. Images of older lid-sutured (**A**) and *rge* chicks (**B–D**). (**A**) Eyecup of 50-week-old lid-sutured chick. There are more orientations and a higher number of lacquer cracks compared with an 8-week-old lid-sutured eyecup with two lesions crisscrossing each other (red arrow) (**B**) Confocal scanning laser ophthalmoscopy (cSLO) FA of 134-week-old *rge* chicks showing three circular lesions near the pecten. (**C**) Spectral domain OCT (SD-OCT) image of a circular lesion illustrating the marked loss of tissue and the posterior bowing of sclera at the lesion site. (**D**) A 3D image of the circular lesion showing similar findings. **B, C, D** reprinted with permission from Vutipongsatorn K, Nagaoka N, Yokoi T, et al. Correlations between experimental myopia models and human pathologic myopia. *Retina*. 2019;39:621–635.

may share a similar pathophysiology and that *rge* chicks might be a suitable animal model to study the disease.

Animal Models of Posterior Staphyloma. Posterior staphyloma is a localized, outpouching of the eye wall with a radius of curvature that is less than the surrounding curvature of the eye wall.[79] It is present in approximately 50% of patients with pathologic myopia and little is known about its etiology.[5] Scleral weakness secondary to tissue loss and change in collagen fibrils have been implicated in some studies.[80–82] However, scleral re-enforcement treatments have yielded mixed results.[83–86] Choroidal thinning has also been proposed because it is strongly associated with posterior staphylomas.[87] However, patients with an acquired choroidal thinning still demonstrate axial elongation without developing posterior staphylomas.[88] Furthermore, patients with retinitis pigmentosa can develop posterior staphylomas in areas where the choroid was intact.[89]

Bruch's membrane is an acellular, five-layered extracellular matrix located between the RPE and choroid.[90] With a thickness of 2 to 4 µm, it facilitates the transport of nutrients and metabolic byproducts between the choriocapillaris and the RPE, as well as providing structural support to the globe. Bruch's membrane and its surrounding structures are markedly thinned or absent along the staphyloma edges.[91] Additionally, eyes with a secondary Bruch's membrane defect, such as in toxoplasmotic macular scars, can show a collateral scleral staphyloma.[92] Furthermore, because its thickness remains constant while other layers thin out in axially elongated globes, Jonas et al.[93] proposed that Bruch's membrane may play an active role in the process of emmetropization, myopization and potentially staphyloma development as well.

Rge Chicks. As seen in Figure 3C, the OCT images of 134-week-old *rge* chicks show an outward bowing of the sclera in the regions of a Bruch's membrane defect. Because the extent of scleral displacement is limited, it is difficult to conclude if these scleral deformations were certainly staphylomas. However, it seems reasonable to suggest that this may be an early stage of a transition toward a staphyloma formation. A longer observation period may be necessary to monitor the development of scleral deformation.

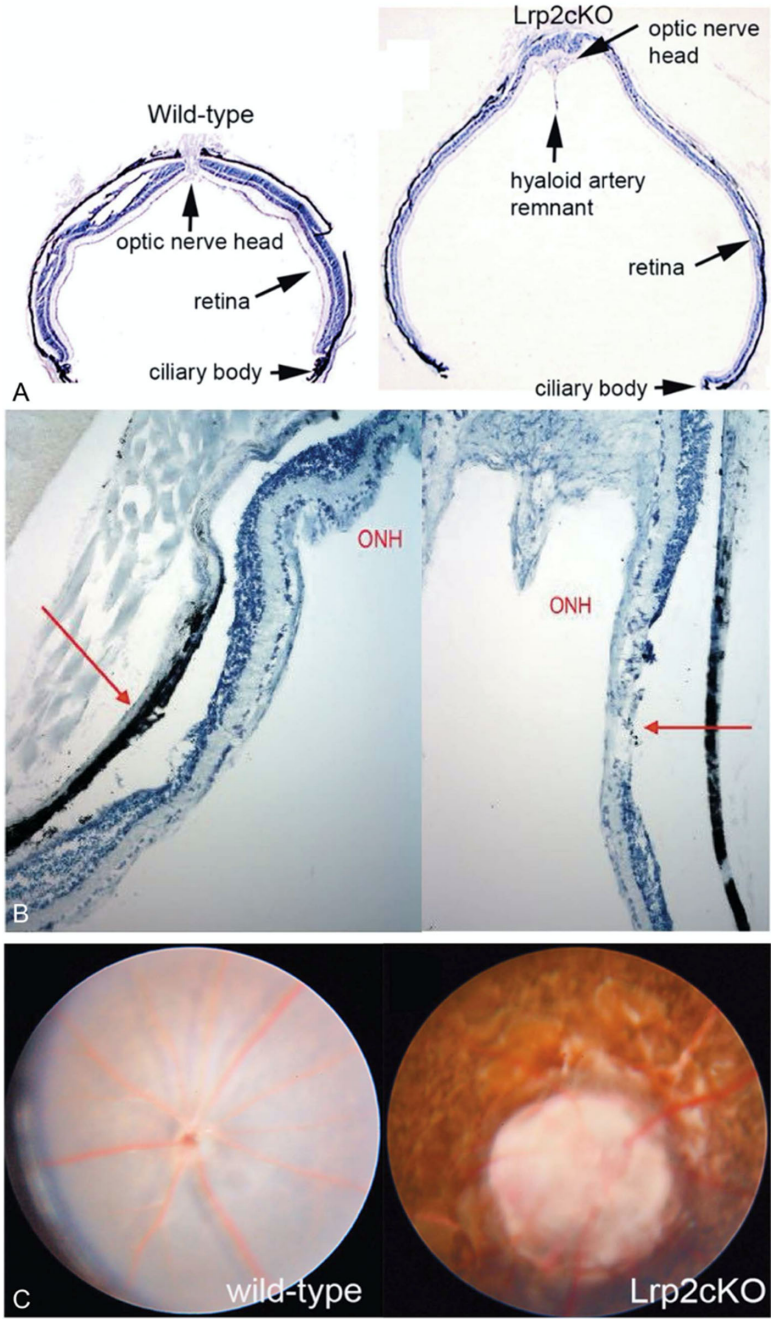

Figure 4. Images taken from 134-week-old *rge* chicks. (**A**) Confocal scanning laser ophthalmoscopy (cSLO) FA showing three circular lesions near the pecten. (**B**) Spectral domain OCT (SD-OCT) image of a circular lesion illustrating the marked loss of tissue and the posterior bowing of sclera at the lesion site. (**C**) A 3D image of the circular lesion showing similar findings.

LRP2 Knockout Mouse. Currently, there is one animal model that definitively develops posterior staphyloma, which is the *LRP2* knockout mouse.[94] *LRP2* (low-density lipoprotein receptor–related protein 2) encodes megalin—a transmembrane receptor found on the apical side of absorptive epithelia. It regulates the level of certain circulating compounds such as lipoproteins, sterols, vitamin-binding proteins, and hormones.[95] Its mutation is associated with rare genetic conditions such as Donnai–Barrow syndrome and Stickler syndrome, both of which present with facial dysmorphology, hearing loss, ocular defects and chorioretinal atrophy.[96]

Histologic sections and magnetic resonance imaging (MRI) show evidence of axial elongation and posterior staphyloma from days 15 and 21, respectively (Figs. 4A and 4B). A separation of the choroid and RPE began at the edge of the staphyloma. Both layers became progressively thinner before disappearing at the optic nerve head. Bruch's membrane could not be identified clearly on these images. Furthermore, there was a marked thinning of the retina and pycnotic cell bodies were detected throughout the excavated region. This finding indicated an area of peripapillary atrophy apparently corresponding with the region with peripapillary staphyloma in this model. This formation is compatible

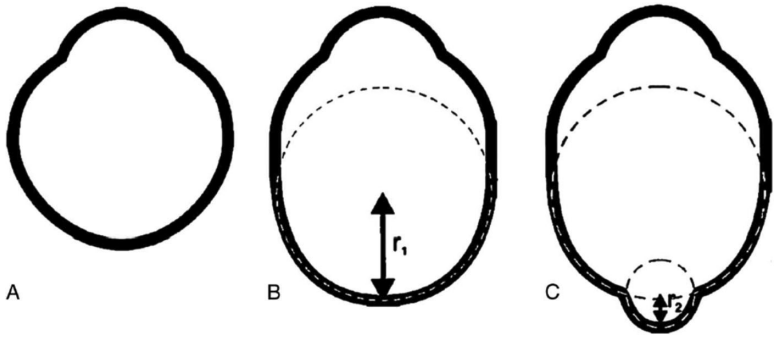

Figure 5. Proposed nomenclature for staphylomas. (**A**) Normal eye shape. (**B**) Axial elongation occurring in the equatorial region that does not induce altered curvature in the posterior aspect of the eye. This eye has axial myopia but no staphyloma. (**C**) A second curvature occurs in the posterior portion of the eye with a small radius (r_2) than the surrounding eye wall (r_1). This secondary curve is staphyloma, Reproduced with permission from Spaide RF. *Staphyloma: part 1. Pathologic Myopia*: Springer; 2014:167-176.

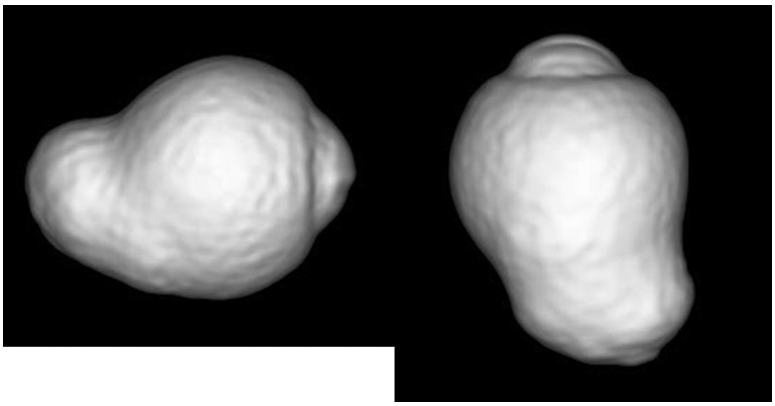

Figure 6. Three-dimensional MRI of the eye with posterior staphyloma. A clear outpouching of a part of the posterior segment of the eye is observed in the image viewed from the side (left) as well as in the image viewed from the inferior (right).

with a posterior bowing of the area of peripapillary gamma zone in patients with pathologic myopia.[97] Figure 4C shows a posterior bowing of the area of gamma zone.

Apart from posterior staphyloma, mutant mice also developed retinal and scleral thinning and chorioretinal atrophy, similar to patients with pathologic myopia. Furthermore, they maintained a similar IOP throughout their lifespan, which is consistent with the findings from patients with pathologic myopia as well. Thus, *LRP2* knockout mouse may serve as an animal model to study the etiology of pathologic myopia.

Clinical Aspects of Pathologic Myopia

Posterior Staphyloma

Posterior staphylomas are hallmarks of pathologic myopia and are among other major causes or sequels of developing myopic maculopathy.[3,18,77,98–100] The presence of a posterior staphyloma is part of a recently updated definition of pathologic myopia that was characterized by the occurrence of myopic choroidal atrophy equal to or more serious than diffuse choroidal atrophy or by the presence of a posterior staphyloma.[3,4]

As described by Spaide,[79] a posterior staphyloma is an outpouching of a circumscribed posterior fundus region and has a curvature radius that is smaller than the curvature radius of the adjacent eye wall (Fig. 5).[4,5] Posterior staphylomas should be differentiated from a simple scleral backward bowing which is commonly seen on OCT images of highly myopic eyes.

Applying three-dimensional (3D)-MRI, Moriyama et al. recently analyzed the shape of the whole eye,[5,101,102] so that even large posterior staphylomas could be imaged entirely (Fig. 6). Based on 3D-MRI images of the eye, they showed that the difference in the ocular shape is correlated with the development of vision-threatening conditions in eyes with pathologic myopia.[5] Applying 3D-MRI and wide-field fundus imaging, Ohno-Matsui[102] recently classified posterior staphylomas into six types: the wide macular type, the narrow macular type, the peripapillary type, the nasal type, the inferior type, and other configurations (Fig. 7). This classification was based on the previous categorization of staphylomas by Curtin[103] into 10 types, among which the types I to V were primary staphylomas and the types VI to X were compound staphylomas. The most predominant staphyloma type was the wide, macular type (74% of eyes with staphyloma), followed by the narrow, macular type of staphyloma (14% of eyes with staphyloma). However, 3D-MRI was not feasible as a screening technique and, owing to a relatively low spatial resolution, subtle changes of shallow staphylomas were difficult to detect.

A new prototype of a wide-field swept source OCT system has recently been developed and uses not one but

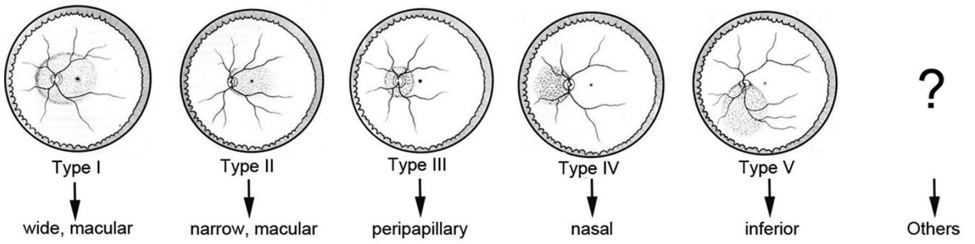

Figure 7. Classification of staphyloma. A new classification of posterior staphyloma according to its location and extent. The staphyloma type is renamed according to its location and distribution. Type I → wide, macular staphyloma, Type II → narrow, macular staphyloma, Type III → peripapillary staphyloma, Type IV → nasal staphyloma, Type V → inferior staphyloma, Others → staphylomas other than type I to V. Reprinted with permission from Ohno-Matsui K. Proposed classification of posterior staphylomas based on analyses of eye shape by 3D-MRI. *Ophthalmology*. 2014;121:1798-1809. © 2014 American Academy of Ophthalmology. Published by Elsevier Inc.

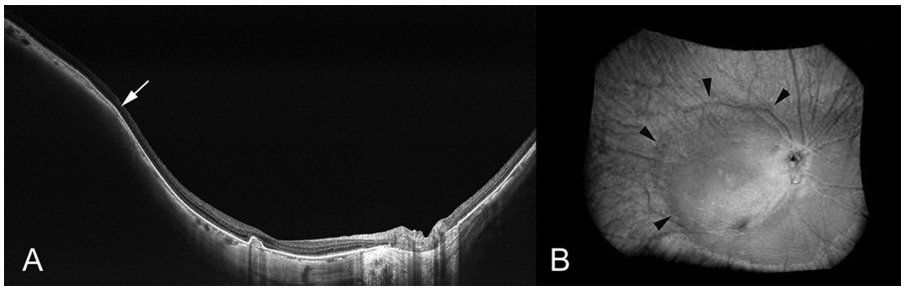

Figure 8. Ultra-wide-field optical coherence tomographic image of staphyloma. (**A**) In a horizontal OCT section across the fovea, the edge of the staphyloma (arrow) shows consistent features with a gradual thinning of the choroid from the periphery toward the staphyloma edge as well as a gradual re-thickening of the choroid from the staphyloma edge in direction to the posterior pole, accompanied by a change in the curvature of the sclera at the staphyloma edge. The staphylomatous region shows a posterior outpouching of the sclera nasal to the staphyloma edge. (**B**) Three-dimensionally reconstructed image shows the staphyloma edge clearly (outlined by arrowheads). Reprinted with permission from Shinohara K, Shimada N, Moriyama M, et al. Posterior staphylomas in pathologic myopia imaged by widefield optical coherence tomography. *Invest Ophthalmol Vis Sci*. 2017;58:3750-3758. Licensed under a Creative Commons Attribution 4.0 International License (CC BY).

multiple scan lines and generates scan maps allowing the 3D reconstruction of posterior staphylomas in a region of interest of 23 × 20 mm and a depth of 5 mm. Shinohara et al.[104] showed that wide-field OCT can provide tomographic images of posterior staphylomas in a resolution and size that have been unachievable so far and that may replace 3D-MRI in assessing posterior staphylomas. Using wide-field OCT, the edge of staphylomas showed consistent features with a gradual thinning of the choroid from the periphery toward the staphyloma edge and a gradual rethickening of the choroid from the staphyloma edge in direction to the posterior pole, accompanied by a change in the curvature radius of the sclera at the staphyloma edge (Fig. 8).

In a study by Tanaka et al.,[105] 55 eyes of 30 patients with a mean age of 12.3 years and a mean axial length of 27.9 mm were studied. Seven of the 55 eyes (12.7%) had a posterior displacement of the sclera and were diagnosed as having a staphyloma. Although staphylomas are generally considered to be pathological changes that develop in later life, the results showed that posterior staphylomas can be present at a much younger age than they had been believed.

Ultra-wide-field OCT is considered to be a useful method to identify children with pathologic myopia. One of the strengths of ultra-wide-field OCT is that structures of the neural retina can be visualized and a relationship between staphylomas and chorioretinal complications can be examined. Shinohara et al.[106] showed that, in eyes with staphylomas, myopic macular retinoschisis is observed only within the area of staphylomas. Myopic macular retinoschisis is also seen in eyes without staphyloma, in which cases myopic macular retinoschisis is seen in a diffuse fashion. Takahashi et al.[107] analyzed a relationship between vitreous adhesion and staphylomas.

Finally, therapies targeting staphylomas are eagerly expected. Before vision-threatening complications occur, preventing and treating staphylomas are considered to be ideal treatments.

Myopic Choroidal Atrophy

Myopic maculopathy, also known as myopic macular degeneration, is a key feature of pathologic myopia. Curtin and Karlin[70] first described five myopic fundus changes that are associated with an increase of axial length, including optic nerve crescent, chorioretinal atrophy, central pigment spot, lacquer cracks, and posterior staphyloma. Later, Avila et al.[108] developed a grading system of myopic maculopathy on a scale of increasing severity from 0 to 5 as follows: M_0, normal-appearing posterior pole; M_1, choroidal pallor and tessellation; M_2, M_1 plus posterior staphyloma; M_3, M_2 plus lacquer cracks; M_4, M_3 plus focal areas of deep choroidal atrophy; and M_5, large geographic areas of deep chorioretinal atrophy shown as "bare sclera." In an atlas of pathologic myopia,[109] Tokoro updated and organized the lesions of myopic maculopathy. Tokoro[109] classified myopic macular lesions into four categories based on ophthalmoscopic findings: (1) tessellated fundus, (2) diffuse choroidal atrophy, (3) patchy choroidal atrophy, and (4) macular hemorrhage.

Table 2. META-PM Classification and an Impact on Vision

META-PM Classification*	Visual Impairment	Pathologic Myopia
Category		
Tessellated fundus (category 1)	None	–
Diffuse chorioretinal atrophy (category 2)	Mild	+
Patchy chorioretinal atrophy (category 3)	Parafoveal scotoma	+
Macular atrophy (category 4)	Central scotoma	+
Plus lesions		
Myopic MNV (including Fuchs' spots)	Central scotoma, distorted vision	+
Lacquer cracks	Temporal scotoma owing to simple hemorrhage, distorted vision (in some cases)	+

* Modified from Ohno-Matsui K, Kawasaki R, Jonas JB, et al. International photographic classification and grading system for myopic maculopathy. Am J Ophthalmol. 2015;159:877e883.

Pathologic myopia is defined as equal or greater than myopic maculopathy category 2, or presence of "plus lesion," or the presence of posterior staphyloma.

Lacquer cracks were included in the diffuse atrophy category and macular hemorrhage was subclassified into two types of lesions—myopic MNV and simple macular hemorrhage. Later, Hayashi et al.[98] investigated the natural course of 806 eyes of 429 consecutive patients with high myopia (myopic refractive error of >8 D or an axial length of ≥26.5 mm) who had follow-up for 5 to 32 years. Hayashi et al.[98] made some modifications to Tokoro's classification based on clinical impression; they categorized lacquer cracks and myopic MNV as independent lesions. This longitudinal observation of all myopic maculopathy lesions has made a great contribution to the subsequent establishment of universal classification (META-PM classification).[3]

The META-PM Classification of Myopic Maculopathy. Recently an international panel of researchers in myopia reviewed previous studies and proposed a simplified, uniform classification system for pathologic myopia (Table 2). In this simplified system (the META-PM classification), myopic maculopathy lesions are categorized into five categories from no myopic retinal lesions (category 0), tessellated fundus only (category 1), diffuse chorioretinal atrophy (category 2), patchy chorioretinal atrophy (category 3), to macular atrophy (category 4). Three additional features were added to these categories and were included as "plus signs": (1) lacquer cracks, (2) myopic MNV, and (3) Fuchs spot. The reason for separating these plus signs from the categories is that these three plus lesions affect or potentially affect central visual acuity and may develop from, or coexist, in eyes with any categories of the myopic maculopathy. Based on this classification, pathologic myopia is defined as equal to or greater than myopic maculopathy category 2, or presence of plus lesion, or the presence of a posterior staphyloma.

Features of Each Lesion of Myopic Maculopathy.

Tessellated (or Tigroid) Fundus (Category 1). Tessellated fundus is defined by the increased visibility of large choroid vessels owing to axial elongation (Fig. 9). Tessellation begins to develop around the optic disc, especially in the area between the optic disc and the central fovea. A tessellated fundus alone does not affect the central vision, unlike the other lesions of myopic maculopathy (Table 2). A tessellated fundus, along with the myopic conus, is one of the preliminary visible signs in eyes with myopia in general and often observed in children with high myopia.[110] Wong et al.[111] also reported that a tessellated fundus and peripapillary atrophy were the most common findings in highly myopic Chinese adolescents (aged 12–16 years).

Highly myopic patients with a tessellated fundus are significantly younger than the patients with other lesions of myopic maculopathy.[21,77,98,112] Fang et al.[77] and Xiao et al.[21] both showed that highly myopic eyes with a tessellated fundus had less myopia and a shorter axial length than those in the category 2 or above. Tokoro[109] reported that approximately 90% of eyes with only a tessellated fundus had an axial length of less than 26 mm. The proportion of tessellation decreases linearly with longer axial length and tessellation is not seen in eyes with an axial length of more than 31 mm. In other words, almost all eyes with axial length of more than 31 mm would have progressed to advanced myopic maculopathy (i.e., diffuse atrophy or patchy atrophy).

The mean (or median) subfoveal choroidal thickness in eyes with tessellated fundus in high myopia varies from 80 to 166 µm,[7,112–114] and is decreased almost by one-half compared with those with no myopic maculopathy in high myopia.[7,113] The distribution pattern of the choroidal thickness in eyes with tessellation was different with those in eyes with no maculopathy, but was similar to greater myopic maculopathy categories (e.g., diffuse atrophy and patchy atrophy). This finding suggested that the tessellation might be the first sign for myopic eyes to become pathologic.

Hayashi et al.[98] showed that only 13.4% of eyes with a tessellated fundus showed a progression after a follow-up period of 5 to 32 years; 10.1% developed diffuse chorioretinal atrophy, 2.9% developed lacquer cracks, and 0.4% developed a MNV in the first time progression. In the population-based Beijing Eye Study, progression was observed in 19% eyes with tessellation with 10 years of follow-up.[100] Another large series of 810 highly myopic eyes that were followed for more than 10 years (mean follow-up, 18 years) showed a higher progression rate (27%).[77] Because the eyes with greater myopic maculopathy categories showed a greater progression rate, it is suggested that myopic maculopathy tends to progress more quickly after the tessellated fundus stage. A tessellated fundus might be a relatively stable condition, and highly myopic eyes might stay in this condition for a relatively long period.

Diffuse Choroidal Atrophy (Category 2). Diffuse choroidal atrophy is observed as an ill-defined yellowish

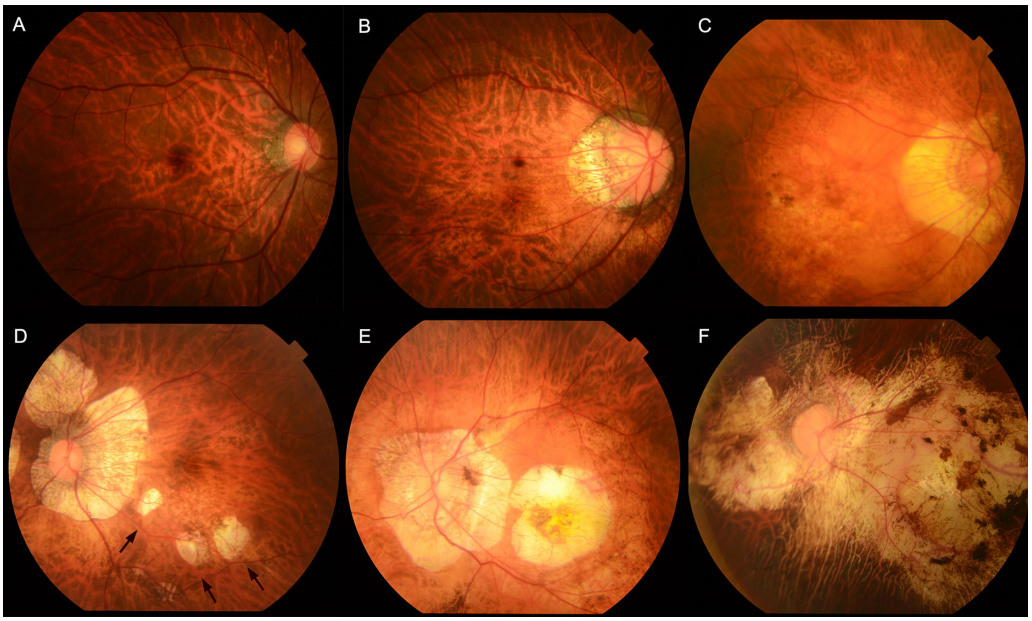

Figure 9. Fundus photographs showing different type of myopic maculopathy. (**A**) Right fundus showing a tessellated fundus with an axial length of 28.1 mm in a 37-year-old woman. The best-corrected visual acuity (BCVA) is 1.2. (**B**) Right fundus showing PDCA with an axial length of 29.76 mm in a 45-year-old woman. The BCVA is 0.8. (**C**) Right fundus showing MDCA with an axial length of 31.77 mm in a 76-year-old man. The BCVA is 0.5. (**D**) Left fundus showing patchy atrophy (arrows) with an axial length of 30.46 mm in a 60-year-old woman. The BCVA is 0.9. (**E**) Left fundus showing myopic MNV-related macular atrophy with an axial length of 33.16 mm in a 74-year-old woman. The BCVA is 0.15. (**F**) Left fundus showing patchy atrophy-related macular atrophy with an axial length of 32.95 mm in a 61-year-old woman. The BCVA is 0.2.

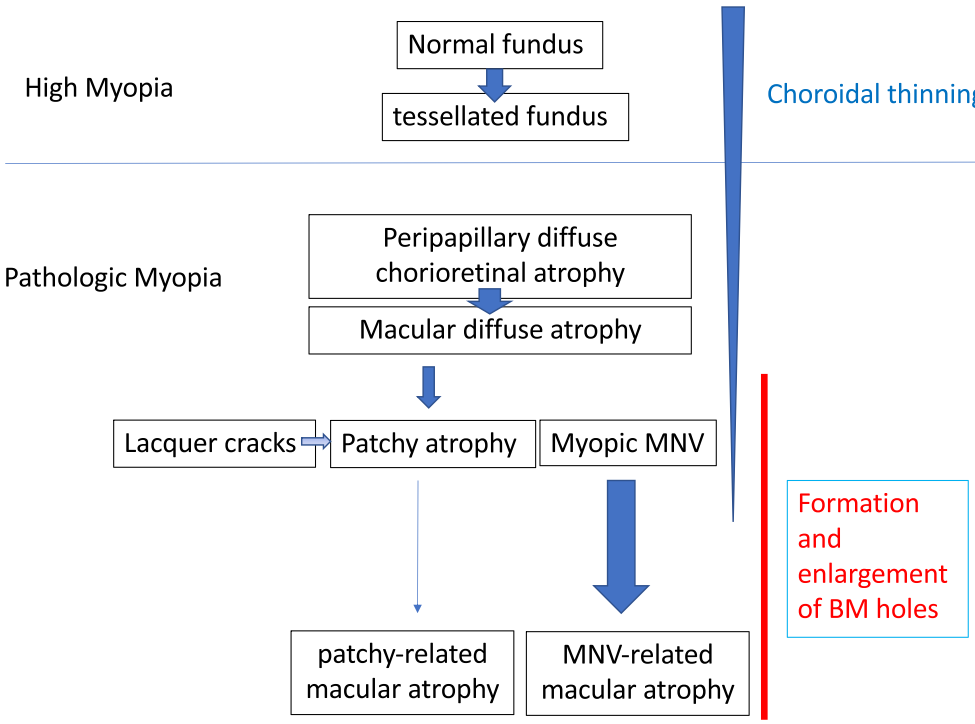

Figure 10. Diagram showing the progression patterns of high myopia to the different categories of pathologic myopia. Bruch's membrane, Bruch's membrane. Reproduced and modified with permission from Fang Y, Yokoi T, Nagaoka N, et al. Progression of myopic maculopathy during 18-year follow-up. *Ophthalmology*. 2018;125(6):863-877. © 2018 by the American Academy of Ophthalmology.

lesion in the posterior fundus of highly myopic eyes. The lesion is not uniformly yellow, but shows a granular appearance. However, the fundus color may look different according to the degree of fundus pigmentation among races. Diffuse choroidal atrophy primarily appear around the optic disc and increases with age and finally covers the entire posterior pole.[109] Thus, diffuse choroidal atrophy is subclassified to peripapillary diffuse choroidal atrophy (PDCA)[30] and macular diffuse choroidal atrophy (MDCA).[77] The frequency of diffuse atrophy increases with age as well as with an increase of axial length.[28,115] Tokoro el al.[115] found that diffuse atrophy usually occurred at around the age 40 and was observed in about 30% to 40% of patients after age 40. Recently, Liu et al.[28] adopted the META-PM classification to evaluate the frequency and distribution of the diffuse choroidal atrophy according to the age, axial length and the best-corrected visual acuity. In this large Chinese highly myopic cohort, the proportion of diffuse choroidal atrophy in age groups of 7 to 11, 12 to 18, 19 to 39, and more than 40 years old was 20.9%, 9.2%, 23.1%, and 52.9%, respectively. The incidence of diffuse choroidal atrophy increased with longer axial length, from 3.6% in eyes with an axial length of less than 26.50 mm to 62.8% in eyes with an axial length of 28.50 mm or greater.

Fluorescein angiography (FA) revealed a mild hyperfluorescence owing to tissue staining in the late phase of the angiogram.[109] On indocyanine green angiography (ICGA), a pronounced decrease of the choroidal capillaries and medium and large-size choroidal vessels can be seen in the area of diffuse atrophy. OCT shows a marked thinning of the choroid in the area of diffuse atrophy. The subfoveal choroidal thickness in eyes with macular diffuse atrophy is usually less than 100 µm and the mean choroidal thickness is 50 µm based on a clinic-based study.[7] In most cases, the choroid is almost absent, although it is sporadically present large choroidal vessels. Larger choroidal blood vessels can be observed to protrude to the retina. However, even in the area where most of the choroidal layer is absent, the RPE layer and outer retina are present. It might explain the relatively preserved vision in eyes with diffuse atrophy. With the use of OCTA, choriocapillaris flow impairment can be detected, even though the visualization of the choroidal circulation remains a challenge for interpretation in eyes with pathologic myopia. The OCTA in eyes with diffuse atrophy shows the low-density choriocapillaris, with the presence of medium and large choroidal vessels.[111,116] Although the choroid becomes thinned in eyes with a tessellated fundus, the degree of choroidal thinning is much more serious in eyes with diffuse atrophy[7] and such disproportionate thinning of choroid compared with the surrounding tissue (RPE, outer retina, and sclera) might be a key phenomenon in diffuse atrophy as well as pathologic myopia.

Patchy Choroidal Atrophy (Category 3). Patchy choroidal atrophy can be seen as a grayish-white, well-defined atrophy.[109] Owing to an absence of RPE and most of the choroid, the sclera can be observed through transparent retinal tissue. The median size of patchy atrophy was 1.73 mm^2, varying from 0.03 to 101.3 mm^2,[117] with the diameter of less than one or more lobules of the choriocapillaris. Pigment clumping is observed within the area of patchy atrophy, especially along the margin of the atrophy or along the large choroidal vessels. Abruptly emerging vessels are commonly observed within or near the edge of patchy atrophy, especially for those with large size.[118] Patchy atrophy was found in 10.5% of patients in a clinic-based Japanese highly myopic cohort.[117] The percentage of patchy atrophy increases linearly with age and reaches 32.5% after age 60 years.[115] The prevalence of patchy atrophy is 3.3% in eyes with an axial length from 27.0 to 27.9 mm, and exceeds 25% and 50% if the axial length is longer than 31 mm and 32 mm, respectively.[115] With time, the patchy atrophy enlarges and coalesces with each other.[77,98,119]

FA as well as ICGA show a choroidal filling defect in the area of patchy atrophy suggesting that this lesion is a complete closure of choriocapillaris.[109] Fundus autofluorescence shows hypoautofluorescence with distinct border owing to a loss of RPE in the area of patchy atrophy. Using OCT, patchy atrophy is characterized by the lack of RPE and outer retina with loss of most of choroid. Thus, the inner retinal layers have direct contact with the inner scleral surface. Swept source OCT also showed that discontinuities of Bruch's membrane in the area of patchy atrophy.[117,120] The RPE terminates outside of the margin of the macular Bruch membrane defect. Patchy atrophy could be regarded as a Bruch's membrane rupture, not solely an atrophy.

Patchy atrophy is subclassified into three types: patchy atrophy that develops from lacquer cracks P(Lc); patchy atrophy that develops within the area of an advanced diffuse chorioretinal atrophy P(D); and patchy atrophy which can be seen along the border of the posterior staphyloma.[98] The shape of patchy atrophy may help to differentiate these types, because P(D) is usually circular or elliptical and P(Lc) is often longitudinally oval. P(Lc) is considered an enlargement of Bruch's membrane defect owing to lacquer cracks, and P(D) might also represent a Bruch's membrane hole[121] developing within the area of advanced stage of diffuse atrophy.

Almost all eyes (95%) with patchy atrophy progressed after a mean follow-up of 18 years, in which an enlargement of the original patchy atrophy was found predominantly in 98% and new patchy atrophy was found in 47% followed by development of myopic MNV in 21.7% and patchy-related macular atrophy in 8.3%.[77] Miere et al.[122] also reported that all patchy atrophies had significantly enlarged over at least 12 months using quantitative measurement. Such high percentages of progression of eyes with patchy atrophy could be explained by the biomechanical properties of Bruch's membrane so that as soon as a defect is created, the Bruch's membrane defect would enlarge over time with ongoing axial elongation. However, it is uncommon for extrafoveal patchy atrophy to later involve the central fovea. This means that it is rare for patchy atrophy to cause the central vision loss although this lesion leads to a paracentral absolute scotoma[123] owing to a loss of photoreceptors within the atrophic area (Table 3).

Macular Atrophy (Category 4). Macular atrophy is a well-demarcated, grayish-white or whitish, atrophic lesion centered on the fovea. The imaging features are similar to those of patchy chorioretinal atrophy. The main difference between patchy atrophy and macular atrophy is its location relative to the central fovea. Based on the long-term follow-up observation, it is suggested that macular atrophy could be subclassified into MNV-related macular atrophy and patchy atrophy-related macular atrophy. MNV-related macular atrophy develops centered in the central fovea and enlarges toward the periphery, and patchy atrophy-related macular atrophy develops outside of the foveal area and enlarging, or coalescing with other patchy atrophies, into the foveal center.[77] The differentiation is mainly based on its morphologic features or is assisted by the history of MNV. The

Table 3. Summary of Phase III Clinical Trials Using Anti-VEGF Agents for Myopic Choroidal Neovascularization

Study	Treatment Groups	No. of Eyes	Mean BCVA Change at Study Primary End Point	Mean BCVA Change at Study Final Visit	Mean No. of Anti-VEGF Injections Over Study Period
RADIANCE[158]	Ranibizumab 0.5 mg guided by BCVA stabilization	106	+10.5 letters at month 3	+13.8 letters at month 12 month	4.6 ranibizumab injections over 12 months
	Ranibizumab 0.5 mg guided by disease activity	116	+10.6 letters at month 3	+14.4 letters at month 12 month	3.5 ranibizumab injections over 12 months
	vPDT then eligible to add ranibizumab 0.5 mg after month 3	55	+2.2 letters at month 3	+9.3 letters at month 12	2.4 ranibizumab injections from month 3 to 12
BRILLANCE[160]	Ranibizumab 0.5 mg guided by visual stabilization	182	+9.5 letters at month 3	+12.0 letters at month 12	4.6 ranibizumab injections over 12 months
	Ranibizumab 0.5 mg guided by disease activity	184	+9.8 letters at month 3	+13.1 letters at month 12	3.0 ranibizumab injections over 12 months
	vPDT then eligible to add ranibizumab after month 3	91	+4.5 letters at month 3	+10.3 letters at month 12	3.2 ranibizumab injections from month 3 to 12
MYRROR[161]	Aflibercept 2 mg	91	+12.1 letters at week 24	+13.5 letters at week 48	4.2 aflibercept injections over 48 weeks
	Sham followed by aflibercept 2 mg after week 24	31	–2.0 letters at week 24	+3.9 letters at week 48	3.0 aflibercept injections from week 24 to 48
SHINY[162]	Conbercept 0.5 mg	132	+12.0 letters at month 3	+13.3 letters at month 9	4.8 conbercept injections over 9 months
	Sham followed by conbercept 0.5 mg after month 3	44	+0.6 letters at month 3	+11.3 letters at month 9	3.6 conbercept injections from month 3 to 9

BCVA, best-corrected visual acuity.

majority of macular atrophy is an atrophic stage of MNV, with a very few percentages related to secondary foveal involvement by enlargement of patchy atrophy.

During an 18-year follow-up, loss of best-corrected visual acuity was associated with the development of MNV, MNV-related macular atrophy, and enlargement of MNV-related macular atrophy.[77] At the last visit, most of eyes with a best-corrected visual acuity of less than 0.1 (20/200) had macular atrophy.

Lacquer Cracks (Plus Lesion). Lacquer cracks can be detected as fine, irregular, yellow lines in and around the macula. They are considered to represent healed and mechanical breaks of the RPE, Bruch's membrane, and the choriocapillaris complex.[67,68] Multiple lacquer cracks can often be seen in branching and crisscrossing patterns. The prevalence of lacquer cracks ranged from 4.2% to 15.7% in highly myopic eyes in several cohorts.[27,67–69,124] Lacquer cracks can develop at a relatively early age in patients with pathologic myopia. Klein and Curtin[68] reported that the mean age of patients with lacquer cracks was 32 years with a range of 14 to 52 years. Previous studies also indicated that lacquer cracks occur most often in eyes with an axial length between 29.0 mm and 32.0 mm.[27,67–69,71,124–127]

The diagnosis of lacquer cracks is made based on multimodal imaging. ICGA is considered the gold standard for lacquer crack detection, observed as linear hypofluorescence in the late phase.[126] On FA, lacquer cracks show a consistent linear hyperfluorescence during the entire angiographic phase, a window defect owing to RPE atrophy overlying the defects of Bruch's membrane in the early phase and a staining of healed scar tissue filling the Bruch's membrane defect in the late phase. Fundus autofluorescence shows hypoautofluorescence, which is due to the atrophied RPE overlying the rupture. Lacquer cracks are easily overlooked on OCT because they are too narrow to detect. However, when the lesions are within the OCT scans, lacquer cracks appear as discontinuities of the RPE and increased transmission into the deeper tissue beyond the RPE.[71,127] OCTA shows partial defect of choriocapillaris in the region of lacquer cracks.[116]

Xu et al.[71] reported that 53.7% of eyes with lacquer cracks progressed during a mean follow-up of 3.5 years. Three progression patterns were found: increase in number (43.9%), elongation (9.8%), and progression to patchy atrophy (14.6%). The most common pattern was an increase in number of lacquer cracks. New lacquer cracks tend to occur perpendicularly from the existing lacquer cracks (branching) or in parallel with the existing lacquer cracks. An elongation of an existing lacquer crack is also seen in a small percentage of eyes. Lacquer cracks increase their width and progress to patchy atrophy. In some eyes, this progression is not a uniform widening of a pre-existing lacquer cracks, but small circular areas of patchy atrophy first develop along the lines of lacquer cracks, and then these circular areas enlarge and fuse with each other.

Although lacquer cracks are often observed in the vicinity of MNV,[108] it is unusual for MNV to develop secondarily from the existing lacquer cracks. This finding suggests that the lacquer cracks that are seen as yellowish linear lesions represent healed scar tissue. When lacquer cracks are newly formed, MNV might develop through the Bruch's membrane rupture. However, once the Bruch's membrane rupture is healed with scar tissue, a secondary MNV rarely occurs.

It is rare for lacquer cracks to develop across the central fovea itself. Thus, lacquer cracks themselves do not generally impair the central vision; however, the subretinal bleeding that develops at the onset of the rupture of Bruch's membrane could cause the impairment of central vision even after absorption of the hemorrhage (Table 2).

Myopic MNV (Plus Sign). MNV is a major cause of central vision impairment in pathologic myopia. It has been included as a plus sign in the META-PM classification. MNV included three phases: the active phase with proliferation of a fibrovascular membrane including MNV, exudation, and hemorrhage; the scar phase exemplified by a Fuchs spot; and the atrophic phase represented by MNV-related macular atrophy. Thus, Fuchs spots were not considered to be independent lesions and they were a scar phase of MNV. Further details are discussed in the section on Myopic MNV.

New Classification and Grading System. Although the META-PM classification is well-suited to identify various stages of myopic maculopathy, this classification is only based on fundus photographs that could lead to an accurate diagnosis of atrophic lesions because of the different visual presentations according to the degree of fundus pigmentation among races. In addition, other myopic macular lesions such as myopic traction maculopathy and dome-shaped macula were not included. Thus, an OCT-based classification has been developed.[7] Further details are discussed under the section on OCT-based Classification of Myopic Maculopathy.

Recently, Ruiz-Medrano et al.[128] also published a comprehensive review summarizing the main features of pathologic myopia and proposed a new classification system based on three key factors—atrophy, traction, and neovascularization—or the ATN classification system. This proposed classification system does not make any changes to the current atrophy classification (five categories in the META-PM classification). Tractional component is newly included containing five stages of inner or/and outer foveoschisis, foveal detachment, macular hole, and retinal detachment. Three plus signs in the META-PM classification are considered as neovascular components.

Progression of Myopic Maculopathy. Based on the META-PM classification, Fang et al.[77] conducted a retrospective case series study including 810 eyes of 432 highly myopic patients who had been followed for 10 or more years. After a mean follow-up of 18 years, the progression of myopic maculopathy was observed in 58.6% for all eyes, with 74.3% for eyes with pathologic myopia at baseline. The three most frequent progression patterns were (1) an extension of peripapillary diffuse atrophy to macular diffuse atrophy in diffuse atrophy, (2) an enlargement of the original atrophic lesion in patchy atrophy, and (3) the development of patchy atrophy in lacquer cracks. From two Chinese population-based longitudinal studies, the 10-year progression rate of myopic maculopathy was 35.5% in elderly Chinese (aged ≥40 years) (the Beijing Eye Study)[100] and the 5-year progression rate was also 35.3% in rural Chinese adult population (aged ≥30 years) (the Handan Eye Study).[129] In another large highly myopic Chinese cohort (the Zhongshan Ophthalmic Center-Brien Holden Vision Institute High Myopia Cohort Study), approximately 15% of 657 highly myopic eyes had progression of myopic maculopathy over 2 years.[130] Older age, longer axial length, and the presence of posterior staphyloma are the main factors associated with the development and progression of myopic maculopathy.

A Scheme Depicting the Progression Patterns of Myopic Maculopathy (Fig. 10). First, the progression

from category 0 (no myopic maculopathy) to category 1 (fundus tessellation) was not associated with a decrease in visual acuity. Although tessellation is not considered as pathologic myopia, a remarkable thinning of the choroid begins with the appearance of tessellation, which is the first sign of the progression of myopic maculopathy. Second, diffuse atrophy (category 2) primarily occurs in the peripapillary region (PDCA) and eventually extends into the macula (MDCA). Third, the eyes with patchy atrophy have a hole in the macular Bruch's membrane that either forms by an enlargement of lacquer cracks or develops in regions of advanced diffuse atrophy with a more vulnerable Bruch's membrane. Fourth, both patchy atrophy and macular atrophy (MNV related and patchy related) tend to enlarge with time. Fifth, macular atrophy is almost always MNV related, although patchy-related macular atrophy can occasionally occur.

Conclusion. The characteristics of each lesion of myopic maculopathy have been clarified by multimodal imaging with advanced technique. The wide use of the META-PM classification system allows researchers to perform direct comparisons across studies and provides a common tool for clinical trials and epidemiologic studies. Further studies targeting the pathogenesis of myopic maculopathy will be of benefit to find an effective treatment and finally impede the progression of myopic maculopathy.

Myopic MNV

Pathogenesis of Myopic MNV. The pathogenesis of myopic MNV is not understood fully, and several theories, such as the mechanical theory and the heredodegenerative theory have been proposed to explain the development of myopic MNV.[108,131–133] The background changes in an eye with pathologic myopia are believed to contribute to the pathogenesis of myopic MNV. These structural changes involve multiple layers of the eye, including the RPE, Bruch's membrane, choriocapillaris, and choroid, as well as the sclera, and are mostly driven by axial elongation. These changes can be observed clinically as an increasing severity of myopic macular degeneration. Specific lesions particularly associated with myopic MNV include lacquer cracks, patchy atrophy, and large myopic conus. Marked thinning of the choroid and loss of large choroidal vessels suggest that impaired choroidal perfusion may contribute to the development of progressive atrophy in a myopic macula.[134–136] Lacquer cracks are present in many eyes with myopic MNV and have been proposed to be an important predisposing lesion.[69] Lacquer cracks are believed to represent ruptures in Bruch's membrane and therefore mechanical stretching has been proposed as a potential underlying factor.[137] Alterations in the cytokine levels have also been described in eyes with pathologic myopia and may contribute to the pathogenesis of myopic MNV.[138] In eyes with myopic MNV, an increased VEGF level has been found in the aqueous humor compared with eyes undergoing cataract surgery.[139] There have also been a suggestion that genetic or hereditary factors may play a role in the development of myopic MNV.[48] Single nucleotide polymorphism in the complement factor I gene has been associated with myopic MNV.[48]

Diagnosis of Myopic MNV. The diagnosis of myopic MNV is based on clinical findings. Patients may present with blurring, scotoma, or distortion of vision. Upon ophthalmoscopy, features of pathologic myopia such as diffuse or patchy choroidal atrophy or myopic conus are usually present.[69,140] The myopic MNV typically appears as a flat, small, greyish subretinal lesion beneath, or in close proximity to, the fovea with or without hemorrhage.[4,108,131–133] SD-OCT is a useful screening tool because it is noninvasive and can be performed rapidly. On SD-OCT, myopic MNV presents as a highly reflective area contiguous above the RPE (type 2 MNV), usually with minimal subretinal fluid (SRF).

A clinical diagnosis of myopic MNV is usually confirmed by FA, which demonstrates the presence of the neovascularization, which appears as a well-defined hyperfluorescence in the early phase with leakage in the late phase in a classic MNV pattern. More recently, OCTA has been shown to detect myopic MNV noninvasively with high sensitivity and specificity.[141–143] The key advantage of OCTA lies in its noninvasive nature, which allows repeated scans to be performed at each visit. As such, some centers now accept the diagnosis of myopic MNV to be made by either form of angiography. However, because OCTA is a relatively new technology, users need to be aware of limitations including various artefacts and segmentation error.[144] A key limitation of OCTA is that activity cannot be assessed reliably based on OCTA alone. Interpreting OCTA together with structural OCT is therefore recommended to fully assess the presence, type, area, and activity of the MNV.

Assessment of Myopic MNV Activity. An accurate assessment of activity of MNV is important in determining when to start treatment and whether further treatment is no longer warranted. A demonstration of leakage in FA has been the gold standard for evaluating the activity of MNV.[133] However, FA cannot be repeated frequently owing to its invasiveness. Increasingly, SD-OCT has overtaken FA as the main modality for assessing activity, particularly during follow-up. During the active phase, myopic MNV typically appears as a dome-shaped, hyperreflective elevation above the RPE with ill-defined borders.[145] In addition, a lack of RPE coverage may also help to differentiate an active MNV from an inactive or scarred MNV.[146] SD-OCT is extremely useful in assessing features of coexisting myopic tractional maculopathy, which may be exacerbated by the treatment of MNV by anti-VEGF therapy.[147] Although OCTA may detect the area of neovascularization, it does not reflect the level of activity. Flow signal within the MNV often persists in the scar or atrophic phase of myopic MNV.

Differential Diagnoses. Differential diagnoses to consider for myopic MNV include a simple macular bleed in a highly myopic eye, which is often associated with lacquer cracks. Using FA, simple macular bleeding appears as blocked fluorescence only and high flow signal is absent in OCTA. On SD-OCT, simple bleeds appear as a projection of the hemorrhage along the Henle's fiber layer.[148] The late phase of ICGA is also useful to confirm the absence of MNV and for detecting coexisting lacquer cracks as linear hypofluorescences. Several inflammatory conditions may present with signs that can be confused with myopic MNV. The most common conditions are acute multifocal choroiditis and panuveitis, as well as punctate inner choroidopathy with or without secondary MNV.[4,133] In myopic individuals greater than 50 years of age, neovascular AMD may be confused with myopic MNV. Polypoidal lesions may arise at the edge of staphyloma or in eyes with tilted disc syndrome. Idiopathic MNV is diagnosed by excluding other causes; that is, it is a diagnosis of exclusion. Finally, serous detachment with or without neovascularization may occur in eyes with a dome-shaped maculopathy.

Treatment of Myopic MNV. The natural history of myopic MNV is generally poor without treatment.[149–151] In a 10-year follow-up study that evaluated the long-term visual outcome of myopic MNV without treatment, visual acuity was decreased significantly at 10 years, with the proportion of eyes having a visual acuity of 20/200 or less increasing from 29.6% to 88.9% and 96.3% at 5 and 10 years, respecrtively.[150] Therefore, the treatment of myopic MNV is warranted to prevent progressive visual loss.

Based on the Verteporfin in Photodynamic Therapy (VIP) Study,[152] verteporfin photodynamic therapy (vPDT) became the first approved treatment for myopic MNV as vPDT treated eyes had better mean best-corrected visual acuity compared with sham treatment. However, vPDT was unable to result in a gain in mean visual acuity at 2 years.[152] Moreover, vPDT also resulted in a significantly more frequent development of chorioretinal atrophy and significantly worse visual acuity compared with intravitreal anti-VEGF therapy.[153] Therefore in the era of anti-VEGF therapy, the standard-of-care treatment for myopic MNV is the use of intravitreal anti-VEGF therapy and vPDT is not recommended.[133,154–157]

The efficacy and safety of intravitreal anti-VEGF therapy for the treatment of myopic MNV has been evaluated in a number of large, phase III, multicenter, randomized, controlled clinical trials, including RADIANCE,[158,159] BRILLIANCE,[160] MYRROR,[161] and SHINY (Table 3).[162,163] Both the RADIANCE and BRILLIANCE studies evaluated the use of intravitreal ranibizumab 0.5 mg versus vPDT,[158–160] whereas MYRROR and SHINY compared the use of intravitreal aflibercept 2 mg and intravitreal conbercept 0.5 mg versus sham treatment, respectively.[161,162] Results from these randomized controlled trials have all demonstrated conclusively that intravitreal ranibizumab, aflibercept, and conbercept resulted in significant mean visual acuity gains in patients with myopic MNV at their primary end points with an excellent safety profile. These positive findings have led to approval of these anti-VEGF agents for the treatment of myopic MNV by various health authorities. The off-label use of intravitreal bevacizumab and ziv-aflibercept, which were originally designed to treat systemic neoplasia, have also been evaluated for treating myopic MNV and both agents have resulted in favorable visual acuity gains after treatment.[164–167] However, robust clinical trial data in using intravitreal bevacizumab or ziv-aflibercept for myopic MNV are lacking. The use of these anti-VEGF agents for myopic MNV should therefore be limited to patients with a lack of access to the on-label approved anti-VEGF agents.

In comparison with anti-VEGF treatment for MNV owing to neovascular AMD, the treatment burden in using anti-VEGF therapy for myopic MNV is considerably lower. The recommended treatment strategy in using intravitreal anti-VEGF therapy for myopic MNV is with a single initial injection followed by as-needed injection with regular monitoring using SD-OCT to assess for disease activity.[155,156] This strategy is based on the treatment protocols used in the ranibizumab disease activity-guided arms of the RADIANCE and BRILLIANCE studies[158,160] and in the aflibercept arm of the MYRROR study.[161] The effectiveness of this as-needed treatment approach has been evaluated in various real-world studies.[168,169] The prospective LUMINOUS study demonstrated in the real-world setting that ranibizumab for myopic MNV resulted in a mean visual improvement of 9.7 letters and 1.5 letters at 1 year in treatment-naïve and previously treated eyes, with a low mean number of ranibizumab injections of 3.0 and 2.6 injections over 12 months respectively.[168] Another large-scale prospective real-world study evaluating the use of ranibizumab for myopic MNV in Japan also demonstrated similar findings, with a mean improvement in the logMAR best-corrected visual acuity of 0.19 unit and a low mean number of 2.0 injections over 12 months.[169] The long-term results of the RADIANCE study also confirmed the favorable visual outcomes and low number of retreatment, with a mean visual acuity gain of 16.3 letters and 83% of patients required no further treatment for myopic MNV after up to 48 months of follow-up.[170]

Several studies have evaluated the prognostic factors associated with various treatment outcomes in using anti-VEGF therapy for myopic MNV.[159,171,172] A subgroup analysis of the RADIANCE study showed that ranibizumab treatment resulted in a significant visual acuity gain, regardless of the level of baseline age, ethnicity, lesion area, MNV location, severity of myopia, axial length, and presence or absence of SRF.[159] It was found that eyes with a larger baseline MNV lesion area required more injections over the study period compared with those with a smaller area.[159] A post hoc analysis of eyes in the MYRROR study also showed that the severity of myopic macular degeneration severity did not seem to influence the visual or anatomical outcomes after intravitreal aflibercept treatment for myopic MNV.[171] Another study showed that better visual acuity outcomes after ranibizumab or bevacizumab treatment might be associated with a shorter duration of symptoms, better baseline best-corrected visual acuity, and fundus autofluorescence pattern.[172]

One of the main issues concerning the long-term visual outcomes of myopic MNV after anti-VEGF therapy is the development of myopic MNV-related macular atrophy, which can result in a gradual loss of the visual acuity initially gained over the long run.[157,165] Because the current anti-VEGF therapy for myopic MNV only targets the angiogenesis process, future research efforts should therefore consider investigating methods to target macular atrophy associated with myopic MNV to achieve better long-term visual outcomes.

Myopic Traction Maculopathy

Pathogenesis. Myopic traction maculopathy includes a variety of pathologies secondary to tractional force on the retina in highly myopic eyes. Epiretinal membrane, lamellar hole, and many other conditions generating traction to the retina are included. Among myopic traction maculopathies, myopic foveoschisis is unique to pathological myopia and worth to learn as a specific complication. Because of the space limitation, this article will shed a light on this pathology. Myopic foveoschisis is referred to as a posterior retinal detachment without a macular hole in highly myopic eyes, first documented as a case report by Phillips in 1958.[173] Almost 40 years later, Takano and Kishi[174] found that retinoschisis and foveal detachment are common in highly myopic eyes in OCT. Myopic foveoschisis is characterized by various foveal architectural abnormalities, including a foveal cyst, a lamellar hole, and a foveal detachment.[175]

Typical OCT images of this disease showing split between inner and outer retina within posterior staphyloma have led to the hypothesis that the inner retina is less flexible than the outer retina.[176] Factors limiting the inner retinal flexibility include the vitreous cortex adhering to the retina, epiretinal membranes, internal limiting membrane (ILM), and retinal vessels. Preretinal membranes are often hard to recognize in high myopia, however it is present at the microscopic

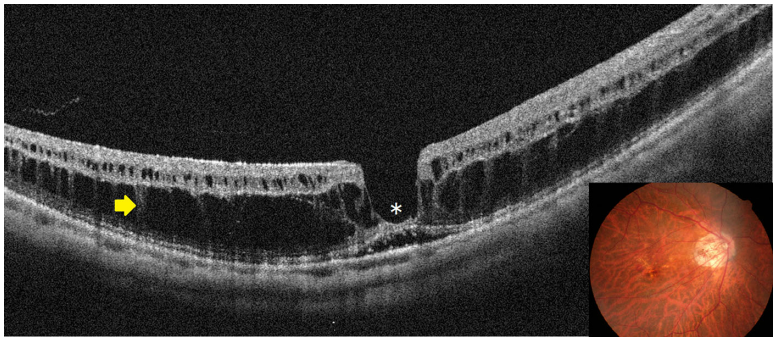

Figure 11. Typical appearance of myopic foveoschisis. The fundus photograph (inset) shows a slightly elevated retina at the posterior pole, although it is not clearly identifiable. A horizontal OCT scan involving the macula shows retinoschisis in multiple retinal layers and a retinal detachment at the fovea (*asterisk*). There is glial tissue bridging the inner and outer layers of the retinoschisis (a so-called column, *arrow*).

level.[177] Any or all of these factors can deteriorate the retinal flexibility.

Retinal detachment arising from a macular hole is a typical complication in highly myopic eyes. The vitreous cortex adhering to the retinal surface around the hole causes tangential traction that generates an inward vector component in deep staphyloma in highly myopic eyes, resulting in a retinal detachment.[178]

Assessment.

Symptoms. Patients are normally aware of central visual distortion corresponding with the involved area for retinoschisis and a relative scotoma for retinal detachment. Patients may be aware of an absolute scotoma at the center of the relative scotoma when a macular hole opens within a retinal detachment. Patients also report visual field loss at the involved area if an extensive retinal detachment is complicated. The Watzke–Allen test is usually negative for macular hole within the area of retinal detachment.

Fundus and OCT Appearance. Myopic foveoschisis can be recognized as a slight elevation of the posterior retina in highly myopic eyes; however, OCT is essential for accurate diagnosis especially in an atrophic fundus. OCT are essential not only for complete assessment of the retinal status but for surgical decision-making. Myopic foveoschisis presents with retinoschisis in multiple retinal layers (Fig. 11). The split retinal layers normally have a bridge between them, the so-called column, which is presumed to be residual Müller cells.[179] ILM separation from the other retinal layers can also be observed, a so-called ILM detachment (Fig. 12A), and is a good indicator of the tractional force from the ILM.[180] The tent-like peak of the inner retina is observed on the OCT image. This finding is coincident with retinal vessels and the so-called retinal microvascular traction, and more clearly observed after vitreous surgery with ILM peeling (Fig. 12B).[181] This tractional force to the retinal vessels are also observed as a paravascular microhole in highly myopic eyes.[182] The ellipsoid zone line of the photoreceptors sometimes disappears in the area of the retinal detachment;[183] however, the ellipsoid zone line is typically well preserved in the area of retinoschisis. This finding suggests that the photoreceptor function is well-preserved in this subtype.

Based on OCT appearance, there are two stages before macular hole formation associated with retinoschisis (Fig. 13). The first stage is the development of the retinoschisis type, in which only retinoschisis is present and not a retinal detachment (Fig. 13A).[176] Several months (sometimes several years) later, a retinal detachment begins around the fovea. This stage is the so-called foveal detachment type (Fig. 13B). After a while, the inner retina above the detachment is stretched and torn. This is how a macular hole appears as a consequence of retinoschisis with a retinal detachment.

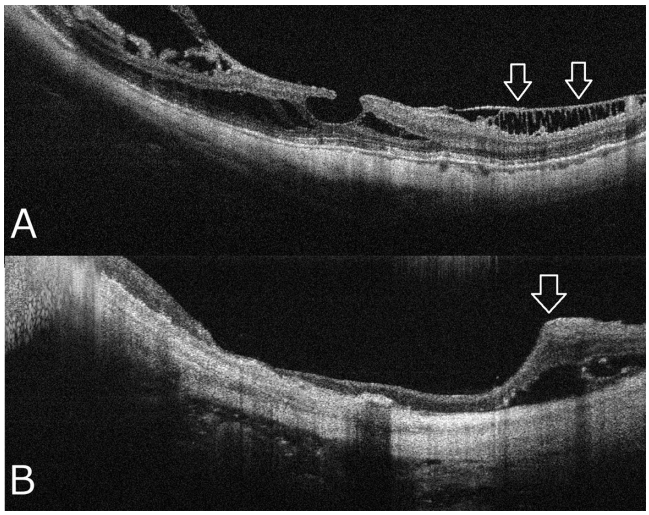

Figure 12. Representative OCT images specific high myopia. (**A**) an ILM detachment (arrows) shows that the ILM layer is detached from the other retinal layers owing to inflexibility of this layer. (**B**) Retinal microfolds (arrow) is associated with the retinal vessels showing microvascular traction on the retina.

There are two types of macular holes in highly myopic eyes. (Fig. 14)[184] One is the type with the edge of the hole thickened with retinal cysts (Fig. 14A). There is no retinal detachment around the hole clinically, and this type usually does not change for months or years. The other has surrounding retinoschisis instead of retinal cysts around the hole (Fig. 14B). This type of macular hole results from myopic foveoschisis and typically progresses rapidly because of underlying traction.

Treatment.

Surgical Indications and Results. Investigators have reported that the vision decreased in 69% of patients, a macular hole developed in 31% after 3 years of follow-up,[185] and in 50% of patients with retinoschisis a macular hole or retinal detachment developed after 2 years.[186] These

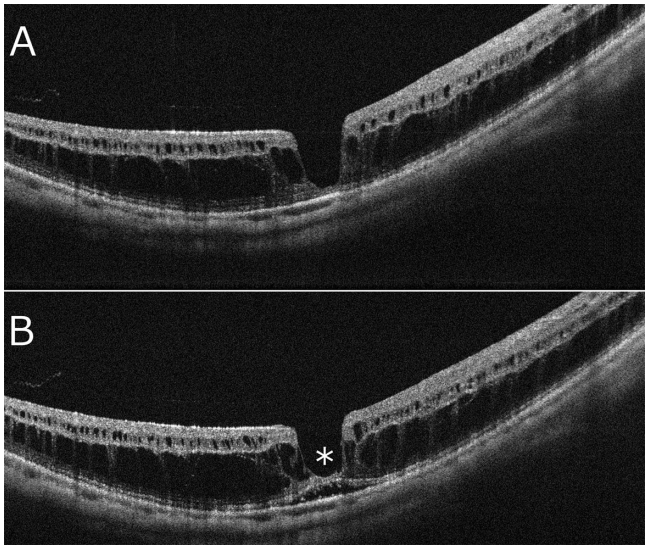

Figure 13. Time course and two distinct subtypes of myopic foveoschisis of the same patient shown in Fig 11. (**A**) The OCT image at the initial visit showing the retinoschisis type characterized by only retinoschisis without a retinal detachment. (**B**) One year later, the foveal detachment type occurs, which is characterized by a small localized retinal detachment (asterisk). The photoreceptors are separated from the RPE.

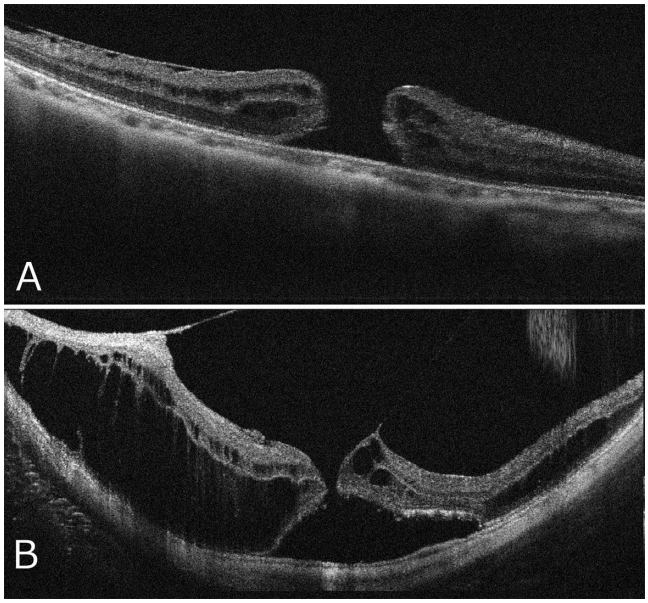

Figure 14. OCT appearance of two distinct subtypes in highly myopic macular holes. (**A**) A macular hole without retinoschisis has only retinal cysts and is normally stable, whereas (**B**) a macular hole with surrounding retinoschisis usually presents a higher likelihood of consequent retinal detachment.

observations encourage surgery on myopic foveoschisis to prevent more serious condition, namely, macular holes.

Asymptomatic myopic foveoschisis is not a good surgical indication because of a significant number of patients who suffer surgically induced visual decrease. The chance of visual improvement after surgery is much greater in cases with a foveal detachment than retinoschisis alone.[187,188] The chance of visual improvement is substantially smaller if a macular hole is present preoperatively.[187]

The mean visual acuity after vitrectomy for macular hole with retinal detachment was less than 20/200, and the initial reattachment rate was about 50% to 70% after vitrectomy.[189] Once a macular hole develops, the hole is difficult to close after vitrectomy in highly myopic eyes.[190] The macular hole closure rate with retinoschisis or retinal detachment is about 40% to 50% based on OCT images.[191] This difficulty probably arises because of the presence of posterior staphyloma for which the retina is extremely stretched. In fact, a longer axial length is generally a poor prognostic factor.[192]

Vitrectomy. The vitreous plays an important role; therefore, creating a posterior vitreous detachment is critical. To create posterior vitreous separation, a vitreous cutter and silicone-tipped backflush needle with active suction are normally used. Because multiple components such as vitreous cortex, epiretinal membrane, and ILMs are tightly adhering to the retinal surface,[193] a diamond-dusted membrane scraper facilitates to peel these extremely thin membranes. Importantly, great care is needed to separate the vitreous at the macula because of the risk of macular hole formation.

The necessity for ILM peeling remains controversial in myopic foveoschisis. However, the ILM is separated from the other retinal layers on OCT images in most eyes,[180] suggesting that the rigidity of the ILM plays a significant role. ILM peeling also can enhance macular hole closure and remove any traction on the retina in myopic macular holes with a retinal detachment and raises the success rate.[194] Indocyanine green or brilliant blue G are commonly used to stain the ILM selectively.

It is hypothesized that traumatic damage at the fovea induced by ILM peeling may cause full-thickness tissue loss at the fovea in myopic foveoschisis. This idea led to an attempt for surgeons to leave the foveal ILM. Recently, a nonfoveal ILM peeling technique was introduced to avoid macular holes.[195] So far, studies reported a significant reduction of the incidence of postoperative macular holes; however, the visual acuity level was similar even with a higher anatomic success rate.[196]

Macular holes in eyes with high myopia are much less likely to close. The inverted ILM flap technique was applied for highly myopic cases. The visual benefit has not been proven, especially in cases with retinal detachment; however, the macular hole closure rate seems to be higher than with the conventional ILM peeling technique.[197] A study using this inverted ILM flap technique has shown a significantly higher success rate than conventional peeling technique.[198] Autologous ILM[199] or partial thickness or full-thickness retinal transplants[200,201] have been reported recently to enhance the closure of myopic macular holes.

Because there is no coagulation maneuver around the macula, it is critical to support the retina for a long time to recover the integrity between the RPE and photoreceptors. It is preferred to use long-acting gas tamponade (i.e., perfluoropropane) to attain a greater anatomic success rate.[202] Silicone oil tamponade is also an effective option.[203]

Postoperative Complications. The opening of a macular hole occurs in between 10% and 20% of patients who underwent vitrectomy for myopic foveoschisis.[187] Cases in which ILM peeling was performed in the presence of an extremely thin, stretched fovea are at risk of developing this complication. We investigated the incidence of postoperative macular hole formation and looked for the risk factors.[204] A preoperative discontinuity of the ellipsoid zone line defect seen on

OCT was a predictor of macular hole development. Other factors, such as age, gender, and visual acuity, did not affect the rate of macular hole formation.

The recurrence of a retinal detachment is a major postoperative complication after vitrectomy for a macular hole with a retinal detachment. Removing residual vitreous cortex and epiretinal membranes is critical during a reoperation. However, it is sometimes difficult to identify the apparent cause of a re-detachment. In those cases, persistent traction, such as microvascular traction, might be responsible. Macular buckling can be considered in these cases. Macular buckling can compensate for any tractional force and showed a slightly higher initial reattachment rate than vitrectomy in eyes with a macular hole with a retinal detachment.[205,206]

Conclusion. With the advancement in ocular imaging technologies, the pathophysiology of myopic macular diseases has become better understood. A number of interesting findings have suggested the presence of underlying traction in highly myopic eyes. The preoperative features of these pathologies should be evaluated carefully, as these are important for decision-making and for assessing more effective surgical procedures in patients with myopic macular complications.

Dome-Shaped Macula

Definition and Clinical Features. In 2008, a French team reported a previously undescribed cause of visual loss in myopic patients that they have called dome-shaped macula.[207] It was characterized by an inward bulge of the macula within the chorioretinal posterior concavity of the eye. This macular bulge was hardly detectable on fundus biomicroscopy, and was mainly visualized by OCT. They have reported five unilateral and five bilateral cases, corresponding with 15 of the 140 myopic eyes in their database. The degree of refractive changes ranged between –2 D and –15 D. A visual loss was found in 11 eyes, with a median visual acuity of 20/50. The authors have also reported various degrees of changes in the RPE, including atrophy and pigment clumping, observed in all eyes. A focal fluorescein leakage was found in seven eyes, but MNV could be ruled out in all cases.[207] The finding has been confirmed by other authors in various countries and continents, allowing a better characterization of the condition. The prevalence of dome-shaped macula has been estimated at between 10.7% and 14.6% in the Chinese myopic population.[208,209] Most reported cases are adult patients, but the condition has also been reported in children and adolescents.[210] Mild-to-moderate myopia is usually reported, but the condition may also be observed in highly myopic eyes, in emmetropic eyes, and, less often, in hyperopic eyes.[211,212] Subtypes of dome-shaped macula have been identified depending on the dome shape: round (Fig. 15) or oval with a vertical (Fig. 16) or horizontal axis (Figs. 17 and 18).[213–215] In these studies, horizontal dome-shaped macula accounted for two-thirds to three-quarters of the cases. It is thus recommended to perform OCT B-scans along different axes to make the diagnosis of dome-shaped macula.

Multimodal Imaging. In the first descriptions, time-domain OCT was used and it was unable to demonstrate if the bulge was due to the sclera or not.[207,212] OCT has shown that the sclera was significantly thicker in the macular area in myopic eyes with dome-shaped macula compared with myopic eyes without dome-shaped macula,[216] whereas there was no difference in the scleral thickness outside the macular area. Thus, the authors have concluded that dome-shaped macula could be the result of a relatively localized change in the scleral thickness beneath the macula in their highly myopic patients. In another study, dome-shaped macula has been found to correspond to a ridge between two outward concavities within the posterior staphyloma.[217] Recently, 3D-MRI has allowed the reconstruction of the entire posterior pole in these eyes and has shown the presence of morphological changes in the entire posterior pole, with a band-shaped inward convexity that extended horizontally from the optic disc through the fovea in most eyes with a horizontal oval dome-shaped macula, and a round inward convexity of the macular area in most eyes with a round dome-shaped macula. This MRI study has also shown a high diversity in convexities that could be the border of a single staphyloma or multiple staphyloma areas.[209] The results from studies assessing the choroidal thickness are more controversial. A relatively thick choroid has been reported in some studies,[211,212] whereas other studies have reported a relatively thin choroid,[218] and a similar choroidal thickness has been found between eyes with and without dome-shaped macula with the same axial length in a comparative case study.[219] However, the mean central choroidal thickness seemed to be thicker than the choroid in the surrounding staphyloma, and the mean central choroidal thickness-to-mean perimacular choroidal thickness ratio seemed to be greater in dome-shaped macula eyes than in other myopic eyes with the same axial length.[220] Thus, a dome-shaped macula seems to be associated with a relatively thicker sclera and choroid at the bulge apex.

Pathogenesis. Dome-shaped macula has been suggested to be a possible compensatory mechanism in myopic anisometropia, after comparing the two eyes of a 49-year-old woman with mild myopic anisometropia.[221] However, little is known about the occurrence of the condition, which may be unilateral or bilateral. Ohno-Matsui et al.[222] have observed a peri dome choroidal deepening. Based on this finding, they have assumed that there might be a dome-induced inward push of the Bruch's membrane at the dome-shaped macula apex, leading to a compression of the subfoveal choroid. They have also observed Bruch's membrane defects in 20% of their studied eyes, suggesting the presence of Bruch's membrane strains on the dome's slopes.[222]

Course and Complications of a Dome-shaped Macula. Long-term studies have shown that the bulge height increases moderately over time.[218,219] This increased height has been shown to be associated with the extension of macular atrophic changes.[219] The scleral thickness slightly decreases over time, both in the fovea and in parafoveal areas.[218]

The main complication of dome-shaped macula is the occurrence of a macular serous retinal detachment (SRD). A macular SRD has been observed in all studies, but its incidence varies from 1.8% of cases in a Japanese cohort to 54% of cases in a French cumulative study.[214,220] A dome-shaped macula is considered a vision-threatening condition, accounting for most cases of visual loss. A SRD is more commonly observed when the bulge height is greater than 350 microns and in eyes with vertical oval dome-shaped macula.[213,223] The pathogenesis of SRD remains unknown but, it has recently been shown that the submacular choroidal blood flow measured on the OCTA B-scan is greater in eyes with SRF than in eyes without SRF.[220] Thus, the changes in the choroidal thickness at the

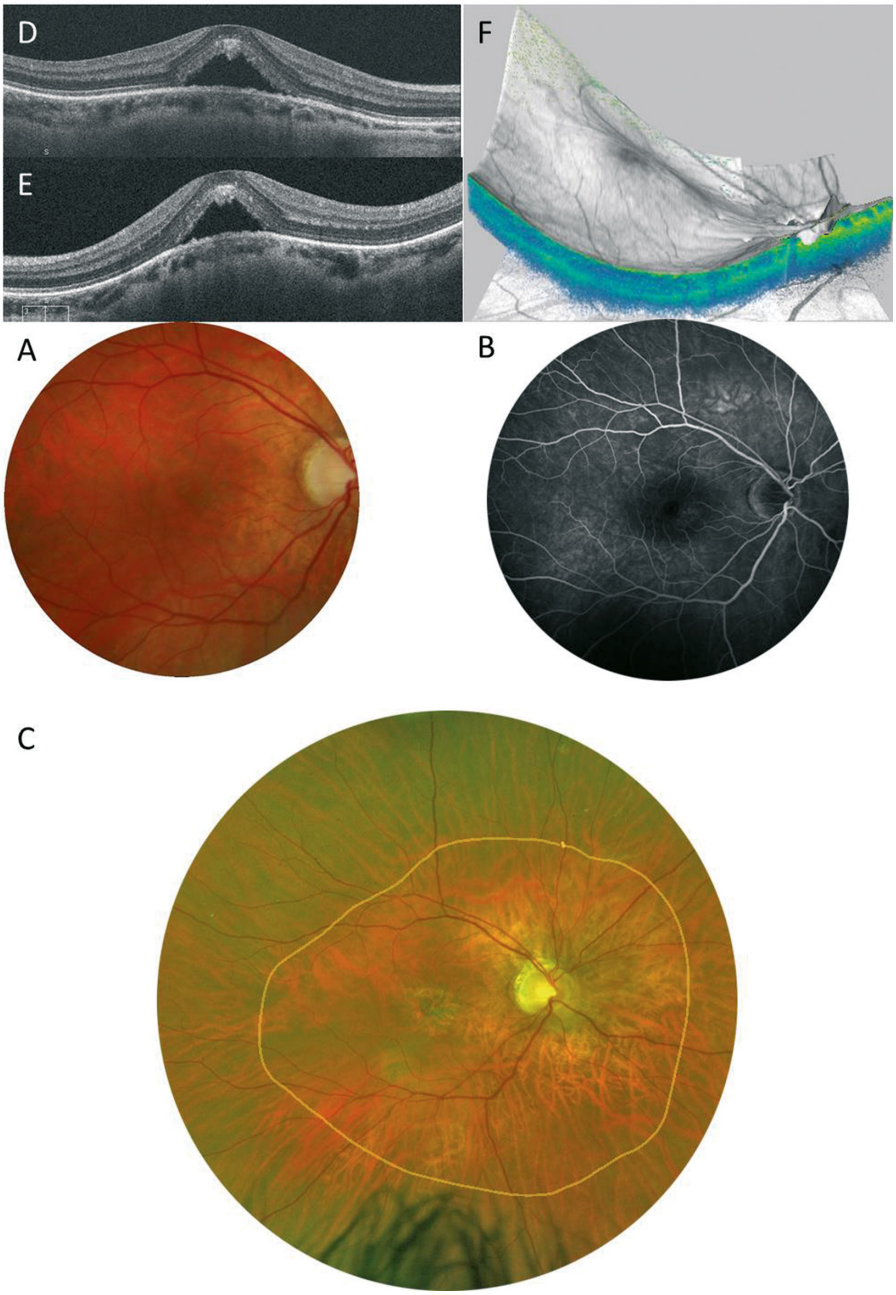

Figure 15. Round dome-shaped macula (DSM). The diagnosis of DSM may be challenging based on fundus examination (**A**, —). The border of the staphyloma (yellow line) appears on the wide-field color photo (**C**). FA (**B**) only shows a slight hyperfluorescence in the macula. The DSM is visible on both SD-OCT horizontal (**D**) and vertical (**E**) B-scans, which also reveal a serous macular detachment. The choroid is relatively thick in the subfoveal area. The 3D reconstruction of the macula (**F**, **G**) clearly shows the round inward bulge of the macula.

transition between the bulge and the staphyloma observed by different teams[217,224] may correspond with abrupt changes in choroidal blood flow, leading to outer blood–retina barrier failure and resulting in the occurrence of SRF. The spontaneous course of SRF is characterized by major changes in SRF height that may sometimes result in the complete resolution of the fluid.[225] The fluid resolution may also correspond with the development of RPE and outer retina atrophy in the macula.[219] Most studies of SRF associated with dome-shaped macula have shown a poorer visual acuity at baseline or during the follow-up[219,226] but in one study, a similar prognosis has been reported between eyes with and without SRF after a 2-year follow-up.[227]

Other reported complications include pigment epithelial detachment at the dome apex,[228] polypoidal choroidal vasculopathy,[229] and MNV that is more easily detected on OCTA.[228,230] A similar response of MNV to ranibizumab has been reported between eyes with and without dome-shaped macula in a comparative series[231] and in the RADIANCE trial.[232]

Differential Diagnosis. Dome-shaped macula and its complications are very similar to the inferior staphyloma commonly observed in eyes with tilted disc syndrome. Indeed, both conditions include a change in the eyeball curvature[233] that may lead to complications such as pigmentary changes, MNV, polypoidal choroidal vasculopathy, and

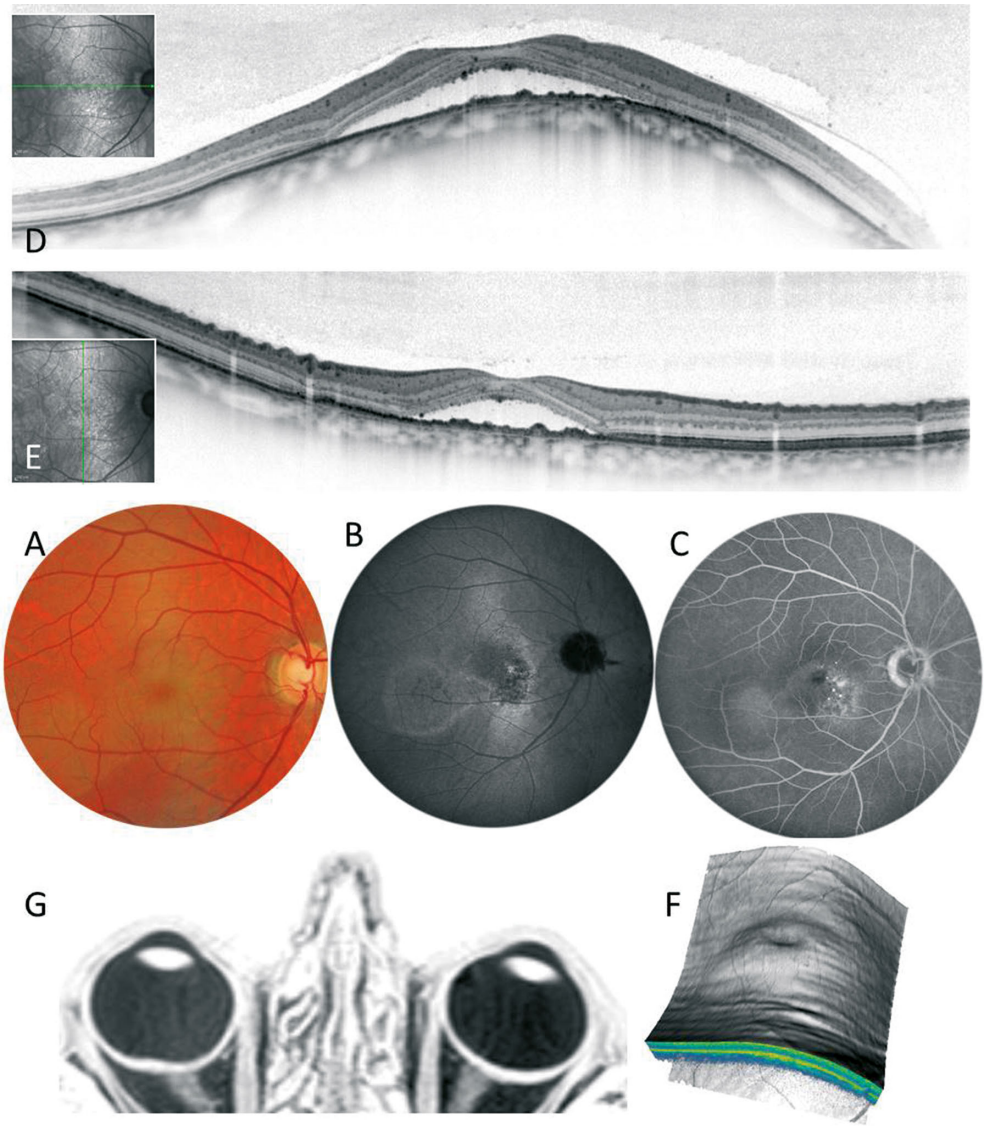

Figure 16. Vertical dome-shaped macula (DSM). Fundus examination (**A**) is not contributive. Fundus autofluorescence (**B**) shows a hypoautofluorescence revealing RPE atrophy in the macula, surrounded by hyperautofluorescent areas. FA shows an uneven hyperfluorescence with leaking points (**C**). The difference in curvature is obvious when comparing the OCT horizontal (**D**) and vertical (**E**) B-scans, or on the 3D reconstruction of the posterior pole (**F**). A SRD is present. MRI shows a macular focal thickening of the eye wall in the right eye (**G**, arrow).

SRF.[234–236] Similarities between these conditions have been highlighted in different studies,[237–239] and similar hypotheses have been suggested to explain the occurrence of SRF.[240] A condition close to dome-shaped macula called ridge-shaped macula has been recently described in younger patients (<20 years of age). It is characterized by a macular elevation in only one meridian across the fovea, observed in the horizontal direction across the vertical scan of OCT. In this study, no staphyloma and no Bruch's membrane defect were associated.[241]

Therapeutic Attempts. No treatment for dome-shaped macula is available currently. Its complications such as MNV or polypoidal choroidal vasculopathy should be treated promptly with anti-VEGF agents. Different therapies have been proposed for SRF complicating dome-shaped macula, including photodynamic therapy,[242,243] spironolactone,[244] aflibercept,[245] and topical carbonic anhydrase inhibitors.[246] A transient improvement has been observed after surgery for epiretinal membrane.[247] However, all studies were case reports or small series and no comparison with a control group was performed. To date, no effective treatment is available for SRF complicating dome-shaped macula.

Glaucoma

The definition of pathologic myopia as suggested by the META-PM Study Group describes the morphological abnormalities in the macular region of highly myopic eyes, while coexisting changes in the optic nerve head have been mostly omitted.[3] Optic nerve damage, however, relatively often coexists with maculopathy in eyes with pathologic myopia, and not quite rarely, it is an additional cause for visual field defects and vision impairment.[248–250] In population-based studies of various ethnicities, the increase in the prevalence of glaucomatous or glaucoma-like optic neuropathy occurred beyond a myopic refractive error of –8 D or an

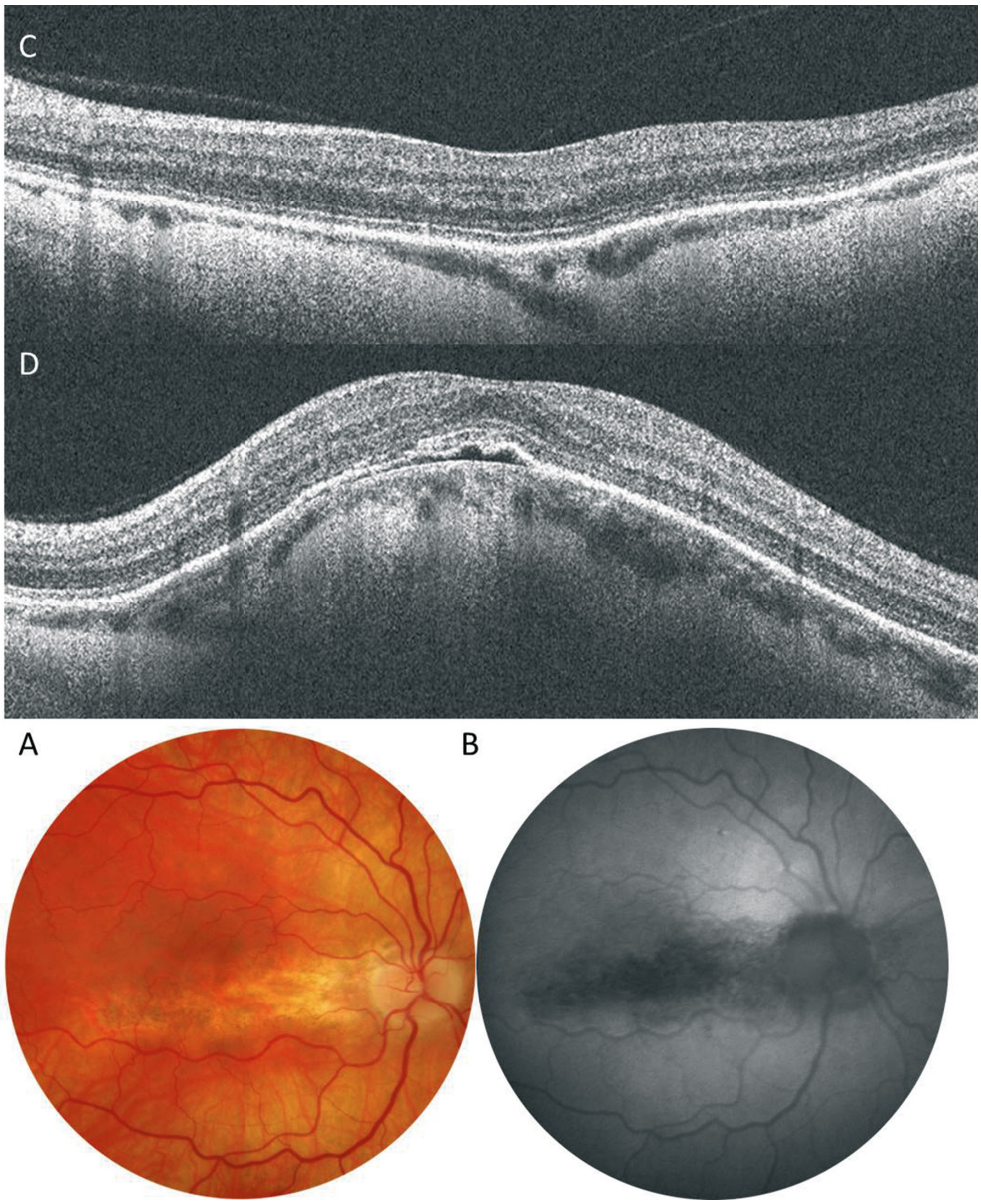

Figure 17. Horizontal dome-shaped macula (DSM). Fundus photography (**A**) and fundus autofluorescence (**B**) show a horizontal band of RPE atrophy. The horizontal (**C**) and vertical (**D**) B-scans show a horizontal DSM associated with a shallow SRD.

axial length of more than 26.5 mm.[248,250] It suggested that the prevalence of glaucoma in eyes with low to moderate levels of myopia or in eyes with an axial length shorter than 26.5 mm was similar to that for emmetropic eyes. The same values of a myopic refractive error of –8 D or an axial length of 26.5 mm were the cut-off values for the definition of high myopia, when an enlargement of the optic disc and parapapillary regions was used as biomarker for the presence of high myopia.[251,252]

For the diagnosis and for a better understanding of glaucoma in myopic eyes, the appearance of the optic nerve head is of great importance. The optic nerve head changes can be divided into those occurring in non–highly myopic eyes, and those in highly myopic eyes. In non–highly myopic eyes, the major change associated with axial elongation is the shifting of Bruch's membrane opening in spatial relationship to the lamina cribrosa, usually in direction to the macula.[253] Considering the optic nerve head being composed of three layers, the Bruch's membrane opening as the inner layer, the choroidal opening as the middle layer, and the opening in the peripapillary scleral flange with the lamina cribrosa as the outer layer, the Bruch's membrane opening shift into the temporal direction leads to an overhanging of Bruch's membrane into the intrapapillary region at the nasal optic disc margin, and to a lack of Bruch's membrane in the temporal parapapillary region. It explains the development of the parapapillary gamma zone that is usually located in the temporal to temporal inferior parapapillary region and that is defined by the absence of Bruch's membrane.[254–258] A hypothetical cause for the Bruch's membrane opening shift backward in direction to the macula may be a production of new Bruch's membrane in the equatorial region for axial elongation in the process of emmetropization and myopization.[93] As a sequel of the Bruch's membrane opening

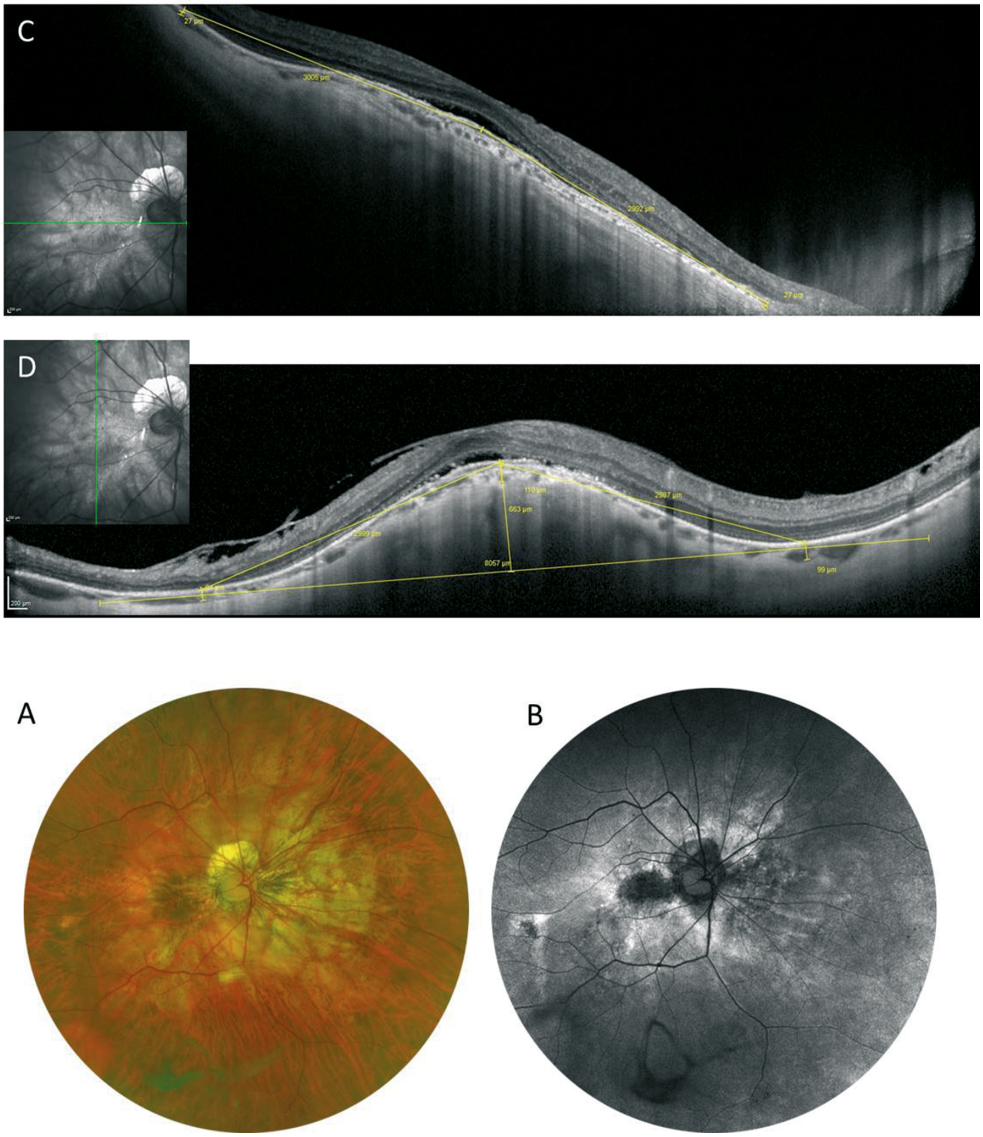

Figure 18. Horizontal dome-shaped macula (DSM). Fundus photography (**A**) and fundus autofluorescence (**B**) show RPE atrophy in the macula. The vertical (**C**) scan shows a horizontally oriented bulge. The sclera is thicker beneath the macula than at its periphery.

shift, occurring usually in the horizontal plane, the optic disc shape, as assessed on ophthalmoscopy, changes from a mostly circular shape to a vertical oval form. Another reason for the ophthalmoscopic change to a vertical optic disc shape is a perspective distortion of the ophthalmoscopic image of the optic disc, owing to the lateralization of the optic disc.[259] In non–highly myopic eyes, the size of the optic disc is not correlated significantly with the axial length of the refractive error.[260] Correspondingly, the size of the Bruch's membrane opening is not related to the axial length in non–highly myopic eyes.[253]

In high myopia, the size of the Bruch's membrane opening and of the optic disc (defined as the region with the lamina cribrosa as its bottom), and consequently the size of the lamina cribrosa, increase with longer axial length.[253,260] The enlargement of the Bruch's membrane opening leads to the development of a circular gamma zone, that is, the Bruch's membrane opening enlargement is more marked than the enlargement of the optic disc (and lamina cribrosa) is. In association with the enlargement of the optic disc and lamina cribrosa, the latter gets elongated and thinned. The lamina cribrosa thinning deceases the distance between the intraocular compartment with the IOP and the retrobulbar compartment with the orbital cerebrospinal fluid pressure.[261,262] Both pressures form the translaminar cribrosa pressure difference which is of high importance for glaucomatous optic neuropathy.[263,264] The decreased distance between both compartments leads to a steepening of the translaminar cribrosa pressure gradient what may be one of the reasons for the increased glaucoma susceptibility in highly myopic eyes.[248–250] Another reason for the increased glaucoma susceptibility may be morphological changes inside of the lamina cribrosa in association with its stretching.

In the parapapillary region, highly myopic eyes show, in addition to the gamma zone, the development and enlargement of the parapapillary delta zone.[258] The delta zone is the equivalent of an elongated (stretched) and

thinned peripapillary scleral flange (within the gamma zone).[265] The latter is the continuation of the inner portion of the posterior scleral into the lamina cribrosa, with the collagen fibers of the peripapillary border tissue of the scleral flange crisscrossing at the border of the scleral flange to the lamina cribrosa.[266] The peripapillary scleral flange forms the anterior border of the orbital cerebrospinal fluid space and is covered only by the peripapillary retinal nerve fiber layer.[265] It forms the biomechanical anchor for the lamina cribrosa.[267] The outer portion of the posterior sclera merges with the optic nerve dura mater, with the circular arterial circle of Zinn–Haller usually located at the merging line.[265] The arterial circle serves roughly as a ophthalmoscopic peripheral demarcation line of delta zone.[267] The axial elongation-associated lengthening of the peripapillary scleral flange thus leads to an increased distance between the arterial circle and the lamina cribrosa that is nourished by the branches of the arterial circle. The increased distance between the arterial circle and the lamina cribrosa may be a further reason for an increased vulnerability of the optic nerve head in high myopia.[248–250] Fitting with the role of the peripapillary scleral flange as the biomechanical anchor of the lamina cribrosa, a clinical study has suggested that a larger delta zone is associated with a higher prevalence of glaucomatous optic neuropathy in highly myopic eyes.[249] In a parallel manner, a larger optic disc was correlated with a higher glaucoma susceptibility, whereas in contrast the size of gamma zone was not significantly related to the prevalence of glaucoma.[249]

The importance of the peripapillary border tissues for the biomechanics of the optic nerve head and the glaucoma susceptibility has remained elusive so far. The peripapillary border tissue are differentiated into the peripapillary border tissue of the scleral flange (Elschnig) and the peripapillary border tissue of the choroid (Jacoby).[266] The first one is the continuation of the optic nerve pia mater and, as mentioned elsewhere in this article, crisscrosses with the fibers of the scleral flange when the flange continues into the lamina cribrosa. The second one is interposed between the peripapillary border tissue of the scleral flange (Elschnig) and the end of Bruch's membrane. It forms the border between the choroidal space and the intrapapillary prelaminar compartment.[266] Because the inner shells of the eye, that is, the uvea, Bruch's membrane, and the retina, are directly or indirectly connected to the outer ocular shell, that is, the sclera, only at the scleral spur anteriorly and through the peripapillary choroidal border tissue posteriorly, the latter may have biomechanical importance for the whole globe in general, and in particular for the connection between the inner ocular shells bearing the IOP and the lamina cribrosa. Owing to the development of the gamma zone, the distance between the end of Bruch's membrane and the optic border elongates.[266] It leads to a thinning of the peripapillary choroidal border tissue. It has been discussed that, in some highly myopic eyes, the choroidal border tissue may rupture, leading to a free Bruch's membrane end and a corrugation of Bruch's membrane in its vicinity.[268] The peripapillary border tissues may, thus, be of some importance for the increased glaucoma susceptibility in high myopia.

In agreement with the histologic findings and with observations made in population-based investigations, a recent clinical study revealed that the prevalence of glaucomatous optic neuropathy increased from approximately 12.0% in eyes with an axial length of less than 26.5 mm to 28.5% in eyes with an axial length of 26.5 mm or greater and less than 28.0 mm, to 32.6% in eyes with an axial length of 28 mm or greater and less than 29 mm, to 36.0% in eyes with an axial length of 29 mm or greater and less than 30 mm, and to 42.1% in eyes with an axial length of 30 mm or greater.[252] After adjusting for axial length, a higher glaucoma prevalence was correlated with a larger delta zone and a larger optic disc. These findings indicate that clinically a large optic disc and/or large delta zone should arouse the suspicion of a coexisting glaucomatous optic nerve damage in highly myopic eyes.

From a practical point of view, the detection of glaucomatous optic nerve damage gets more difficult with longer axial length. Axial elongation leads to a flattening of the physiological cup, so that the difference between the height of the neuroretinal rim and the bottom of the optic cup decreases, and makes the outlining of the cup/rim border more difficult.[269,270] In addition, the pinkish color of the neuroretinal rim is reduced, so that the color contrast between the rim and cup is decreased. The increased brightness of the parapapillary region, mainly owing to the gamma zone and delta zone, decreased the detectability of the retinal nerve fiber layer, and the occurrence of both zones make the detection of glaucoma-associated beta zone difficult. Also, highly myopic eyes with glaucomatous optic neuropathy tend to have an IOP within the normal range, and perimetric defects are often unspecific, because they may be caused by refractive abnormalities, myopic macular changes, and/or nonglaucomatous optic nerve damage.[271] The most important sign for the presence of glaucomatous optic nerve damage in highly myopic eyes may be the ophthalmoscopically detected intrapapillary vessel kinking relatively close to the disc border so that the inferior–superior–nasal–temporal rule of the shape of the neuroretinal rim is no longer fulfilled.[252,260]

The detection of glaucoma progression as compared with the detection of the presence of glaucoma is even more difficult, in particular in highly myopic eyes. Observation of changes in the outer visual field may perhaps help for the detection of glaucoma progression since most other psychophysical and morphometric techniques may fail.

Although glaucomatous optic neuropathy in highly myopic eyes can be defined by the intrapapillary vessel kinking relatively close to the optic disc border, studies are lacking that show the dependence of the effect of this optic nerve damage on the IOP.[271] One may therefore speak of glaucomatous or glaucoma-like optic neuropathy.[252] In addition, there may be a nonglaucomatous optic nerve damage in eyes with a large gamma zone on the temporal side. In a recent population-based study, a higher prevalence of high myopia or myopic maculopathy was correlated with a thinner retinal nerve fiber layer after exclusion of glaucomatous eyes.[250] It fits with clinical observations that highly myopic eyes without myopic maculopathy category III or IV and without a glaucoma-like optic nerve head could show a deep central scotoma. One may discuss that the elongated distance between the disc and fovea, caused by the enlargement of gamma zone, led to a stretching of the macular retinal ganglion cell axons and to their loss. Such a mechanism may mimic glaucomatous optic nerve damage. It has remained unclear whether a myopic traction maculopathy, with the inner limiting membrane lifting the retinal ganglion cell layer and thus relatively shortening the distance between the retinal ganglion cells and the optic disc, may be partially protective against such a nonglaucomatous optic nerve damage in highly myopic eyes. If that

concept is valid, it may be taken into account, if surgery of myopic maculopathy is considered.

In conclusion, the prevalence of glaucomatous optic neuropathy increases with a longer axial length in highly myopic eyes and can reach values of more than 50%. Glaucoma should therefore be ruled in for any highly myopic eye, in particular in those with a secondarily enlarged optic disc and a large parapapillary delta zone.

OCT-Based Classification of Myopic Maculopathy

OCT has dramatically improved our understanding of various retinal pathologies in last two decades. Recent advances in OCT technology, including enhanced depth imaging OCT and swept source OCT, provided the high-resolution images and highly reliable measurements of choroid in highly myopic eyes. It has been well-known that the choroid in high myopia is markedly thin.[7,87,112,113,136,272–286] All of the previous studies supported the theory that choroidal attenuation may have a great contribution to the pathogenesis of myopic maculopathy. In addition, swept source OCT revealed that patchy atrophy and myopic MNV-related macular atrophy were not simply an atrophy, but were a macular Bruch's membrane defect.[117,120,287] Furthermore, OCT enables to detect new macular lesions which were not identified by fundus photographs, such as myopic traction maculopathy and dome-shaped macula.

Although the META-PM classification is very useful, the diagnosis of diffuse atrophy relies solely on its yellowish appearance on ophthalmoscopy. However, the fundus color may look different according to the degree of fundus pigmentation among races, which could impact the accurate diagnosis of atrophic lesions. Earlier studies showed that diffuse atrophy was characterized by an extreme thinning of the choroid (almost absence of the entire choroid) in OCT images.[7,112,113,288] Thus, adding the choroidal thickness into the classification makes the diagnosis possible, objective, and more accurate. In addition, other myopic macular lesions that can only be diagnosed with OCT, such as myopic traction maculopathy and dome-shaped macula, can be included in the OCT-based classification of myopic maculopathy (Table 4).

Key OCT Features Determining Pathologic Myopia.

Extreme Choroidal Thinning. It is well-known that the choroid in highly myopic eyes is thinner compared with normal eyes.[7,87,112,113,136,272–286] In eyes with pathologic myopia (defined as myopic eyes equal to or more serious than diffuse atrophy), the thinning of the choroid is extreme. In many cases, almost the entire thickness of the choroid disappears with sporadically remaining large choroidal vessels.[7,288]

A marked thinning of the choroid starts temporal to the optic disc in childhood, as PDCA.[30] The presence of PDCA in children with high myopia is considered to be an indicator for the eventual development of advanced myopic maculopathy in later life.[30] On OCT images, PDCA in children is characterized by a profound and abrupt thinning of the choroid in the temporal parapapillary region.[289] The thinning of the choroid is abrupt and local; thus, it is critically different from a generalized impairment of choroidal circulation. Subsequently, Yokoi et al.[289] also compared the OCT finding between a hospital-based group of highly myopic children with PDCA and a population-based control group of children. It was shown that 76% of the PDCA group had a choroidal thickness at 2500 µm nasal to the foveola that was thinner than 60 µm, which was not found in the control group.[289] It indicated that this potential cut-off value of choroidal thickness may be helpful for the detection and diagnosis of PDCA in myopic children. With time, the area of extreme choroidal thinning enlarges and it is recognized as MDCA.[77]

Bruch's Membrane Holes. The defects of Bruch's membrane in the macular region were reported in a histologic study of highly myopic eyes.[121] These macular Bruch's membrane defects were accompanied by a complete loss of RPE and choriocapillaris and an almost complete loss of the outer and middle retinal layers and of the middle-sized choroidal vascular layer. Later, by using swept source OCT, Bruch's membrane defects were found in association with two different macular lesions specific to pathologic myopia, that is, with myopic MNV-related macular atrophy and with patchy atrophy.[117,120,287] These studies showed that patchy atrophy and MNV-related macular atrophy which had previously been considered to be chorioretinal atrophies were not simply an atrophy, but were a hole of Bruch's membrane.

Lacquer cracks are also considered to be breaks of Bruch's membrane; however, the defect is difficult to detect by OCT because the lesions tend to be too narrow. In some cases, lacquer cracks are observed as discontinuities of the RPE and increased hypertransmission into the deeper tissue beyond the RPE.[71,127]

Other Myopic Lesions (Myopic Traction Maculopathy and Dome-shaped Macula). Myopic traction maculopathy[290,291] and dome-shaped macula[207] are the most common complications related to pathologic myopia. OCT is an indispensable tool to diagnose both entities, although their presence can be suspected ophthalmoscopically in a few cases. Myopic traction maculopathy is generally defined by OCT examinations, including schisis-like inner retinal fluid, schisis-like outer retina fluid, foveal detachment, lamellar or full-thickness macular hole, and/or macular detachment.[292] Dome-shaped macula was initially described by Gaucher et al. using OCT as an inward bulge in the macular area within a staphyloma, which may be responsible for visual loss in myopic patients.[207] According to the following expanded definition, it can be diagnosed quantitatively as macular bulge height of greater than 50 µm in the most convex scan in either vertical or horizontal scan.[217]

Establishment of an OCT-Based Classification.

The Choroidal Thickness Profile in Myopic Maculopathy Is Different From Normal Fundus in Highly Myopic Eyes. There are three studies illustrating the relationship between the choroidal thickness and different lesions of myopic maculopathy based on META-PM classification (Fig. 19).[7,113,136] A clinic-based cross-sectional study was conducted for 1487 highly myopic eyes which were examined by swept source OCT.[7] In this study, the subfoveal choroid was the thickest in the horizontal scan in highly myopic eyes with normal fundus, which was the same pattern with non–highly myopic eyes.[293] In contrast, in eyes with myopic maculopathy, that is, being equal or more severe than a tessellated fundus, the temporal choroid was the thickest. In the vertical scan, the inferior choroid was the thinnest in the normal fundus, whereas in eyes with myopic maculopathy, the subfoveal choroid was the thinnest. This observation was also confirmed in vertical scan by another study comparing choroidal thickness in eyes with tessellated and normal fundus.[114] What is more, the distribution pattern

Table 4. OCT-based Classification of Myopic Maculopathy

Stage of MM	New Terminology	Details	Old Terminology
Ia	Peripapillary choroidal thinning	CT of <56.5 μm at 3000 μm nasal from the fovea, outside of gamma zone.	PDCA
Ib	Macular choroidal thinning	CT of <62 μm subfoveally.	MDCA
Plus sign	Linear Bruch's membrane defects	Yellowish linear lesions. Discontinuities of the RPE and increased hypertransmission into deeper tissues beyond the RPE in OCT image.	Lacquer cracks
II	Extrafoveal Bruch's membrane defects	Well-defined, grayish white, round lesion(s) in the macular, extrafoveal area. The Bruch's membrane defect is usually surrounded by a slightly wider RPE defect the size and shape of which determines the ophthalmoscopic size and shape of the lesion. In the region of the Bruch's membrane defect, the outer retinal layer, the RPE, the choriocapillaris and most of the medium-sized choroidal vessel layer are absent, and a medium-sized or large choroidal vessel may occasionally be present. The middle and inner retinal layers, more or less thinned, are in direct contact with the inner scleral surface	Patchy atrophy
Plus sign	Myopic CNV	CNV occurring in eyes with at least peripapillary or macular choroidal thinning	CNV
III	Foveal Bruch's membrane defect	The OCT-based histology is similar to the histology of extrafoveal Bruch's membrane defects.	Macular atrophy
IIIb	Foveal Bruch's membrane defect, CNV-related	Well-defined, round lesion including the fovea and expanding centrifugally around the fovea. The edges of the macular Bruch's membrane defect are often upturned. In the center, remnants of Bruch's membrane can be present, folded up in the process of the RPE-associated scar formation.	CNV-MA
IIIa	Foveal Bruch's membrane defects, patchy related	Develops outside of the foveal area and enlarges in direction to the fovea or coalesces with other extrafoveal Bruch's membrane defects in direction to the fovea.	Patchy MA
Plus sign	Macular traction maculopathy	Schisis-like inner retinal splitting, schisis-like outer retina splitting, foveal detachment, lamellar or full-thickness macular hole and/or macular detachment.	—
Plus sign	Dome-shaped macula and macular ridge	Dome-like, inward bulge of the RPE line in all meridians with a height of >50 um above a base line connecting the RPE lines on both side outside the dome.Macula ridge: Inward bulge of the RPE line in either horizontal or vertical scan with a height of >50 um above a base line connecting the RPE lines.	

CT, choroidal thickness; CNV, choroidal neovascularization; CNV-MA=choroidal neovascularization-related macular atrophy; Patchy MA, patchy atrophy-related macular atrophy.

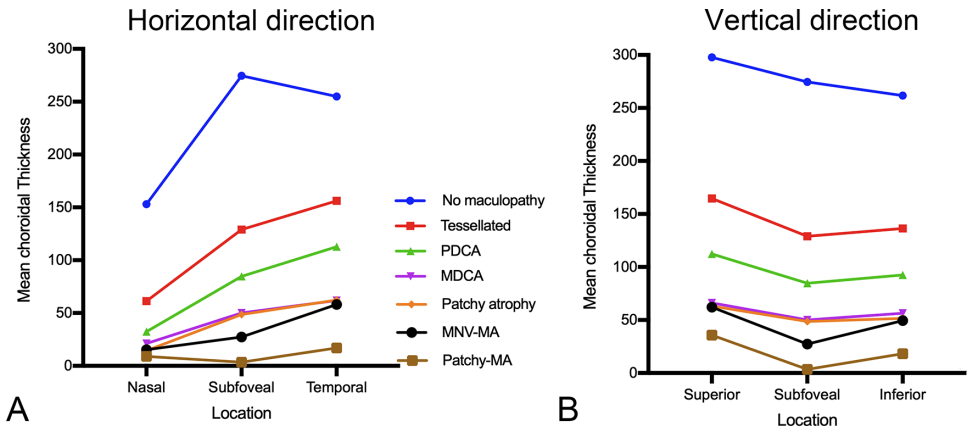

Figure 19. Graph showing the pattern of distribution of choroidal thickness (CT) at different locations for each type of myopic maculopathy in the horizontal (**A**) and in the vertical direction (**B**). The CT was measured at the subfoveal region and at 3 mm nasal, temporal, superior, and inferior to the fovea. MA = macular atrophy.

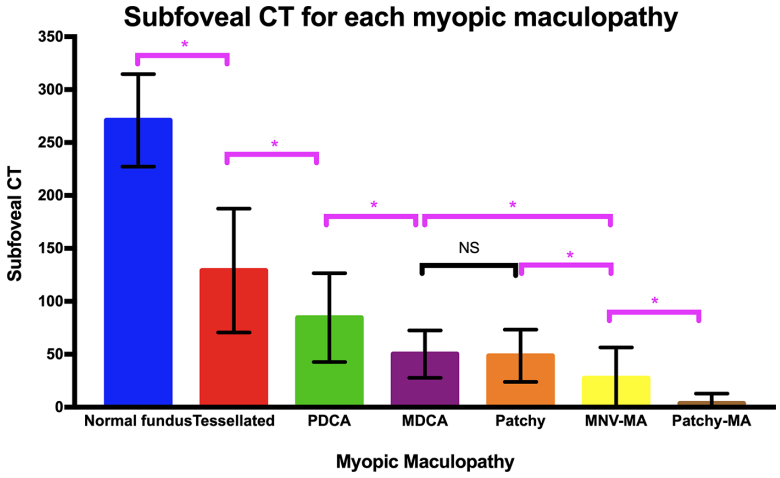

Figure 20. The subfoveal CT (mean with standard deviation) in each myopic maculopathy are shown. The CT decreased significantly from normal fundus to tessellated fundus, to PDCA, and to MDCA in all locations. There is no significant difference in choroidal thickness between eyes with MDCA and patchy atrophy. *$P < 0.05$. CT = choroidal thickness; MA = macular atrophy; NS = not significant.

of choroidal thickness in eyes with a tessellation was similar to the eyes with other myopic maculopathy in greater categories, such as, PDCA, MDCA, and patchy atrophy. This finding suggested that the tessellation might be the first sign for myopic eyes to become pathologic.

Progressive Choroidal Thinning From Tessellation to PDCA, and to MDCA, But Not Thereafter. It was shown that the mean subfoveal choroidal thickness in eyes with a normal fundus was 274.5 µm, tessellated fundus was 129.1 µm, PDCA was 84.6 µm, MDCA was 50.2 µm, patchy atrophy was 48.6 µm, MNV-related macular atrophy was 27.3 µm, and patchy-related macular atrophy was 3.5 µm (Fig. 20).[7] The choroidal thickness in all locations decreased from normal fundus to tessellated fundus, to PDCA, and to MDCA, as the severity of the myopic maculopathy increased. But there was no significant difference in choroidal thickness between eyes with MDCA and patchy atrophy in all locations except for those at nasally. Because the other two studies did not differentiate MDCA from PDCA, it is reasonable that the choroidal thickness in diffuse atrophy, which might include both PDCA and MDCA, was significantly thicker than those eyes with patchy atrophy.[113,136]

The subfoveal choroidal thickness of eyes with macular atrophy (both MNV related and patchy related or either of them) was significantly thinner than that in any other groups.[7] The subfoveal choroidal thickness in eyes with patchy-related macular atrophy was even thinner than choroidal thickness in MNV-related macular atrophy. It was noted that there was no difference among MNV-related macular atrophy, MDCA, and patchy atrophy in choroidal thickness at temporal, nasal, superior, and inferior locations.

The result from other two studies also indicated that the choroidal thickness was negatively correlated with severity of myopic maculopathy.[113,136] A high myopia clinic-based study from Zhongshan Ophthalmic Center[113] investigated the choroidal thickness in a large population. In this study, the median subfoveal choroidal thickness was 165 µm in normal fundus (C0), 80 µm in tessellated fundus (C1), 49 µm in diffuse atrophy (C2), 35 in patchy atrophy (C3), and 6.5 µm in macular atrophy (C4). It also showed that

the subfoveal choroidal thickness became significantly thinner with the increasing severity of maculopathy in C0 to C4 but the eyes with C3 to C4 shared similar parafoveal choroidal thickness, leading to the conclusion that C4 was not the result of progression from C3 which was consistent with long-term follow-up study by Fang et al.[77]

Cut-Off Value of Choroidal Thickness for Identifying PDCA and MDCA. Fang et al.[7] used a receiver operating characteristic curve and Youden's index to determine the optimal cut-off choroidal thickness value of 56.5 µm in nasal choroidal thickness (3000 µm from fovea) for the diagnosis of PDCA. The performance is particularly excellent in the less than 20 years of age group with a high sensitivity of 90% and a good specificity of 88%. The area under curve of choroidal thickness in each location became lower in the older age group. For the 60 to 79 years group, only the subfoveal choroidal thickness can be used for diagnosis.

The nasal choroidal thickness is not able to differentiate eyes with MDCA from those with PDCA. Instead, the choroidal thickness cut-off value of 62 µm at the subfovea (sensitivity, 71%; specificity, 72%), 73 µm at the temporal location (sensitivity, 67%; specificity, 90%), 83 µm at the superior location (sensitivity, 67%;specificity, 80%), 84.5 µm at the inferior location (sensitivity, 81%; specificity, 65%) can be used to define the eyes with MDCA.[7] Although the area under curve of subfoveal choroidal thickness is not the largest among all the locations, the cut-off value is still based on the subfoveal choroidal thickness, because the measurement at the fovea is easier to take and more accurate than the parafoveal points.

Summary of OCT-Based Classification of Myopic Maculopathy. Combining the hallmarks of myopic maculopathy in pathologic myopia, a new classification based on OCT findings has been proposed. In this new system, diffuse choroidal atrophy, for PDCA and MDCA, is suggested to be called "peripapillary choroidal thinning" and "macular choroidal thinning" (Table 3). Based on these results, the cut-off value of choroidal thickness as a diagnostic tool for diffuse atrophy has been added to this system. That is, peripapillary choroidal thinning is defined as a choroidal thickness of less than 56.5 µm at 3000 µm nasal from the fovea and macular choroidal thinning is defined as a choroidal thickness of less than 62 µm at the subfovea. Patchy atrophy and MNV-related macular atrophy are not simply owing to atrophy, but to holes in Bruch's membrane. Patchy atrophy is seen as a well-defined, grayish white lesion by fundus photograph seldomly involving the central fovea which is appropriate called as "extrafoveal Bruch's membrane defects" by OCT definition. In contrast, foveal Bruch's membrane defects is named for macular atrophy, that is, category 4 in the META-PM classification, for both MNV-related and patchy-related disease. In addition, myopic traction maculopathy and dome-shaped macula both as potential vision-threatening macular complications that only can be detected on OCT are also included in the OCT-based classification of myopic maculopathy.

Further studies are needed to validate whether the cut-off values of choroidal thickness from a single high myopia clinic can work well in clinical practice. More studies should investigate the role of the choroid in high myopia, not only by a measurement of the thickness, but also by examining other parameters, such as choroidal blood flow and the morphologic and vascular features of the choroid. Longitudinal studies on choroidal change will help us to depict a real-world picture of the choroidal changes in patients with high myopia.

Future Perspectives

Diagnostic methods as well as therapies have been greatly advancing for pathologic myopia. In particular, anti-VEGF therapies as well as vitreoretinal surgeries have improved the anatomical and visual outcomes of myopic MNV and myopic traction maculopathy. However, therapeutic approaches are not sufficient for other complications, such as choroidal atrophies and optic nerve damage. The diagnosis of glaucoma is difficult in eyes with pathologic myopia, because of a deformity of the optic disc appearance and the scotoma caused by myopic macular lesions and a large gamma zone. How to diagnose glaucoma in its early stage of patients with pathologic myopia needs to be established in the future, because the optic nerve damage is considered an important cause of blindness in pathologic myopia.

Posterior staphyloma causes a deformity of the area containing visually important tissues, namely, macula and the optic nerve. It is in contrast with most of the axial elongation in myopic eyes in general occurs in the equator of the eye. Thus, a formation of posterior staphyloma mechanically damages these nerve tissues. Before developing irreversible blinding complications, approaches to prevent and treat staphylomas are expected.

Finally, clarifying which genes are responsible for pathologic myopia (not high myopia) is important. With this information, it will finally become clear whether or not pathologic myopia is different from myopia in general. In addition, identifying children who will become pathologically myopic will be possible.

Based on the consistent definition of pathologic myopia and the objective detection of its major feature—posterior staphyloma—future studies regarding the global prevalence of pathologic myopia and its impact on vision and quality of life[294] should be undertaken.

Acknowledgments

The authors thank Monica Jong for facilitation of the process.

Supported by the International Myopia Institute. The publication costs of the International Myopia Institute reports were supported by donations from the Brien Holden Vision Institute, Carl Zeiss Vision, CooperVision, Essilor, and Alcon.

Disclosure: **K. Ohno-Matsui**, Santen (C), Nevakar (C); **P.-C. Wu**, None; **K. Yamashiro**, None; **K. Vutipongsatorn**, None; **Y. Fang**, None; **C.M.G. Cheung**, Novartis, Bayer, Roche, Topcon, Zeiss, Allergan, and Boehringer Ingelheim (F, C); **T.Y.Y. Lai**, Bayer Healthcare (C, F, R), Boehringer Ingelheim (C), Roche (C, F, R), Novartis (C, F, R); **Y. Ikuno**, Novartis Pharma (R); **S.Y. Cohen**, Allergan (C), Bayer (C), Novartis (C), Thea (C), Roche (C); **A. Gaudric**, None; **J.B. Jonas**, Europäische Patentanmeldung 16 720 043.5 and Patent application US 2019 0085065 A1 „Agents for use in the therapeutic or prophylactic treatment of myopia or hyperopia" (P)

References

1. Flitcroft DI, He M, Jonas JB, et al. IMI - defining and classifying myopia: a proposed set of standards for clinical and epidemiologic studies. *Invest Ophthalmol Vis Sci*. 2019;60:M20–M30.

2. Duke-Elder S. (ed) *Pathological Refractive Errors*. St. Louis: Mosby; 1970.
3. Ohno-Matsui K, Kawasaki R, Jonas JB, et al. International photographic classification and grading system for myopic maculopathy. *Am J Ophthalmol*. 2015;159:877–883.
4. Ohno-Matsui K, Lai TY, Lai CC, Cheung CM. Updates of pathologic myopia. *Prog Retin Eye Res*. 2016;52:156–187.
5. Moriyama M, Ohno-Matsui K, Hayashi K, et al. Topographic analyses of shape of eyes with pathologic myopia by high-resolution three-dimensional magnetic resonance imaging. *Ophthalmology*. 2011;118:1626–1637.
6. Wang NK, Wu YM, Wang JP, et al. Clinical characteristics of posterior staphylomas in myopic eyes with axial length shorter than 26.5 mm. *Am J Ophthalmol*. 2016;162:180–190.
7. Fang Y, Du R, Nagaoka N, et al. OCT-based diagnostic criteria for different stages of myopic maculopathy. *Ophthalmology*. 2019;126:1018–1032.
8. Wong TY, Ferreira A, Hughes R, Carter G, Mitchell P. Epidemiology and disease burden of pathologic myopia and myopic choroidal neovascularization: an evidence-based systematic review. *Am J Ophthalmol*. 2014;157:9–25.
9. Hsu WM, Cheng CY, Liu JH, Tsai SY, Chou P. Prevalence and causes of visual impairment in an elderly Chinese population in Taiwan: the Shihpai Eye Study. *Ophthalmology*. 2004;111:62–69.
10. Iwase A, Araie M, Tomidokoro A, et al. Prevalence and causes of low vision and blindness in a Japanese adult population: the Tajimi Study. *Ophthalmology*. 2006;113:1354–1362.
11. Xu L, Wang Y, Li Y, et al. Causes of blindness and visual impairment in urban and rural areas in Beijing: the Beijing Eye Study. *Ophthalmology*. 2006;113:1134.e1–11.
12. Klaver CC, Wolfs RC, Vingerling JR, Hofman A, de Jong PT. Age-specific prevalence and causes of blindness and visual impairment in an older population: the Rotterdam Study. *Arch Ophthalmol*. 1998;116:653–658.
13. Buch H, Vinding T, Nielsen NV. Prevalence and causes of visual impairment according to World Health Organization and United States criteria in an aged, urban Scandinavian population: the Copenhagen City Eye Study. *Ophthalmology*. 2001;108:2347–2357.
14. Cotter SA, Varma R, Ying-Lai M, Azen SP, Klein R, Los Angeles Latino Eye Study Group. Causes of low vision and blindness in adult Latinos: the Los Angeles Latino Eye Study. *Ophthalmology*. 2006;113:1574–1582.
15. World Health Organization (WHO). The impact of myopia and high myopia. Report of the Joint World Health Organization–Brien Holden Vision Institute Global Scientific Meeting on Myopia, University of New South Wales, Sydney, Australia, 16–18 March 2015. Geneva: World Health Organization; 2017. Licence: CC BY-NC-SA 3.0 IGO.
16. Asakuma T, Yasuda M, Ninomiya T, et al. Prevalence and risk factors for myopic retinopathy in a Japanese population: The Hisayama Study. *Ophthalmology*. 2012;119:1760–1765.
17. Gao LQ, Liu W, Liang YB, et al. Prevalence and characteristics of myopic retinopathy in a rural Chinese adult population: the Handan Eye Study. *Arch Ophthalmol*. 2011;129:1199–1204.
18. Vongphanit J, Mitchell P, Wang JJ. Prevalence and progression of myopic retinopathy in an older population. *Ophthalmology*. 2002;109:704–711.
19. Wong YL, Sabanayagam C, Ding Y, et al. Prevalence, risk factors, and impact of myopic macular degeneration on visual impairment and functioning among adults in Singapore. *Invest Ophthalmol Vis Sci*. 2018;59:4603–4613.
20. Liu HH, Xu L, Wang YX, Wang S, You QS, Jonas JB. Prevalence and progression of myopic retinopathy in Chinese adults: the Beijing Eye Study. *Ophthalmology*. 2010;117:1763–1768.
21. Xiao O, Guo X, Wang D, et al. Distribution and severity of myopic maculopathy among highly myopic eyes. *Invest Ophthalmol Vis Sci*. 2018;59:4880–4885.
22. Lin LL, Shih YF, Hsiao CK, Chen CJ. Prevalence of myopia in Taiwanese schoolchildren: 1983 to 2000. *Ann Acad Med Singap*. 2004;33:27–33.
23. Holden BA, Fricke TR, Wilson DA, et al. Global prevalence of myopia and high myopia and temporal trends from 2000 through 2050. *Ophthalmology*. 2016;123:1036–1042.
24. Healey PR, Mitchell P, Gilbert CE, et al. The inheritance of peripapillary atrophy. *Invest Ophthalmol Vis Sci*. 2007;48:2529–2534.
25. Bullimore MA, Brennan NA. Myopia control: why each diopter matters. *Optom Vis Sci*. 2019;96:463–465.
26. Verkicharla PK, Ohno-Matsui K, Saw SM. Current and predicted demographics of high myopia and an update of its associated pathological changes. *Ophthalmic Physiol Opt*. 2015;35:465–475.
27. Chang L, Pan CW, Ohno-Matsui K, et al. Myopia-related fundus changes in Singapore adults with high myopia. *Am J Ophthalmol*. 2013;155:991–999.e991.
28. Liu R, Guo X, Xiao O, et al. Diffuse chorioretinal atrophy in Chinese high myopia: the ZOC-BHVI high myopia cohort study. *Retina*. 2020;40:241–248.
29. Samarawickrama C, Mitchell P, Tong L, et al. Myopia-related optic disc and retinal changes in adolescent children from Singapore. *Ophthalmology*. 2011;118:2050–2057.
30. Yokoi T, Jonas JB, Shimada N, et al. Peripapillary diffuse chorioretinal atrophy in children as a sign of eventual pathologic myopia in adults. *Ophthalmology*. 2016;123:1783–1787.
31. Curtin BJ. The pathogenesis of congenital myopia. A study of 66 cases. *Arch Ophthalmol*. 1963;6:166–173.
32. Shih YF, Ho TC, Hsiao CK, Lin LL. Long-term visual prognosis of infantile-onset high myopia. *Eye (Lond)*. 2006;20:888–892.
33. Morgan I, Rose K. How genetic is school myopia? *Prog Retin Eye Res*. 2005;24:1–38.
34. Morgan IG, He M, Rose KA. Epidemic of pathologic myopia: what can laboratory studies and epidemiology tell us? *Retina*. 2017;37:989–997.
35. Tedja MS, Haarman AEG, Meester-Smoor MA, et al. IMI - myopia genetics report. *Invest Ophthal Vis Sci*. 2019;60:M89–M105.
36. Morgan IG, French AN, Ashby RS, et al. The epidemics of myopia: aetiology and prevention. *Prog Retin Eye Res*. 2018;62:134–149.
37. Wu PC, Huang HM, Yu HJ, Fang PC, Chen CT. Epidemiology of myopia. *Asia Pac J Ophthalmol (Phila)*. 2016;5:386–393.
38. Guan H, Yu NN, Wang H, et al. Impact of various types of near work and time spent outdoors at different times of day on visual acuity and refractive error among Chinese school-going children. *PLoS One*. 2019;14:e0215827.
39. Solouki AM, Verhoeven VJ, van Duijn CM, et al. A genome-wide association study identifies a susceptibility locus for refractive errors and myopia at 15q14. *Nat Genet*. 2010;42:897–901.
40. Verhoeven VJ, Hysi PG, Wojciechowski R, et al. Genome-wide meta-analyses of multiancestry cohorts identify multiple new susceptibility loci for refractive error and myopia. *Nat Genet*. 2013;45:314–318.
41. Kiefer AK, Tung JY, Do CB, et al. Genome-wide analysis points to roles for extracellular matrix remodeling, the

visual cycle, and neuronal development in myopia. *PLoS Genet*. 2013;9:e1003299.

42. Tedja MS, Wojciechowski R, Hysi PG, et al. Genome-wide association meta-analysis highlights light-induced signaling as a driver for refractive error. *Nat Genet*. 2018;50:834–848.
43. Hysi PG, Choquet H, Khawaja AP, et al. Meta-analysis of 542,934 subjects of European ancestry identifies new genes and mechanisms predisposing to refractive error and myopia. *Nat Genet*. 2020;52:401–407.
44. Hysi PG, Young TL, Mackey DA, et al. A genome-wide association study for myopia and refractive error identifies a susceptibility locus at 15q25. *Nat Genet*. 2010;42:902–905.
45. Fernandez-Robredo P, Maestre SR, Zarranz-Ventura J, Mulero HH, Salinas-Alaman A, Garcia-Layana A. Myopic choroidal neovascularization genetics. *Ophthalmology*. 2008;115:1632.e1631.
46. Nakanishi H, Gotoh N, Yamada R, et al. ARMS2/HTRA1 and CFH polymorphisms are not associated with choroidal neovascularization in highly myopic eyes of the elderly Japanese population. *Eye (Lond)*. 2010;24:1078–1084.
47. Akagi-Kurashige Y, Kumagai K, Yamashiro K, et al. Vascular endothelial growth factor gene polymorphisms and choroidal neovascularization in highly myopic eyes. *Invest Ophthal Vis Sci*. 2012;53:2349–2353.
48. Leveziel N, Yu Y, Reynolds R, et al. Genetic factors for choroidal neovascularization associated with high myopia. *Invest Ophthal Vis Sci*. 2012;53:5004–5009.
49. Miyake M, Yamashiro K, Nakanishi H, et al. Evaluation of pigment epithelium-derived factor and complement factor I polymorphisms as a cause of choroidal neovascularization in highly myopic eyes. *Invest Ophthal Vis Sci*. 2013;54:4208–4212.
50. Velazquez-Villoria A, Recalde S, Anter J, et al. Evaluation of 10 AMD associated polymorphisms as a cause of choroidal neovascularization in highly myopic eyes. *PLoS One*. 2016;11:e0162296.
51. Miyake M, Yamashiro K, Akagi-Kurashige Y, et al. Vascular endothelial growth factor gene and the response to anti-vascular endothelial growth factor treatment for choroidal neovascularization in high myopia. *Ophthalmology*. 2014;121:225–233.
52. Hayashi H, Yamashiro K, Nakanishi H, et al. Association of 15q14 and 15q25 with high myopia in Japanese. *Invest Ophthal Vis Sci*. 2011;52:4853–4858.
53. Oishi M, Yamashiro K, Miyake M, et al. Association between ZIC2, RASGRF1, and SHISA6 genes and high myopia in Japanese subjects. *Invest Ophthal Vis Sci*. 2013;54:7492–7497.
54. Wong YL, Hysi P, Cheung G, et al. Genetic variants linked to myopic macular degeneration in persons with high myopia: CREAM Consortium. *PLoS One*. 2019;14:e0220143.
55. Hosoda Y, Yoshikawa M, Miyake M, et al. CCDC102B confers risk of low vision and blindness in high myopia. *Nat Commun*. 2018;9:1782.
56. Miyake M, Yamashiro K, Akagi-Kurashige Y, et al. Analysis of fundus shape in highly myopic eyes by using curvature maps constructed from optical coherence tomography. *PLoS One*. 2014;9:e107923.
57. Wiesel TN, Raviola E. Myopia and eye enlargement after neonatal lid fusion in monkeys. *Nature*. 1977;266:66–68.
58. Fox JG, Barthold S, Davisson M, Newcomer CE, Quimby FW, Smith A, eds. *The Mouse in Biomedical Research: Normative Biology, Husbandry, and Models*. New York: Elsevier; 2006.
59. Qu J, Zhou X, Xie R, et al. The presence of m1 to m5 receptors in human sclera: evidence of the sclera as a potential site of action for muscarinic receptor antagonists. *Curr Eye Res*. 2006;31:587–597.
60. Barathi VA, Kwan JL, Tan QS, et al. Muscarinic cholinergic receptor (M2) plays a crucial role in the development of myopia in mice. *Dis Model Mech*. 2013;6:1146–1158.
61. Schaeffel F, Feldkaemper M. Animal models in myopia research. *Clin Exp Optom*. 2015;98:507–517.
62. Sundin OH. The mouse's eye and Mfrp: not quite human. *Ophthalmic Genet*. 2005;26:153–155.
63. Waldvogel JA. The bird's eye view. *Am Sci*. 1990;78:342–353.
64. Koch T. *Anatomy of the Chicken and Domestic Birds*. Ames: Iowa State University Press; 1973.
65. Coulombre AJ, Coulombre JL. The skeleton of the eye. II. Overlap of the scleral ossicles of the domestic fowl. *Dev Biol*. 1973;33:257–267.
66. Straznicky C, Chehade M. The formation of the area centralis of the retinal ganglion cell layer in the chick. *Development*. 1987;100:411–420.
67. Grossniklaus HE, Green WR. Pathologic findings in pathologic myopia. *Retina*. 1992;12:127–133.
68. Klein RM, Curtin BJ. Lacquer crack lesions in pathologic myopia. *Am J Ophthalmol*. 1975;79:386–392.
69. Ohno-Matsui K, Yoshida T, Futagami S, et al. Patchy atrophy and lacquer cracks predispose to the development of choroidal neovascularisation in pathological myopia. *Br J Ophthalmol*. 2003;87:570–573.
70. Curtin BJ, Karlin DB. Axial length measurements and fundus changes of the myopic eye. I. The posterior fundus. *Trans Am Ophthalmol Soc*. 1970;68:312–334.
71. Xu X, Fang Y, Uramoto K, et al. Clinical features of lacquer cracks in eyes with pathologic myopia. *Retina*. 2019;39:1265–1277.
72. Hirata A, Negi A. Lacquer crack lesions in experimental chick myopia. *Graefes Arch Clin Exp Ophthalmol*. 1998;236:138–145.
73. Tummala H, Ali M, Getty P, et al. Mutation in the guanine nucleotide-binding protein beta-3 causes retinal degeneration and embryonic mortality in chickens. *Invest Ophthalmol Vis Sci*. 2006;47:4714–4718.
74. Dhingra A, Ramakrishnan H, Neinstein A, et al. Gbeta3 is required for normal light ON responses and synaptic maintenance. *J Neurosci*. 2012;32:11343–11355.
75. Vincent A, Audo I, Tavares E, et al. Biallelic mutations in GNB3 cause a unique form of autosomal-recessive congenital stationary night blindness. *Am J Hum Genet*. 2016;98:1011–1019.
76. Montiani-Ferreira F, Kiupel M, Petersen-Jones SM. Spontaneous lacquer crack lesions in the retinopathy, globe enlarged (rge) chick. *J Comp Pathol*. 2004;131:105–111.
77. Fang Y, Yokoi T, Nagaoka N, et al. Progression of myopic maculopathy during 18-year follow-up. *Ophthalmology*. 2018;125:863–877.
78. Ohno-Matsui K, Tokoro T. The progression of lacquer cracks in pathologic myopia. *Retina*. 1996;16:29–37.
79. Spaide RF. *Staphyloma: part 1. Pathologic Myopia*. New York: Springer; 2014:167–176.
80. McBrien NA, Cornell LM, Gentle A. Structural and ultrastructural changes to the sclera in a mammalian model of high myopia. *Invest Ophthalmol Vis Sci*. 2001;42:2179–2187.
81. Avetisov ES, Savitskaya NF, Vinetskaya MI, Iomdina EN. A study of biochemical and biomechanical qualities of normal and myopic eye sclera in humans of different age groups. *Metab Pediatr Syst Ophthalmol*. 1983;7:183–188.
82. Curtin BJ, Iwamoto T, Renaldo DP. Normal and staphylomatous sclera of high myopia. An electron microscopic study. *Arch Ophthalmol*. 1979;97:912–915.

Investigative Ophthalmology & Visual Science

83. Ward B, Tarutta EP, Mayer MJ. The efficacy and safety of posterior pole buckles in the control of progressive high myopia. *Eye (Lond)*. 2009;23:2169–2174.
84. Gerinec A, Slezakova G. Posterior scleroplasty in children with severe myopia. *Bratisl Lek Listy*. 2001;102:73–78.
85. Momose A. Surgical treatment of myopia–with special references to posterior scleral support operation and radial keratotomy. *Indian J Ophthalmol*. 1983;31:759–767.
86. Curtin BJ, Whitmore WG. Long-term results of scleral reinforcement surgery. *Am J Ophthalmol*. 1987;103:544–548.
87. Zhou LX, Shao L, Xu L, Wei WB, Wang YX, You QS. The relationship between scleral staphyloma and choroidal thinning in highly myopic eyes: The Beijing Eye Study. *Sci Rep*. 2017;7:9825.
88. Takahashi H, Takase H, Terada Y, Mochizuki M, Ohno-Matsui K. Acquired myopia in Vogt-Koyanagi-Harada disease. *Int Ophthalmol*. 2019;39:521–531.
89. Xu X, Fang Y, Yokoi T, et al. Posterior staphylomas in eyes with retinitis pigmentosa without high myopia. *Retina*. 2019;39:1299–1304.
90. Curcio CA, Johnson M. Structure, function, and pathology of Bruch's membrane. *Retina*. 2013;1:466–481.
91. Tanaka Y, Shimada N, Ohno-Matsui K. Extreme thinning or loss of inner neural retina along the staphyloma edge in eyes with pathologic myopia. *Am J Ophthalmol*. 2015;159:677–682.
92. Jonas JB, Panda-Jonas S. Secondary Bruch's membrane defects and scleral staphyloma in toxoplasmosis. *Acta Ophthalmol*. 2016;94:e664–e666.
93. Jonas JB, Ohno-Matsui K, Jiang WJ, Panda-Jonas S. Bruch membrane and the mechanism of myopization: a new theory. *Retina*. 2017;37:1428–1440.
94. Cases O, Joseph A, Obry A, et al. Foxg1-Cre mediated Lrp2 inactivation in the developing mouse neural retina, ciliary and retinal pigment epithelia models congenital high myopia. *PLoS One*. 2015;10:e0129518.
95. Kantarci S, Al-Gazali L, Hill RS, et al. Mutations in LRP2, which encodes the multiligand receptor megalin, cause Donnai-Barrow and facio-oculo-acoustico-renal syndromes. *Nat Genet*. 2007;39:957–959.
96. Schrauwen I, Sommen M, Claes C, et al. Broadening the phenotype of LRP2 mutations: a new mutation in LRP2 causes a predominantly ocular phenotype suggestive of Stickler syndrome. *Clin Genet*. 2014;86:282–286.
97. Ohno-Matsui K, Akiba M, Moriyama M, Ishibashi T, Tokoro T, Spaide RF. Imaging retrobulbar subarachnoid space around optic nerve by swept-source optical coherence tomography in eyes with pathologic myopia. *Invest Ophthalmol Vis Sci*. 2011;52:9644–9650.
98. Hayashi K, Ohno-Matsui K, Shimada N, et al. Long-term pattern of progression of myopic maculopathy: a natural history study. *Ophthalmology*. 2010;117:1595–1611.
99. Ohno-Matsui K, Jonas JB. Posterior staphyloma in pathologic myopia. *Prog Retin Eye Res*. 2019;70:99–109.
100. Yan YN, Wang YX, Yang Y, et al. Ten-year progression of myopic maculopathy: the Beijing Eye Study 2001-2011. *Ophthalmology*. 2018;125:1253–1263.
101. Moriyama M, Ohno-Matsui K, Modegi T, et al. Quantitative analyses of high-resolution 3D MR images of highly myopic eyes to determine their shapes. *Invest Ophthalmol Vis Sci*. 2012;53:4510–4518.
102. Ohno-Matsui K. Proposed classification of posterior staphylomas based on analyses of eye shape by three-dimensional magnetic resonance imaging. *Ophthalmology*. 2014;121:1798–1809.
103. Curtin BJ. The posterior staphyloma of pathologic myopia. *Trans Am Ophthalmol Soc*. 1977;75:67–86.
104. Shinohara K, Shimada N, Moriyama M, et al. Posterior staphylomas in pathologic myopia imaged by widefield optical coherence tomography. *Invest Ophthalmol Vis Sci*. 2017;58:3750–3758.
105. Tanaka N, Shinohara K, Yokoi T, et al. Posterior staphylomas and scleral curvature in highly myopic children and adolescents investigated by ultra-widefield optical coherence tomography. *PLOS One* 2019;14:e0218107.
106. Shinohara K, Tanaka N, Jonas JB, et al. Ultra-widefield optical coherence tomography to investigate relationships between myopic macular retinoschisis and posterior staphyloma. *Ophthalmology*. 2018;125:1575–1586.
107. Takahashi H, Tanaka N, Shinohara K, et al. Ultra-widefield optical coherence tomographic imaging of posterior vitreous in eyes with high myopia. *Am J Ophthalmol*. 2019;206:102–111.
108. Avila MP, Weiter JJ, Jalkh AE, Trempe CL, Pruett RC, Schepens CL. Natural history of choroidal neovascularization in degenerative myopia. *Ophthalmology*. 1984;91:1573–1581.
109. Tokoro T (ed) *Atlas of Posterior Fundus Changes in Pathologic Myopia*. Tokyo: Springer-Verlag; 1998:5–22.
110. Kobayashi K, Ohno-Matsui K, Kojima A, et al. Fundus characteristics of high myopia in children. *Jpn J Ophthalmol*. 2005;49:306–311.
111. Wong YL, Ding Y, Sabanayagam C, et al. Longitudinal changes in disc and retinal lesions among highly myopic adolescents in Singapore over a 10-year period. *Eye Contact Lens*. 2018;44:286–291.
112. Wang NK, Lai CC, Chu HY, et al. Classification of early dry-type myopic maculopathy with macular choroidal thickness. *Am J Ophthalmol*. 2012;153:669–677.
113. Zhao X, Ding X, Lyu C, et al. Morphological characteristics and visual acuity of highly myopic eyes with different severities of myopic maculopathy. *Retina*. 2018;38:462–470.
114. Zhou Y, Song M, Zhou M, Liu Y, Wang F, Sun X. Choroidal and retinal thickness of highly myopic eyes with early stage of myopic chorioretinopathy: ressellation. *J Ophthalmol*. 2018;2018:2181602.
115. Tokoro T. *Explanatory Factors of Chorioretinal Atrophy. Atlas of Posterior Fundus Changes in Pathologic Myopia*. Tokyo: Springer; 1998:23–50.
116. Sayanagi K, Ikuno Y, Uematsu S, Nishida K. Features of the choriocapillaris in myopic maculopathy identified by optical coherence tomography angiography. *Br J Ophthalmol*. 2017;101:1524–1529.
117. Du R, Fang Y, Jonas JB, et al. Clinical features of patchy chorioretinal atrophy in pathologic myopia. *Retina*. 2019;40:951–959.
118. Xie S, Fang Y, Du R, et al. Abruptly emerging vessels in eyes with myopic patchy chorioretinal atrophy. *Retina*. 2019;40:1215–1223.
119. Curtin BJ. Ocular findings and complications. In: Curtin BJ (ed), *The Myopias*. New York: Harper and Row; 1985:277–347.
120. Ohno-Matsui K, Jonas JB, Spaide RF. Macular Bruch membrane holes in highly myopic patchy chorioretinal atrophy. *Am J Ophthalmol*. 2016;166:22–28.
121. Jonas JB, Ohno-Matsui K, Spaide RF, Holbach L, Panda-Jonas S. Macular Bruch's membrane defects and axial length: association with gamma zone and delta zone in peripapillary region. *Invest Ophthalmol Vis Sci*. 2013;54:1295–1302.
122. Miere A, Capuano V, Serra R, Jung C, Souied E, Querques G. Evaluation of patchy atrophy secondary to high myopia by semiautomated software for fundus autofluorescence analysis. *Retina*. 2018;38:1301–1306.

Investigative Ophthalmology & Visual Science

123. Lo J, Poon LY, Chen YH, et al. Patchy scotoma observed in chorioretinal patchy atrophy of myopic macular degeneration. *Invest Ophthalmol Vis Sci*. 2020;61:15.
124. Curtin BJ, Karlin DB. Axial length measurements and fundus changes of the myopic eye. *Am J Ophthalmol*. 1971;71:42–53.
125. Wang NK, Lai CC, Chou CL, et al. Choroidal thickness and biometric markers for the screening of lacquer cracks in patients with high myopia. *PLoS One*. 2013;8:e53660.
126. Ohno-Matsui K, Morishima N, Ito M, Tokoro T. Indocyanine green angiographic findings of lacquer cracks in pathologic myopia. *Jpn J Ophthalmol*. 1998;42:293–299.
127. Liu CF, Liu L, Lai CC, et al. Multimodal imaging including spectral-domain optical coherence tomography and confocal near-infrared reflectance for characterization of lacquer cracks in highly myopic eyes. *Eye (Lond)*. 2014;28:1437–1445.
128. Ruiz-Medrano J, Montero JA, Flores-Moreno I, Arias L, Garcia-Layana A, Ruiz-Moreno JM. Myopic maculopathy: Current status and proposal for a new classification and grading system (ATN). *Prog Retin Eye Res*. 2018;69:80–115.
129. Lin C, Li SM, Ohno-Matsui K, et al. Five-year incidence and progression of myopic maculopathy in a rural Chinese adult population: the Handan Eye Study. *Ophthalmic Physiol Opt*. 2018;38:337–345.
130. Li Z, Liu R, Xiao O, et al. Progression of myopic maculopathy in highly myopic Chinese eyes. *Invest Ophthalmol Vis Sci*. 2019;60:1096–1104.
131. Wong TY, Ohno-Matsui K, Leveziel N, et al. Myopic choroidal neovascularisation: current concepts and update on clinical management. *Br J Ophthalmol*. 2015;99:289–296.
132. Neelam K, Cheung CM, Ohno-Matsui K, Lai TY, Wong TY. Choroidal neovascularization in pathological myopia. *Prog Retin Eye Res*. 2012;31:495–525.
133. Lai TY, Cheung CM. Myopic choroidal neovascularization: diagnosis and treatment. *Retina*. 2016;36:1614–1621.
134. Sayanagi K, Ikuno Y, Soga K, Wakabayashi T, Tsujikawa M, Tano Y. Choroidal vascular hypofluorescence in indocyanine green angiography of high myopia. *Br J Ophthalmol*. 2009;93:1687–1690.
135. Wong CW, Teo YCK, Tsai STA, et al. Characterization of the choroidal vasculature in myopic maculopathy with optical coherence tomographic angiography. *Retina*. 2019;39:1742–1750.
136. Wong CW, Phua V, Lee SY, Wong TY, Cheung CM. Is choroidal or scleral thickness related to myopic macular degeneration? *Invest Ophthalmol Vis Sci*. 2017;58:907–913.
137. Klein RM, Green S. The development of lacquer cracks in pathologic myopia. *Am J Ophthalmol*. 1988;106:282–285.
138. Wong CW, Yanagi Y, Tsai ASH, et al. Correlation of axial length and myopic macular degeneration to levels of molecular factors in the aqueous. *Sci Rep*. 2019;9:15708.
139. Tong JP, Chan WM, Liu DT, et al. Aqueous humor levels of vascular endothelial growth factor and pigment epithelium-derived factor in polypoidal choroidal vasculopathy and choroidal neovascularization. *Am J Ophthalmol*. 2006;141:456–462.
140. Nagaoka N, Shimada N, Hayashi W, et al. Characteristics of periconus choroidal neovascularization in pathologic myopia. *Am J Ophthalmol*. 2011;152:420–427.e421.
141. Querques L, Giuffre C, Corvi F, et al. Optical coherence tomography angiography of myopic choroidal neovascularisation. *Br J Ophthalmol*. 2017;101:609–615.
142. Liu B, Bao L, Zhang J. Optical coherence tomography angiography of pathological myopia sourced and idiopathic choroidal neovascularization with follow-up. *Medicine (Baltimore)*. 2016;95:e3264.
143. Bagchi A, Schwartz R, Hykin P, Sivaprasad S. Diagnostic algorithm utilising multimodal imaging including optical coherence tomography angiography for the detection of myopic choroidal neovascularisation. *Eye (Lond)*. 2019;33:1111–1118.
144. Coscas G, Lupidi M, Coscas F. Image analysis of optical coherence tomography angiography. *Dev Ophthalmol*. 2016;56:30–36.
145. Bruyere E, Caillaux V, Cohen SY, et al. Spectral-domain optical coherence tomography of subretinal hyperreflective exudation in myopic choroidal neovascularization. *Am J Ophthalmol*. 2015;160:749–758.e741.
146. Battaglia Parodi M, Iacono P, Bandello F. Correspondence of leakage on fluorescein angiography and optical coherence tomography parameters in diagnosis and monitoring of myopic choroidal neovascularization treated with bevacizumab. *Retina*. 2016;36:104–109.
147. Shimada N, Ohno-Matsui K, Hayashi K, Yoshida T, Tokoro T, Mochizuki M. Macular detachment after successful intravitreal bevacizumab for myopic choroidal neovascularization. *Jpn J Ophthalmol*. 2011;55:378–382.
148. Asai T, Ikuno Y, Nishida K. Macular microstructures and prognostic factors in myopic subretinal hemorrhages. *Invest Ophthalmol Vis Sci*. 2014;55:226–232.
149. Miller DG, Singerman LJ. Natural history of choroidal neovascularization in high myopia. *Curr Opin Ophthalmol*. 2001;12:222–224.
150. Yoshida T, Ohno-Matsui K, Yasuzumi K, et al. Myopic choroidal neovascularization: a 10-year follow-up. *Ophthalmology*. 2003;110:1297–1305.
151. Kojima A, Ohno-Matsui K, Teramukai S, et al. Estimation of visual outcome without treatment in patients with subfoveal choroidal neovascularization in pathologic myopia. *Graefes Arch Clin Exp Ophthalmol*. 2006;244:1474–1479.
152. Blinder KJ, Blumenkranz MS, Bressler NM, et al. Verteporfin therapy of subfoveal choroidal neovascularization in pathologic myopia: 2-year results of a randomized clinical trial–VIP report no. 3. *Ophthalmology*. 2003;110:667–673.
153. Hayashi K, Ohno-Matsui K, Teramukai S, et al. Comparison of visual outcome and regression pattern of myopic choroidal neovascularization after intravitreal bevacizumab or after photodynamic therapy. *Am J Ophthalmol*. 2009;148:396–408.
154. Ng DSC, Lai TYY, Cheung CMG, Ohno-Matsui K Antivascular endothelial growth factor therapy for myopic choroidal neovascularization. *Asia Pac J Ophthalmol (Phila)*. 2017;6:554–560.
155. Cheung CMG, Arnold JJ, Holz FG, et al. Myopic choroidal neovascularization: review, guidance, and consensus statement on management. *Ophthalmology*. 2017;124:1690–1711.
156. Ohno-Matsui K, Ikuno Y, Lai TYY, Gemmy Cheung CM. Diagnosis and treatment guideline for myopic choroidal neovascularization due to pathologic myopia. *Prog Retin Eye Res*. 2018;63:92–106.
157. Yokoi T, Ohno-Matsui K. Diagnosis and treatment of myopic maculopathy. *Asia Pac J Ophthalmol (Phila)*. 2018;7:415–421.
158. Wolf S, Balciuniene VJ, Laganovska G, et al. RADIANCE: a randomized controlled study of ranibizumab in patients with choroidal neovascularization secondary to pathologic myopia. *Ophthalmology*. 2014;121:682–692.e682.
159. Holz FG, Tufail A, Leveziel N, et al. Ranibizumab in myopic choroidal neovascularization: a subgroup analysis by ethnicity, age, and ocular characteristics in RADIANCE. *Ophthalmologica*. 2016;236:19–28.

Investigative Ophthalmology & Visual Science

160. Chen Y, Sharma T, Li X, et al. Ranibizumab versus verteporfin photodynamic therapy in Asian patients with myopic choroidal neovascularization: brilliance, a 12-month, randomized, double-masked study. *Retina*. 2019;39:1985–1994.
161. Ikuno Y, Ohno-Matsui K, Wong TY, et al. Intravitreal aflibercept injection in patients with myopic choroidal neovascularization: the MYRROR study. *Ophthalmology*. 2015;122:1220–1227.
162. Chen Y. Efficacy and safety of conbercept ophthalmic injection in treatment of choroidal neovascularization secondary to pathological myopia (Shiny Trial). *Presented in Angiogenesis, Exudation, and Degeneration 2016 meeting*. Miami, Florida; 2016.
163. Zhou Y, Yang S, Yuan Y, et al. Progression and new onset of macular retinoschisis in myopic choroidal neovascularization eyes after Conbercept therapy: a post-hoc analysis. *Eye (Lond)*. 2020;34:523–529.
164. Lai TY, Luk FO, Lee GK, Lam DS. Long-term outcome of intravitreal anti-vascular endothelial growth factor therapy with bevacizumab or ranibizumab as primary treatment for subfoveal myopic choroidal neovascularization. *Eye (Lond)*. 2012;26:1004–1011.
165. Kasahara K, Moriyama M, Morohoshi K, et al. Six-year outcomes of intravitreal bevacizumab for choroidal neovascularization in patients with pathologic myopia. *Retina*. 2017;37:1055–1064.
166. Chhablani J, Paulose RM, Lasave AF, et al. Intravitreal bevacizumab monotherapy in myopic choroidal neovascularisation: 5-year outcomes for the PAN-American Collaborative Retina Study Group. *Br J Ophthalmol*. 2018;102:455–459.
167. Braimah IZ, Stewart M, Videkar C, Dedhia CJ, Chhablani J. Intravitreal ziv-aflibercept for the treatment of choroidal neovascularisation associated with conditions other than age-related macular degeneration. *Br J Ophthalmol*. 2017;101:1201–1205.
168. Hamilton RD, Clemens A, Minnella AM, et al. Real-world effectiveness and safety of ranibizumab for the treatment of myopic choroidal neovascularization: Results from the LUMINOUS study. *PLoS One*. 2020;15:e0227557.
169. Ohno-Matsui K, Suzaki M, Teshima R, Okami N. Real-world data on ranibizumab for myopic choroidal neovascularization due to pathologic myopia: results from a post-marketing surveillance in Japan. *Eye (Lond)*. 2018;32:1871–1878.
170. Tan NW, Ohno-Matsui K, Koh HJ, et al. Long-term outcomes of ranibizumab treatment of myopic choroidal neovascularization in east-Asian patients from the radiance study. *Retina*. 2018;38:2228–2238.
171. Cheung CMG, Ohno-Matsui K, Wong TY, Li T, Asmus F, Leal S. Influence of myopic macular degeneration severity on treatment outcomes with intravitreal aflibercept in the MYRROR study. *Acta Ophthalmol*. 2019;97:e729–e735.
172. Iacono P, Battaglia Parodi M, Selvi F, et al. Factors influencing visual acuity in patients receiving anti-vascular endothelial growth factor for myopic choroidal neovascularization. *Retina*. 2017;37:1931–1941.
173. Phillips CI. Retinal detachment at the posterior pole. *Br J Ophthalmol*. 1958;42:749–753.
174. Takano M, Kishi S. Foveal retinoschisis and retinal detachment in severely myopic eyes with posterior staphyloma. *Am J Ophthalmol*. 1999;128:472–476.
175. Benhamou N, Massin P, Haouchine B, Erginay A, Gaudric A. Macular retinoschisis in highly myopic eyes. *Am J Ophthalmol*. 2002;133:794–800.
176. Ikuno Y. [Pathogenesis and treatment of myopic foveoschisis]. *Nippon Ganka Gakkai Zasshi*. 2006;110:855–863.
177. Bando H, Ikuno Y, Choi JS, Tano Y, Yamanaka I, Ishibashi T. Ultrastructure of internal limiting membrane in myopic foveoschisis. *Am J Ophthalmol*. 2005;139:197–199.
178. Stirpe M, Michels RG. Retinal detachment in highly myopic eyes due to macular holes and epiretinal traction. *Retina*. 1990;10:113–114.
179. Tang J, Rivers MB, Moshfeghi AA, Flynn HW, Chan CC. Pathology of macular foveoschisis associated with degenerative myopia. *J Ophthalmol*. 2010;2010:175613.
180. Sayanagi K, Ikuno Y, Tano Y. Tractional internal limiting membrane detachment in highly myopic eyes. *Am J Ophthalmol*. 2006;142:850–852.
181. Ikuno Y, Gomi F, Tano Y. Potent retinal arteriolar traction as a possible cause of myopic foveoschisis. *Am J Ophthalmol*. 2005;139:462–467.
182. Falre M. [Parapapillary hole as cause of retinal detachment]. *Ophthalmologica*. 1954;127:351–356.
183. Sayanagi K, Ikuno Y, Soga K, Tano Y. Photoreceptor inner and outer segment defects in myopic foveoschisis. *Am J Ophthalmol*. 2008;145:902–908.
184. Jo Y, Ikuno Y, Nishida K. Retinoschisis: a predictive factor in vitrectomy for macular holes without retinal detachment in highly myopic eyes. *Br J Ophthalmol*. 2012;96:197–200.
185. Gaucher D, Haouchine B, Tadayoni R, et al. Long-term follow-up of high myopic foveoschisis: natural course and surgical outcome. *Am J Ophthalmol*. 2007;143:455–462.
186. Shimada N, Ohno-Matsui K, Baba T, Futagami S, Tokoro T, Mochizuki M. Natural course of macular retinoschisis in highly myopic eyes without macular hole or retinal detachment. *Am J Ophthalmol*. 2006;142:497–500.
187. Ikuno Y, Sayanagi K, Soga K, Oshima Y, Ohji M, Tano Y. Foveal anatomical status and surgical results in vitrectomy for myopic foveoschisis. *Jpn J Ophthalmol*. 2008;52:269–276.
188. Kumagai K, Furukawa M, Ogino N, Larson E. Factors correlated with postoperative visual acuity after vitrectomy and internal limiting membrane peeling for myopic foveoschisis. *Retina*. 2010;30:874–880.
189. Nakanishi H, Kuriyama S, Saito I, et al. Prognostic factor analysis in pars plana vitrectomy for retinal detachment attributable to macular hole in high myopia: a multicenter study. *Am J Ophthalmol*. 2008;146:198–204.
190. Ikuno Y, Sayanagi K, Oshima T, et al. Optical coherence tomographic findings of macular holes and retinal detachment after vitrectomy in highly myopic eyes. *Am J Ophthalmol*. 2003;136:477–481.
191. Ikuno Y, Tano Y. Vitrectomy for macular holes associated with myopic foveoschisis. *Am J Ophthalmol*. 2006;141:774–776.
192. Lim LS, Tsai A, Wong D, et al. Prognostic factor analysis of vitrectomy for retinal detachment associated with myopic macular holes. *Ophthalmology*. 2014;121:305–310.
193. Sakaguchi H, Ikuno Y, Choi JS, Ohji M, Tano T. Multiple components of epiretinal tissues detected by triamcinolone and indocyanine green in macular hole and retinal detachment as a result of high myopia. *Am J Ophthalmol*. 2004;138:1079–1081.
194. Kadonosono K, Yazama F, Itoh N, et al. Treatment of retinal detachment resulting from myopic macular hole with internal limiting membrane removal. *Am J Ophthalmol*. 2001;131:203–207.
195. Ho TC, Chen MS, Huang JS, Shih YF, Ho H, Huang YH. Foveola nonpeeling technique in internal limiting membrane peeling of myopic foveoschisis surgery. *Retina*. 2012;32:631–634.
196. Shimada N, Sugamoto Y, Ogawa M, Takase H, Ohno-Matsui K. Fovea-sparing internal limiting membrane peeling

Investigative Ophthalmology & Visual Science

for myopic traction maculopathy. *Am J Ophthalmol*. 2012;24:24.

197. Kuriyama S, Hayashi H, Jingami Y, Kuramoto N, Akita J, Matsumoto M. Efficacy of inverted internal limiting membrane flap technique for the treatment of macular hole in high myopia. *Am J Ophthalmol*. 2013;24:00141–00144.
198. Wakabayashi T, Ikuno Y, Shiraki N, Matsumura N, Sakaguchi H, Nishida K. Inverted internal limiting membrane insertion versus standard internal limiting membrane peeling for macular hole retinal detachment in high myopia: one-year study. *Graefes Arch Clin Exp Ophthalmol*. 2018;256:1387–1393.
199. Lai CC, Chen YP, Wang NK, et al. Vitrectomy with internal limiting membrane repositioning and autologous blood for macular hole retinal detachment in highly myopic eyes. *Ophthalmology*. 2015;122:1889–1898.
200. Morizane Y, Shiraga F, Kimura S, et al. Autologous transplantation of the internal limiting membrane for refractory macular holes. *Am J Ophthalmol*. 2014;157:861–869.e861.
201. Grewal DS, Mahmoud TH. Autologous neurosensory retinal free flap for closure of refractory myopic macular holes. *JAMA Ophthalmol*. 2016;134:229–230.
202. Uemoto R, Saito Y, Sato S, Imaizumi A, Tanaka M, Nakae K. Better success of retinal reattachment with long-standing gas tamponade in highly myopic eyes. *Graefes Arch Clin Exp Ophthalmol*. 2003;241:792–796.
203. Nishimura A, Kimura M, Saito Y, Sugiyama K. Efficacy of primary silicone oil tamponade for the treatment of retinal detachment caused by macular hole in high myopia. *Am J Ophthalmol*. 2011;151:148–155.
204. Gao X, Ikuno Y, Fujimoto S, Nishida K. Risk factors for development of full-thickness macular holes after pars plana vitrectomy for myopic foveoschisis. *Am J Ophthalmol*. 2013;155:1021–1027.e1021.
205. Ripandelli G, Coppe AM, Fedeli R, Parisi V, D'Amico DJ, Stirpe M. Evaluation of primary surgical procedures for retinal detachment with macular hole in highly myopic eyes: a comparison [corrected] of vitrectomy versus posterior episcleral buckling surgery. *Ophthalmology*. 2001;108:2258–2264; discussion 2265.
206. Parolini B, Frisina R, Pinackatt S, et al. Indications and results of a new l-shaped macular buckle to support a posterior staphyloma in high myopia. *Retina*. 2015;35:2469–2482.
207. Gaucher D, Erginay A, Lecleire-Collet A, et al. Dome-shaped macula in eyes with myopic posterior staphyloma. *Am J Ophthalmol*. 2008;145:909–914.
208. Zhao X, Ding X, Lyu C, et al. Observational study of clinical characteristics of dome-shaped macula in Chinese Han with high myopia at Zhongshan Ophthalmic Centre. *BMJ Open*. 2018;8:e021887.
209. Dai F, Li S, Wang Y, et al. Correlation between posterior staphyloma and dome-shaped macula in high myopic eyes. *Retina*. 2019;40:2119–2126.
210. Shin E, Park KA, Oh SY. Dome-shaped macula in children and adolescents. *PLoS One*. 2020;15:e0227292.
211. Viola F, Dell'Arti L, Benatti E, et al. Choroidal findings in dome-shaped macula in highly myopic eyes: a longitudinal study. *Am J Ophthalmol*. 2015;159:44–52.
212. Errera MH, Michaelides M, Keane PA, et al. The extended clinical phenotype of dome-shaped macula. *Graefes Arch Clin Exp Ophthalmol*. 2014;252:499–508.
213. Caillaux V, Gaucher D, Gualino V, Massin P, Tadayoni R, Gaudric A. Morphologic characterization of dome-shaped macula in myopic eyes with serous macular detachment. *Am J Ophthalmol*. 2013;156:958–967.
214. Liang IC, Shimada N, Tanaka Y, et al. Comparison of clinical features in highly myopic eyes with and without a dome-shaped macula. *Ophthalmology*. 2015;122:1591–1600
215. Zhao X, Lian P, Li S, Liu B, Ding X, Lu L. Patterns of choroidal deepening in highly myopic eyes with dome-shaped macula. *Curr Eye Res*. 2019;45:1–7.
216. Imamura Y, Iida T, Maruko I, Zweifel SA, Spaide RF. Enhanced depth imaging optical coherence tomography of the sclera in dome-shaped macula. *Am J Ophthalmol*. 2011;151:297–302.
217. Ellabban AA, Tsujikawa A, Matsumoto A, et al. Three-dimensional tomographic features of dome-shaped macula by swept-source optical coherence tomography. *Am J Ophthalmol*. 2013;155:320–328.e322.
218. Ellabban AA, Tsujikawa A, Muraoka Y, et al. Dome-shaped macular configuration: longitudinal changes in the sclera and choroid by swept-source optical coherence tomography over two years. *Am J Ophthalmol*. 2014;158:1062–1070.
219. Soudier G, Gaudric A, Gualino V, et al. Long-term evolution of dome-shaped macula: increased macular bulge is associated with extended macular atrophy. *Retina*. 2016;36:944–952.
220. Soudier G, Gaudric A, Gualino V, et al. Serous retinal detachment in dome-shaped macula is associated with greater central choroidal blood flow measured by optical coherence tomography angiography. *Ophthalmologica*. 2020;243:129–135.
221. Keane PA, Mitra A, Khan IJ, Quhill F, Elsherbiny SM. Dome-shaped macula: a compensatory mechanism in myopic anisometropia? *Ophthalmic Surg Lasers Imaging*. 2012;43 Online:e52–54.
222. Ohno-Matsui K, Fang Y, Uramoto K, et al. Peri-dome choroidal deepening in highly myopic eyes with dome-shaped maculas. *Am J Ophthalmol*. 2017;183:134–140.
223. Hocaoglu M, Ersoz MG, Sayman Muslubas I, Arf S, Karacorlu M. Factors associated with macular complications in highly myopic eyes with dome-shaped macular configuration. *Graefes Arch Clin Exp Ophthalmol*. 2019;257:2357–2365.
224. Deobhakta A, Ross AH, Helal J, Jr., Maia A, Freund KB. Localized choroidal thickness variation and pigment epithelial detachment in dome-shaped macula with subretinal fluid. *Ophthalmic Surg Lasers Imaging Retina*. 2015;46:391–392.
225. Tamura N, Sakai T, Tsuneoka H. Spontaneous resolution of foveal detachment in dome-shaped macula observed by spectral domain optical coherence tomography. *Clin Ophthalmol*. 2014;8:83–86.
226. Burke TR, Wu AD, Shen Y, Rajendram R. Longitudinal follow-up of dome-shaped macula. *Eye (Lond)*. 2020;34:1903–1908.
227. Garcia-Ben A, Garcia-Basterra I, Gonzalez-Gomez A, et al. Comparison of long-term clinical evolution in highly myopic eyes with vertical oval-shaped dome with or without untreated serous retinal detachment. *Br J Ophthalmol*. 2019;103:385–389.
228. Ohsugi H, Ikuno Y, Oshima K, Yamauchi T, Tabuchi H. Morphologic characteristics of macular complications of a dome-shaped macula determined by swept-source optical coherence tomography. *Am J Ophthalmol*. 2014;158:162–170.e161.
229. Naysan J, Dansingani KK, Balaratnasingam C, Freund KB. Type 1 neovascularization with polypoidal lesions complicating dome shaped macula. *Int J Retina Vitreous*. 2015;1:8.
230. Marchese A, Arrigo A, Sacconi R, et al. Spectrum of choroidal neovascularisation associated with dome-shaped macula. *Br J Ophthalmol*. 2019;103:1146–1151.
231. Cai B, Yang J, Li S, et al. Comparison of the efficacy of intravitreal ranibizumab for choroidal neovascularization

Investigative Ophthalmology & Visual Science

due to pathological myopia with and without a dome-shaped macula. *Medicine (Baltimore)*. 2017;96:e9251.
232. Ceklic L, Wolf-Schnurrbusch U, Gekkieva M, Wolf S. Visual acuity outcome in RADIANCE study patients with dome-shaped macular features. *Ophthalmology*. 2014;121:2288–2289.
233. Shinohara K, Moriyama M, Shimada N, et al. Analyses of shape of eyes and structure of optic nerves in eyes with tilted disc syndrome by swept-source optical coherence tomography and three-dimensional magnetic resonance imaging. *Eye*. 2013;27:1233–1241.
234. Cohen SY, Quentel G, Guiberteau B, Delahaye-Mazza C, Gaudric A. Macular serous retinal detachment caused by subretinal leakage in tilted disc syndrome. *Ophthalmology*. 1998;105:1831–1834.
235. Nakanishi H, Tsujikawa A, Gotoh N, et al. Macular complications on the border of an inferior staphyloma associated with tilted disc syndrome. *Retina*. 2008;28:1493–1501.
236. Cohen SY, Dubois L, Nghiem-Buffet S, et al. Spectral domain optical coherence tomography analysis of macular changes in tilted disk syndrome. *Retina*. 2013;33:1338–1345.
237. Pardo-Lopez D, Gallego-Pinazo R, Mateo C, et al. Serous macular detachment associated with dome-shaped macula and tilted disc. *Case Report Ophthalmol*. 2011;2:111–115.
238. Coco RM, Sanabria MR, Alegria J. Pathology associated with optical coherence tomography macular bending due to either dome-shaped macula or inferior staphyloma in myopic patients. *Ophthalmologica*. 2012;228:7–12.
239. Tan ACS, Yzer S, Freund KB, Dansingani KK, Phasukkijwatana N, Sarraf D. Choroidal changes associated with serous macular detachment in eyes with staphyloma, dome-shaped macula or tilted disk syndrome. *Retina*. 2017;37:1544–1554.
240. Ueno C, Gomi F, Ikuno Y, Nakai K, Sawa M, Nishida K. Choroidal thickness in eyes with tilted disk syndrome. *Retina*. 2014;34:497–503.
241. Xu X, Fang Y, Jonas JB, et al. Ridge-shaped macula in young myopic patients and its differentiation from typical dome-shaped macula in elderly myopic patients. *Retina*. 2020;40:225–232.
242. Chinskey ND, Johnson MW. Treatment of subretinal fluid associated with dome-shaped macula. *Ophthalmic Surg Lasers Imaging Retina*. 2013;44:593–595.
243. Arapi I, Neri P, Mariotti C, et al. Considering photodynamic therapy as a therapeutic modality in selected cases of dome-shaped macula complicated by foveal serous retinal detachment. *Ophthalmic Surg Lasers Imaging Retina*. 2015;46:217–223.
244. Dirani A, Matet A, Beydoun T, Mantel I, Behar-Cohen F. Resolution of foveal detachment in dome-shaped macula after treatment by spironolactone: report of two cases and mini-review of the literature. *Clin Ophthalmol*. 2014;8:999–1002.
245. Giacomelli G, Mencucci R, Sodi A, et al. Aflibercept in serous foveal detachment in dome-shaped macula: short-term results in a retrospective study. *Ophthalmic Surg Lasers Imaging Retina*. 2017;48:822–828.
246. Chen NN, Chen CL, Lai CH. Resolution of unilateral dome-shaped macula with serous detachment after treatment of topical carbonic anhydrase inhibitors. *Ophthalmic Surg Lasers Imaging Retina*. 2019;50:e218–e221.
247. Soudier G, Gaudric A, Gualino V, Nardin M, Speeg-Schatz C, Gaucher D. Epiretinal membrane in dome-shaped macula complicated with serous retinal detachment: transient efficacy of surgery. *Case Rep Ophthalmol*. 2017;8:515–520.
248. Xu L, Wang Y, Wang S, Wang Y, Jonas JB. High myopia and glaucoma susceptibility the Beijing Eye Study. *Ophthalmology*. 2007;114:216–220.
249. Jonas JB, Weber P, Nagaoka N, Ohno-Matsui K. Glaucoma in high myopia and parapapillary delta zone. *PLoS One*. 2017;12:e0175120.
250. Bikbov MM, Gilmanshin TR, Kazakbaeva GM, et al. Prevalence of myopic maculopathy among adults in a Russian population. *JAMA Netw Open*. 2020;3:e200567.
251. Jonas JB. Optic disk size correlated with refractive error. *Am J Ophthalmol*. 2005;139:346–348.
252. Xu L, Wang YX, Wang S, Jonas JB. Definition of high myopia by parapapillary atrophy. The Beijing Eye Study. *Acta Ophthalmol*. 2010;88:e350–351.
253. Zhang Q, Xu L, Wei WB, Wang YX, Jonas JB. Size and shape of Bruch's membrane opening in relationship to axial length, gamma zone, and macular Bruch's membrane defects. *Invest Ophthalmol Vis Sci*. 2019;60:2591–2598.
254. Kim TW, Kim M, Weinreb RN, Woo SJ, Park KH, Hwang JM. Optic disc change with incipient myopia of childhood. *Ophthalmology*. 2012;119:21–26.e21-23.
255. Lee KM, Choung HK, Kim M, Oh S, Kim SH. Positional change of optic nerve head vasculature during axial elongation as evidence of lamina cribrosa shifting: Boramae Myopia Cohort Study Report 2. *Ophthalmology*. 2018;125:1224–1233.
256. Guo Y, Liu LJ, Tang P, et al. Parapapillary gamma zone and progression of myopia in school children: the Beijing Children Eye Study. *Invest Ophthalmol Vis Sci*. 2018;59:1609–1616.
257. Kim M, Choung HK, Lee KM, Oh S, Kim SH. Longitudinal changes of optic nerve head and peripapillary structure during childhood myopia progression on OCT: Boramae Myopia Cohort Study Report 1. *Ophthalmology*. 2018;125:1215–1223.
258. Jonas JB, Jonas SB, Jonas RA, et al. Parapapillary atrophy: histological gamma zone and delta zone. *PLoS One*. 2012;7:e47237.
259. Dai Y, Jonas JB, Ling Z, Sun X. Ophthalmoscopic-perspectively distorted optic disc diameters and real disc diameters. *Invest Ophthalmol Vis Sci*. 2015;56:7076–7083.
260. Jonas JB, Gusek GC, Naumann GO. Optic disc, cup and neuroretinal rim size, configuration and correlations in normal eyes. *Invest Ophthalmol Vis Sci*. 1988;29:1151–1158.
261. Jonas JB, Berenshtein E, Holbach L. Anatomic relationship between lamina cribrosa, intraocular space, and cerebrospinal fluid space. *Invest Ophthalmol Vis Sci*. 2003;44:5189–5195.
262. Jonas JB, Berenshtein E, Holbach L. Lamina cribrosa thickness and spatial relationships between intraocular space and cerebrospinal fluid space in highly myopic eyes. *Invest Ophthalmol Vis Sci*. 2004;45:2660–2665.
263. Berdahl JP, Allingham RR, Johnson DH. Cerebrospinal fluid pressure is decreased in primary open-angle glaucoma. *Ophthalmology*. 2008;115:763–768.
264. Ren R, Jonas JB, Tian G, et al. Cerebrospinal fluid pressure in glaucoma: a prospective study. *Ophthalmology*. 2010;117:259–266.
265. Ren R, Wang N, Li B, et al. Lamina cribrosa and peripapillary sclera histomorphometry in normal and advanced glaucomatous Chinese eyes with various axial length. *Invest Ophthalmol Vis Sci*. 2009;50:2175–2184.
266. Jonas RA, Holbach L. Peripapillary border tissue of the choroid and peripapillary scleral flange in human eyes. *Acta Ophthalmol*. 2020;98:e43–e49.
267. Jonas JB, Jonas SB. Histomorphometry of the circular peripapillary arterial ring of Zinn-Haller in normal eyes

and eyes with secondary angle-closure glaucoma. *Acta Ophthalmol*. 2010;88:e317–322.
268. Jonas JB, Jonas RA, Ohno-Matsui K, Holbach L, Panda-Jonas S. Corrugated Bruch's membrane in high myopia. *Acta Ophthalmol*. 2018;96:e147–e151.
269. Jonas JB, Gusek GC, Naumann GO. Optic disk morphometry in high myopia. *Graefes Arch Clin Exp Ophthalmol*. 1988;226:587–590.
270. Tan NYQ, Sng CCA, Jonas JB, Wong TY, Jansonius NM, Ang M. Glaucoma in myopia: diagnostic dilemmas. *Br J Ophthalmol*. 2019;103:1347–1355.
271. Jonas JB, Nagaoka N, Fang YX, Weber P, Ohno-Matsui K. Intraocular pressure and glaucomatous optic neuropathy in high myopia. *Invest Ophthalmol Vis Sci*. 2017;58:5897–5906.
272. Fujiwara T, Imamura Y, Margolis R, Slakter JS, Spaide RF. Enhanced depth imaging optical coherence tomography of the choroid in highly myopic eyes. *Am J Ophthalmol*. 2009;148:445–450.
273. Ikuno Y, Tano Y. Retinal and choroidal biometry in highly myopic eyes with spectral-domain optical coherence tomography. *Invest Ophthalmol Vis Sci*. 2009;50:3876–3880.
274. Nishida Y, Fujiwara T, Imamura Y, Lima LH, Kurosaka D, Spaide RF. Choroidal thickness and visual acuity in highly myopic eyes. *Retina*. 2012;32:1229–1236.
275. Takahashi A, Ito Y, Iguchi Y, Yasuma TR, Ishikawa K, Terasaki H. Axial length increases and related changes in highly myopic normal eyes with myopic complications in fellow eyes. *Retina*. 2012;32:127–133.
276. Flores-Moreno I, Lugo F, Duker JS, Ruiz-Moreno JM. The relationship between axial length and choroidal thickness in eyes with high myopia. *Am J Ophthalmol*. 2013;155:314–319.
277. Ho M, Liu DT, Chan VC, Lam DS. Choroidal thickness measurement in myopic eyes by enhanced depth optical coherence tomography. *Ophthalmology*. 2013;120:1909–1914.
278. Flores-Moreno I, Ruiz-Medrano J, Duker JS, Ruiz-Moreno JM. The relationship between retinal and choroidal thickness and visual acuity in highly myopic eyes. *Br J Ophthalmol*. 2013;97:1010–1013.
279. Gupta P, Saw SM, Cheung CY, et al. Choroidal thickness and high myopia: a case-control study of young Chinese men in Singapore. *Acta Ophthalmol*. 2015;93:e585–592.
280. Pang CE, Sarraf D, Freund KB. Extreme choroidal thinning in high myopia. *Retina*. 2015;35:407–415.
281. Abdolrahimzadeh S, Parisi F, Plateroti AM, et al. Visual acuity, and macular and peripapillary thickness in high myopia. *Curr Eye Res*. 2017;42:1468–1473.
282. Lee JH, Lee SC, Kim SH, et al. Choroidal thickness and chorioretinal atrophy in myopic choroidal neovascularization with anti-vascular endothelial growth factor therapy. *Retina*. 2017;37:1516–1522.
283. Xiong S, He X, Deng J, et al. Choroidal thickness in 3001 Chinese children aged 6 to 19 years using swept-source OCT. *Sci Rep*. 2017;7:45059.
284. Liu B, Wang Y, Li T, et al. Correlation of subfoveal choroidal thickness with axial length, refractive error, and age in adult highly myopic eyes. *BMC Ophthalmol*. 2018;18:127.
285. Fledelius HC, Jacobsen N, Li XQ, Goldschmidt E. Choroidal thickness at age 66 years in the Danish high myopia study cohort 1948 compared with follow-up data on visual acuity over 40 years: a clinical update adding spectral domain optical coherence tomography. *Acta Ophthalmol*. 2018;96:46–50.
286. Chalam KV, Sambhav K. Choroidal thickness measured with swept source optical coherence tomography in posterior staphyloma strongly correlates with axial length and visual acuity. *Int J Retina Vitreous*. 2019;5:14.
287. Ohno-Matsui K, Jonas JB, Spaide RF. Macular Bruch membrane holes in choroidal neovascularization-related myopic macular atrophy by swept-source optical coherence tomography. *Am J Ophthalmol*. 2016;162:133–139.
288. Marchese A, Carnevali A, Sacconi R, et al. Retinal pigment epithelium humps in high myopia. *Am J Ophthalmol*. 2017;182:56–61.
289. Yokoi T, Zhu D, Bi HS, et al. Parapapillary diffuse choroidal atrophy in children is associated with extreme thinning of parapapillary choroid. *Invest Ophthalmol Vis Sci*. 2017;58:901–906.
290. Panozzo G, Mercanti A. Optical coherence tomography findings in myopic traction maculopathy. *Arch Ophthalmol*. 2004;122:1455–1460.
291. Baba T, Ohno-Matsui K, Futagami S, et al. Prevalence and characteristics of foveal retinal detachment without macular hole in high myopia. *Am J Ophthalmol*. 2003;135:338–342.
292. Johnson MW. Myopic traction maculopathy: pathogenic mechanisms and surgical treatment. *Retina*. 2012;32(Suppl 2):S205–S210.
293. Margolis R, Spaide RF. A pilot study of enhanced depth imaging optical coherence tomography of the choroid in normal eyes. *Am J Ophthalmol*. 2009;147:811–815.
294. Takashima T, Yokoyama T, Futagami S, et al. The quality of life in patients with pathologic myopia. *Jpn J Ophthalmol*. 2001;45:84–92.
295. Wen D, Liu SZ, Mao JF, Tan XP. [Apoptosis and c-myc protein expression in the retinal of form-deprivation myopia]. *Zhong Nan Da Xue Xue Bao Yi Xue Ban*. 2006;31(2):236–240. Chinese. PMID: 16706123.
296. Mao JF, Liu SZ, Wen D, et al. Basic fibroblast growth factor suppresses retinal neuronal apoptosis in form-deprivation myopia in chicks. *Current Eye Research*. 2006; 31(11): 983–987.

Investigative Ophthalmology & Visual Science